Adsorption of volatile organic compounds and regeneration of activated carbons – Development of a simulation tool

Shivaji Ganesan Ramalingam

l'université nantes angers le mans
PÔLE DE RECHERCHE ET D'ENSEIGNEMENT SUPÉRIEUR

ECOLE DES MINES DE NANTES

Thèse de Doctorat

Shivaji Ganesan Ramalingam

Mémoire présenté en vue de l'obtention

du grade de Docteur de l'Ecole des Mines de Nantes

Sous le label de l'Université Nantes Angers Le Mans

Discipline : *Génie des procèdes*

Spécialité : Energie et Environnement

Laboratoire : GEPEA

Soutenue le 11 Juillet 2012

École doctorale : SPIGA

Thèse N° 2012EMNA0052

Adsorption de Composes Organiques Volatils et Régénération de charbon actifs – Développement d'outils de simulation

JURY

Rapporteurs :	**M.Gavin Walker**, Professeur, Queens University Belfast
	Mdme. Marie-Helene Manero, Professeur, Laboratoire de Génie Chimique
Examinateurs :	**M.Marc Clausse**, Professeur Associé (HDR), ESIEE Paris
	M.Michel Baudu, Professeur, Université de Limoges
	Mdme.Pascaline Pré, Maître-assistante (HDR), Ecole des Mines de Nantes
	M.Sylvain Giraudet, Maître de conférences, Ecole Nationale Supérieure de Chimie de Rennes
	Mdme.Laurence Le Coq, Professeur, Ecole des Mines de Nantes
	M.Pierre Le Cloirec, Professeur, Ecole Nationale Supérieure de Chimie de Rennes
	M.Christophe Stavrakakis, Ingénieur, ADEME
	M.Oliver Baudouin, Directeur des Procédés, PROSIM
	M.Eric Demangel, Chef de marché, CECA - ARKEMA

REMERCIEMENTS

Je tiens à exprimer toute ma reconnaissance au Professeur Laurence LE COQ, directeur de département DSEE et Professeur Pierre LE CLOIREC, directeur l'Ecole Nationale Supérieure de Chimie de Rennes pour m'avoir permis de préparer mon doctorat dans les meilleures conditions. Je tiens à les remercier tout particulièrement pour leurs efforts et pour le soutien qu'ils m'ont témoigné tout au long de cette étude placée sous leur direction.

Je tiens également à exprimer tous mes sincères remerciements à Madame Pascaline PRE et Monsieur Sylvain GIRAUDET pour avoir co-encadré cette thèse. Je tiens encore à leur exprimer ma profonde gratitude pour leur aide et leurs précieux conseils.

Je suis très honoré de la présence au titre de rapporteurs de Professeur Gavin WALKER et Professeur Marie-Helene MANERO d'avoir accepté de participer à ce jury.

Je souhaite vivement remercier le Professeur Michel BAUDU de l'Université de Limoges pour m'avoir fait l'honneur de présider mon jury de thèse et à Monsieur Marc CLAUSSE de Le CNAM (Paris) d'avoir accepté de participer à ce jury.

Ce travail a été effectué avec le concours financier de l'Agence de l'Environnement et de la Maîtrise de l'Energie, représentée par Monsieur Christophe STAVRAKAKIS. Je le remercie d'avoir participé au jury de cette thèse.

Je suis aussi très reconnaissant à Monsieur Serge NICOLAS (GRL ARKEMA) et Monsieur Olivier BAUDOUIN (PROSIM), pour leur encadrement et leurs soutiens.

Je remercie aussi toutes les équipes du DSEE : professeurs, secrétaires (particulièrement, Madame Dominique Briand), techniciens, doctorants et stagiaires.

Je tiens enfin à exprimer toute ma gratitude à Geraldine MAZOYER et à ma famille dont le soutien a été essentiel tout au long de mes études, et tout particulièrement au cours de ce travail.

LIST OF PUBLICATIONS

Publications

1. S.G. Ramalingam, J. Saussac, P. Pré, S. Giraudet, L. Le Coq, P. Le Cloirec, S. Nicolas, O. Baudouin, S. Déchelotte, A. Medevielle, Hazardous Dichloromethane recovery in combined temperature and vacuum pressure swing adsorption process, Journal of Hazardous Materials, 198 (2011) 95-102

2. S.G. Ramalingam, P. Pré, S. Giraudet, L. Le Coq, P. Le Cloirec, O. Baudouin, S. Déchelotte, Recovery comparisons - Hot Nitrogen Vs Steam regeneration of toxic dichloromethane from activated carbon beds in oil sands process, Journal of Hazardous Materials, 205 – 206 (2012) 222-228

3. S.G. Ramalingam, L. Hamon, P. Pré, S. Giraudet, L. Le Coq, P. Le Cloirec, O. Baudouin, S. Déchelotte, Global statistical predictor model for characteristic adsorption energy or organic vapors – solid interactions: use in dynamic process simulation, Journal of Colloid and Interface Science, 377 (2012) 375-378

4. S.G. Ramalingam, P. Pré, S. Giraudet, L. Le Coq, P. Le Cloirec, O. Baudouin, S. Déchelotte, Different families of Volatile Organic Compounds pollution control by microporous activated carbon in Temperature Swing Adsorption, Journal of Hazardous Materials, 221-222 (2012) 242 -247

5. S.G. Ramalingam, P. Pré, S. Giraudet, L. Le Coq, P. Le Cloirec, O. Baudouin, S. Déchelotte, Strategy for the selection of activated carbon: In adsorption and regeneration of Volatile Organic Compound in industrial applications, Previewed in Chemical Engineering Journal

International Conferences

1. S.G. Ramalingam, J. Saussac, P. Pré, S. Giraudet, L. Le Coq, P. Le Cloirec, S. Nicolas, O. Baudouin, S. Déchelotte, A. Medevielle, Organic vapor recovery by combined temperature and vacuum pressure swing adsorption (VTSA) process, Carbon, Shanghai, China, 25-29 July 2011

2. S.G. Ramalingam, P. Pré, S. Giraudet, L. Le Coq, P. Le Cloirec, O. Baudouin, S. Déchelotte, Recovery comparisons - Organic vapor recovery in Temperature Swing Adsorption (TSA) process, SFGP, Lille, France, 29 Nov – 1 Dec 20 2011

LIST OF FIGURES

LIST OF TABLES

NOMENCLATURE

a_p - ratio between the external surface and the volume of the particle (m^{-1})

b_0 - parameter of the model (atm^{-1})

b_1 - parameter of the model, (T^{-1})

Cp_a – specific heat capacity of adsorbed phase ($J.kg^{-1}.K^{-1}$)

Cp_p – specific heat capacity of the adsorbent ($J.kg^{-1}.K^{-1}$)

C_i –VOC concentration in the gas phase, ($mol.m^{-3}$)

Cp_g – specific heat capacity of gas phase ($J.kg^{-1}.K^{-1}$)

D_L – axial mass dispersion coefficient ($m^2.s^{-1}$)

D_{gl} - global mass transfer coefficient ($m^2.s^{-1}$)

d_c – diameter of the column (m)

D_L – diffusivity ($m^2.s^{-1}$)

D_H – axial heat dispersion coefficient ($W.m^{-1}.K^{-1}$)

d_p – equivalent particle diameter (m)

e – thickness of the column (m)

H – enthalpy of gas phase ($J.kg^{-1}$)

h_w – heat transfer coefficient of wall ($W.m^2.K$-1)

h_p – heat transfer coefficient with solid particle ($W.m^2.K$-1)

ΔH_i – enthalpy of adsorption/desorption of the compound i ($J.mol^{-1}$)

H_{vap} - latent heat of vaporisation ($kJ.mol^{-1}$)

K_f - external mass transfer coefficient ($m.s^{-1}$)

K – global mass transfer coefficient (s^{-1})

PI - VOC ionisation potential (eV)

P_i – equilibrium VOC partial pressure (atm)

q_i – adsorbed VOC concentration ($mol.kg^{-1}$)

qi^* - adsorbed VOC concentration at the equilibrium with the gas phase ($mol.kg^{-1}$)

q_i^* – VOC adsorbed quantity at the equilibrium ($mol.kg^{-1}$)

q_{mo} – parameter of the model ($mol.kg^{-1}$)

q_{m1}– parameter of the model (T^{-1})

q_i – VOC concentration in the adsorbed phase ($mol.kg^{-1}$)

r_p - partcicle equivalent radius (m)

r_{mic}, adsorbent average micropore opening (nm).

T – temperature of gas (°C)

T_p – temperature of solid particle (°C)

v – superficial velocity ($m.s^{-1}$)

V_m - molar VOC volume ($m^3.mol^{-1}$)

v – superficial gas velocity ($m.s^{-1}$)

y - VOC molar fraction in the gas

ϱ_p – bulk adsorbent density ($kg.m^{-3}$)

ϱ_g – density of gas phase, ($kg.m^{-3}$)

ε – bed porosity

λ – thermal conductivity of the material of the column (W/m/K)α - VOC polarisability (10^{-24} cm^3)

γ - surface tension of the liquid solvent ($mN.m^{-1}$)

μ – dynamic viscosity (Pa.s)

n – constant parameter of the model

c_e - experimental concentration at the thermodynamic equilibrium ($mol.m^{-3}$)

W_0 - hypothetical microporous volume that can be filled by adsorbate (cm^3 g^{-1})

V_m - molar volume of the adsorbed phase (cm^3 mol^{-1})

E - characteristic energy, *i.e.* the adsorption potential of the couple adsorbent-adsorbate (KJ mol^{-1})

p_s - vapor saturation pressure of the adsorbate (Pa)

ACRONYMS

VOC – Volatile Organic Compounds

FED – Factorial Experiment Design

DR – Dubinin-Raduskevich

ANOVA – Analysis Of Variance

MLR – Multiple Linear Regression

LIST OF CHAPTERS

1. General Introduction

Volatile Organic Compounds (VOCs) are used as solvents or directly involved in chemical reactions in chemical, pharmaceutical processes, and hydrocarbon industries. Some of them cause serious risks such as cancer and contribute a major proportion to air pollution [1-3]. According to the European Union (EU), volatile organic compound is defined as an organic compound having a boiling point less than or equal to 250 °C measured at a standard pressure of 101.3 kPa [1]. The demand for the reduction in the level of VOC from all the sources in EU member states has been entered into force and so they are monitored in all member states (Directive 2004/42/EC of the European Parliament and of the Council of 21 April 2004 on the limitation of emissions of volatile organic compounds due to the use of organic solvents in decorative paints and varnishes and vehicle refinishing products and amending Directive 1999/13/EC [1]. Figure 1.1 shows the VOC emissions per capita with respect to the country during the period 1990 - 2005. Among the least populated countries, Canada and Norway have higher VOC emissions per capita compared with the other countries such as France, Belgium, and Netherlands. The scale of VOC emissions is significant in case of Canada and Norway, because of their strong hydrocarbon industry compared to other countries.

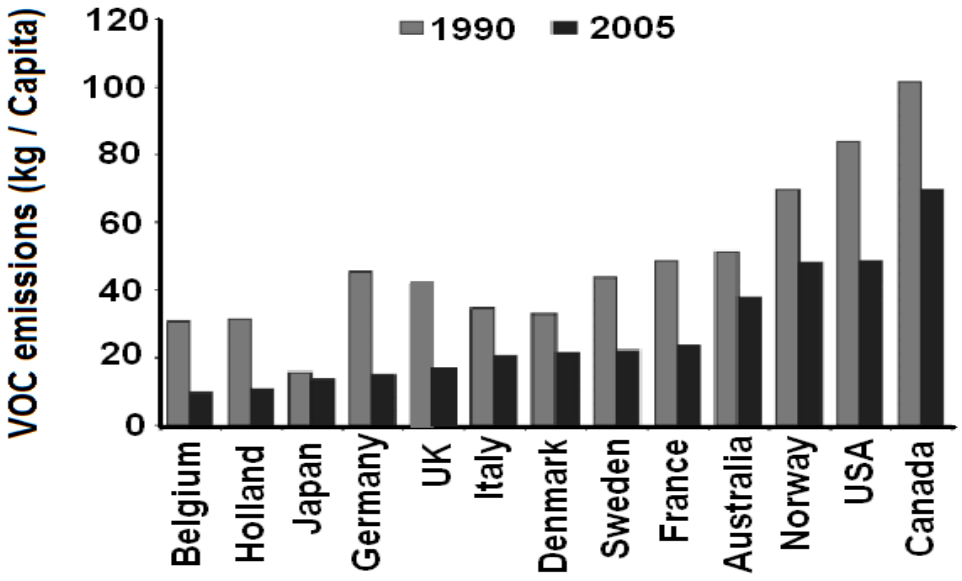

Figure 1.1 – VOC emissions per capita by country (Source: OECD)

Figure 1.2 [Source: Waterleau company - Belgium] summarizes the different techniques to control or recover the VOC. Adsorption is one of the novel techniques used in the remediation process of VOC, which could be used depending on the concentration and flow rate of the gas stream. In this research work the focus will be on recovering the VOCs of concentration ranging from 30 – 50 g.Nm^3. This concentration has been chosen based on the ARKEMA's industrial client belonging to food and hydrocarbon sector. According to the sources from ARKEMA, the flow rate entering the adsorption process ranges from 500 – 10000 Nm^3.hr^{-1}.

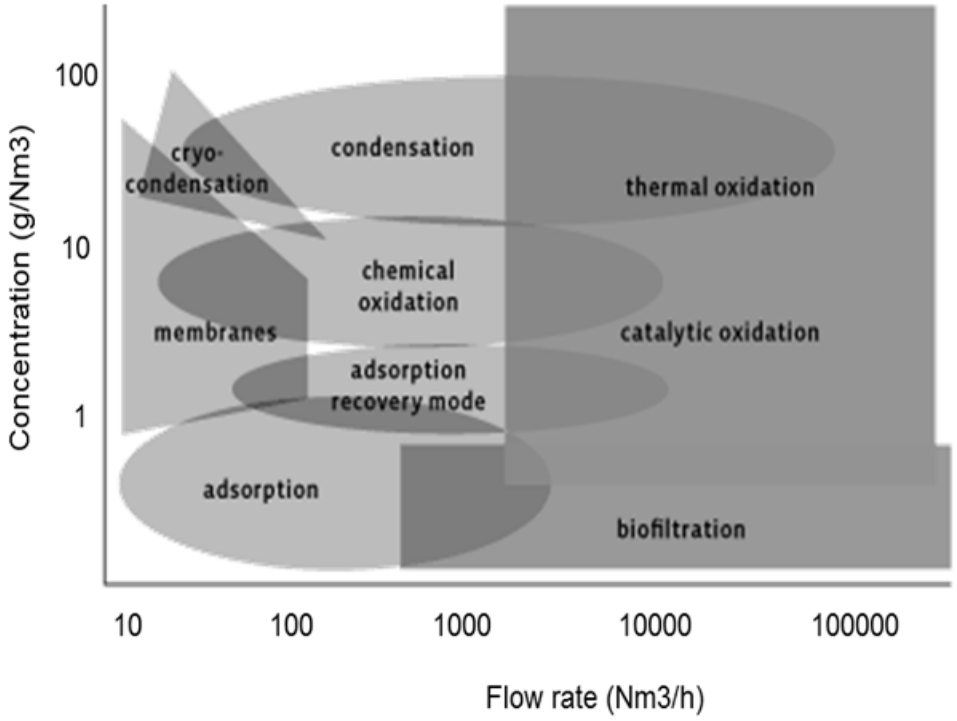

Figure 1.2 – Different techniques for recovery / emission control of VOC (Source: Waterleau)

In the dynamic adsorption and regeneration steps, the activated carbon is the heart of the process to recover the VOCs. According to the Global Industry Inc. activated carbon report (Apr 2011), the consumption of activated carbon keeps on increasing because of their major applications in industries for air treatment and purification. But the needs of activated carbon market in the developing Asian giant countries (like China and India) were already shifted and it would be growing extra-ordinarily in the coming future.

After the adsorption process, the adsorbent can be either regenerated or disposed off based on economics, its use and the kind of adsorbate that was adsorbed. There is a huge amount of risk

involved in exposing the spent absorbent, because they accumulate heat and desorb to air causes a dangerous risk for human health and other living things. Disposing the adsorbent would lead to air, water and land pollution risks. So regeneration of the adsorbent could be considered if it is economically and technically viable. In this research work, a complete investigation of different modes of regeneration such as thermal regeneration (using steam or hot nitrogen gas - TSA), Vacuum Temperature Swing Adsorption (VTSA) has been carried out.

Figure 1.3 shows an example of the adsorption and regeneration of ethyl acetate, which has been used as solvent to extract caffeine from coffee powder. Once the caffeine is extracted, the gas mixture containing ethyl acetate is passed through the adsorption column. At the end of the saturation step, the organic vapors are recovered (by passing hot nitrogen / steam) from the activated carbon bed to reuse it in the caffeine extraction.

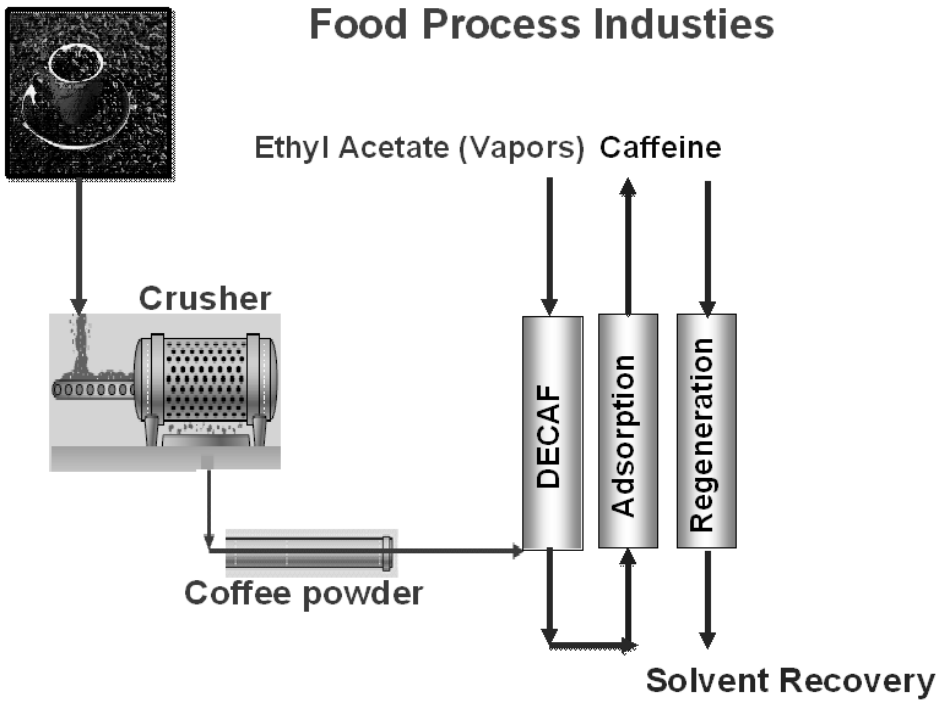

Figure 1.3 –Temperature Swing Adsorption (TSA) application in solvent recovery

The overall objective of the research program is the experimental and simulation studies of the adsorption and regeneration steps in the case of VOC removal which accounts into industrial emissions by Temperature Swing Adsorption (TSA) and Vacuum Temperature Swing Adsorption

(VTSA) processes. This is achieved by the following steps: (1) to establish the isotherm equilibrium data for 5 VOCs and 8 activated carbons at 293, 313, 333, and 353 K (totally 120 isotherm experiments) and then use them in the simulation model; (2) to develop a simulation model for adsorption and regeneration process; (3) to design and optimize the experimental setup of Thermal Swing Adsorption (TSA) which has been established in Ecole des Mines de Nantes; (4) to design and optimize the experimental setup of Vacuum Temperature Swing Adsorption processes (VTSA) which has been established in GRL ARKEMA unit ; (5) Simulation validation of experimental results of TSA and VTSA process. Once after the completion of all the objectives, the goal is to develop and launch a complete simulation package for adsorption and regeneration steps of VOCs with the co-operation from PROSIM Corporation. Figure 1.4 summarizes the different steps involved in this research framework to achieve the goal of developing a simulation tool for the adsorption and regeneration of Volatile Organic Compounds (VOCs).

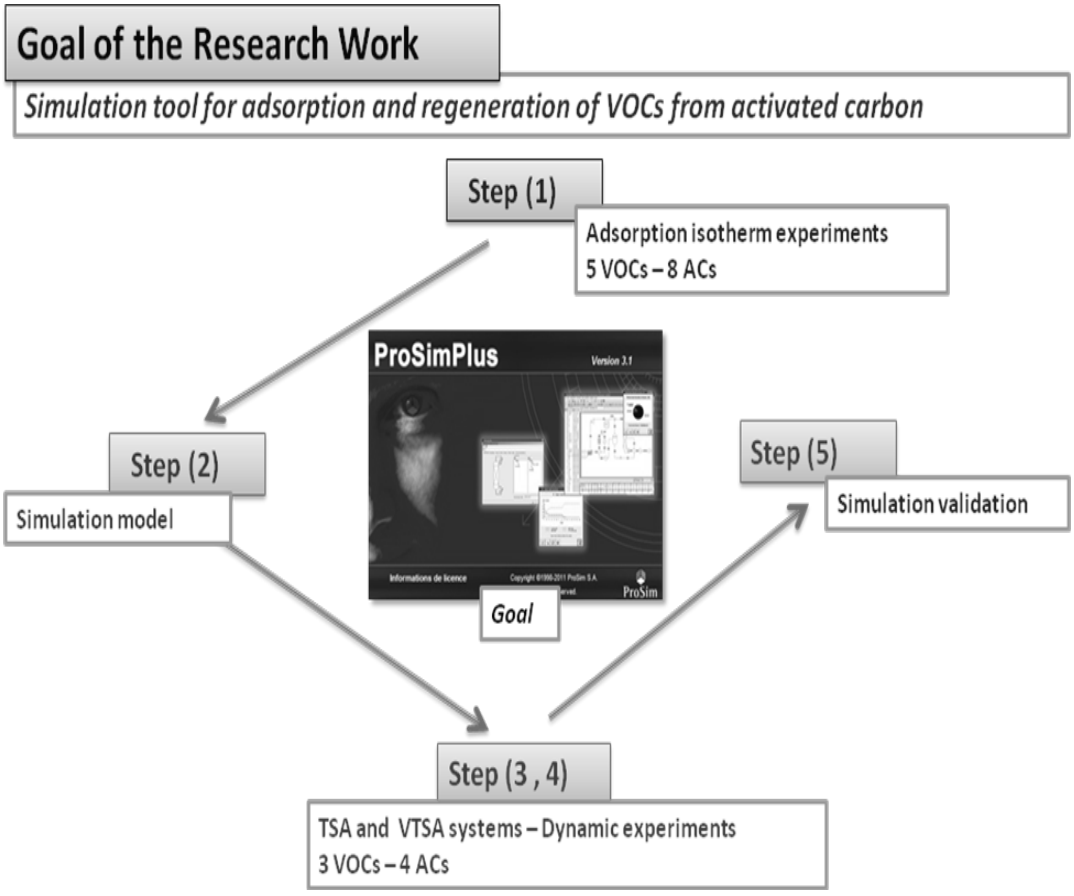

Figure 1.4 – Summary of architecture of the research work

2. Literature Review

2.1. Adsorption of Volatile Organic Compounds (VOCs)

2.1.1. VOC sources and its need for treatment

Industrial emissions of volatile organic compounds (VOC) of different types from gas, oil, paint, solvent and other chemical sectors cause serious health and environmental risks [1-3]. Especially, for example dichloromethane has adverse toxic effects on human central nervous system and environment. And so, the European parliament thus decided to ban its use with concentration equal to or greater than 0.1% weight [4]. Figure 2.1 shows the pie-chart distribution of VOC sources by sectors out of 7500 kt of VOC in the European Economic Area for the year 2009 (Source: European Environmental Agency). With this research work of remediation process (adsorption and regeneration) of VOC, it would be possible to primarily find a solution for the VOC emissions due to: (1) solvent and product use (35.8%); (2) Industrial processes (15.1%).

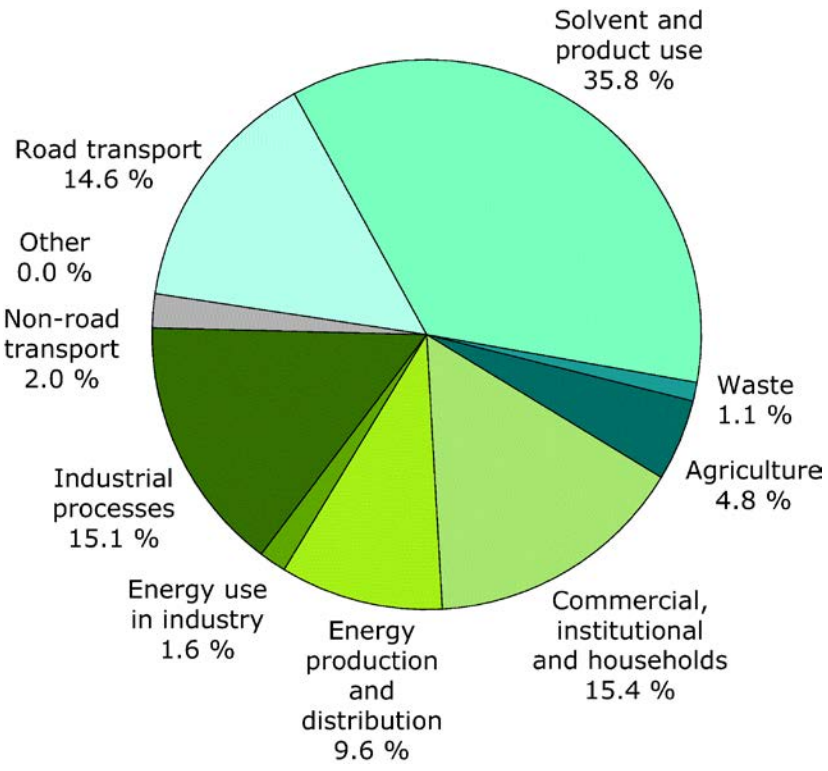

Figure 2.1 – Pie-chart distribution of VOC sources in European Economic Area in 2009

Figure 2.2 shows the change in VOC emissions by sectors from the 1990 – 2008 in the European Economic Area (Source: European Environmental Agency). By primarily remediating the VOC emissions due to (1) industrial processes; (2) solvent and product use, there would be further change in reductions of VOC emissions for the future.

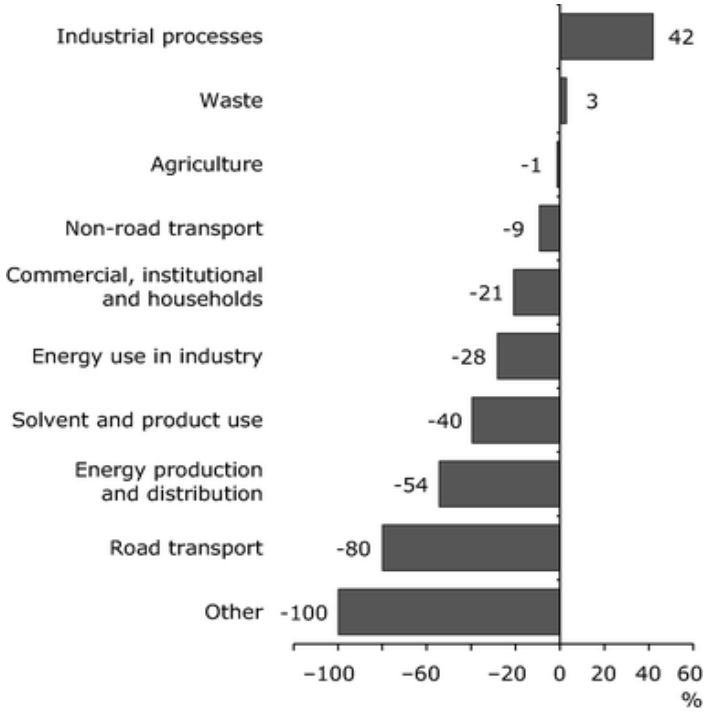

Figure 2.2 - Change in VOC emissions in European Economic Area - by sector (1990-2009)

2.1.2. Adsorption and its mechanism – to control VOC emissions

Adsorption is a phenomenon of combination of diffusions (like Knudsen, molecular and surface diffusions) of contaminants in the surface of granular activated carbon [5-7]. The diffusion of gas molecules inside the pores of activated carbon particles is generally explained by three different mechanisms [8]. Figure 2.3 describes the mechanism of the different diffusion that could occur during adsorption.

- Molecular diffusion;
- Knudson diffusion;

- Surface diffusion

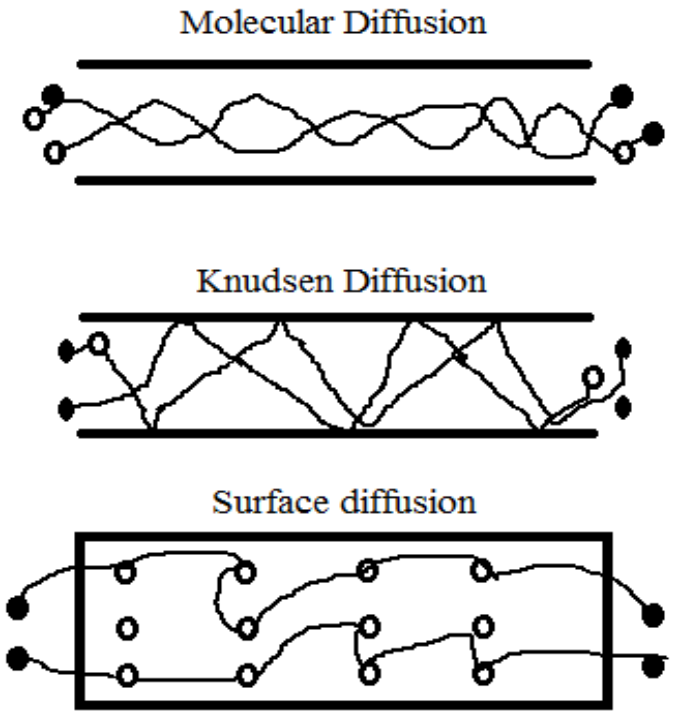

Figure 2.3 – Schematic diagram of different types of diffusion

Theoretically, the three diffusions explain the diffusion phenomenon inside the pore, but the boundaries between these mechanisms are not obvious. The limits depend on the ratio between the size of molecules and the pore size of adsorbent. Moreover, one or more mechanisms may be used during the adsorption process, so it is common to consider the three mechanisms at the same time.

After adsorption, to recover the VOC molecules (contaminants) at higher concentration, a kinetic energy is required in the form of temperature (thermal energy) or vacuum for regeneration. In theory, there will be a repulsion force and weak nuclear force of attraction (due to Van der Waal's force of attraction) between the surface of the adsorbent and the pollutant molecule. There is always a short distance between the surface of adsorbent and the molecule of the VOC and so the potential energy from the nuclear force of attraction makes the molecules to diffuse into the pores of the adsorbent [6-7].

To recover the VOC molecules at higher concentration, it needs kinetic energy in the form of temperature (thermal energy) makes to fly the VOC molecules from the adsorbent bed. Carbon is the first material to have higher surface area with this property [6-7].

2.1.3. Classification of adsorption

Adsorption can be broadly based on the (1) adsorbent concentration; (2) the modes of operation of adsorption [9]. The following section will represent the types of adsorption based on the above criteria.

1. Types based on adsorbate concentration

Based on the adsorbate concentration removal, if the removal of adsorbate is of trace elements (generally upto 1 percent of mass fraction in the feed stream), then it is called purification process. Or the removal of adsorbate present to the higher level (greater than 1 percent of the mass flow fraction percent in the feed stream), and then it is called bulk separation process. The following table shows the industrial examples of the bulk separation and purification process [9].

Table 2.1 - Examples of bulk separation and purification process

Bulk separation process	Purification process
• Normal Paraffin, iso-paraffin, aromatics • N_2/O_2 • CO, CH_4, CO_2, N_2 • Acetone/vent streams • Ethylene/vent streams • Water/Ethanol • p-Xylene, o-Xylene, m-Xylene • p-Diethyl benzene/Isomers mixture • Fructose, Glucose • Detergent range olefins/Paraffin	• Organics/vent streams • Water/natural gas, air, synthesis gas • Sulphur compounds/natural gas, H_2 • VOCs /air • Odours/air • NO_x/N_2 • SO_2/vent streams • Water/organics, oxygenated organics, chlorinated organics • Odor, taste bodies/drinking water

2. Types of mode of operation

Adsorption processes can be classified into two main types: (1) Pressure Swing Adsorption (PSA); (2) Temperature Swing Adsorption (TSA) [9]. Figure 2.4 and 2.5 show the example of the typical example of PSA and TSA processes. PSA process is generally applied when the adsorbate is of higher concentration (> than 1%) of the feed gas and the pressure range is (2 – 20 bars, depending the separation). An example is CO_2 removal from biogas. And, TSA process is applied for concentration of the adsorbate ranging from 1 to 100 $g.m^{-3}$ of the feed gas stream and the temperature range is (120 – 250 °C). An example is the removal of VOCs (ranging from 1 -100 $g.m^{-3}$) in the production of biomethane from landfill waste.

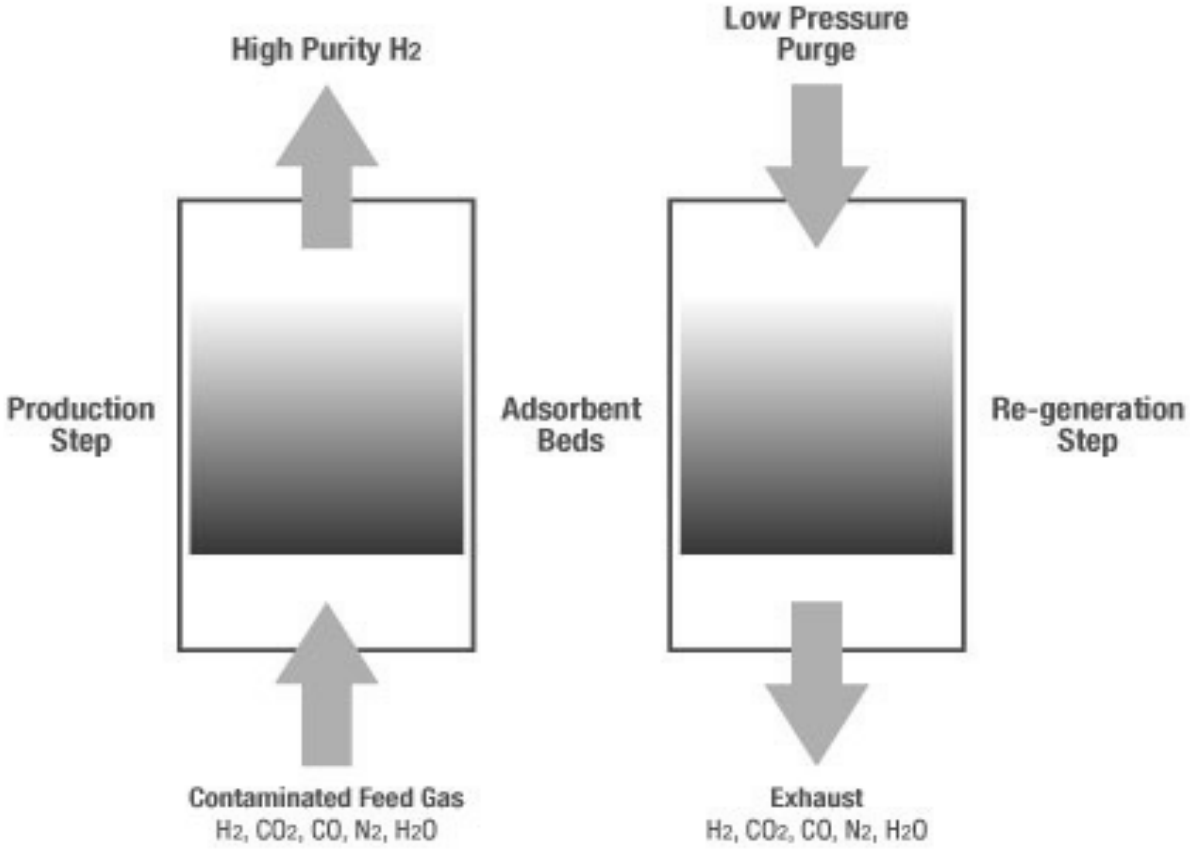

Figure 2.4 – Pressure Swing Adsorption (PSA) for hydrogen production

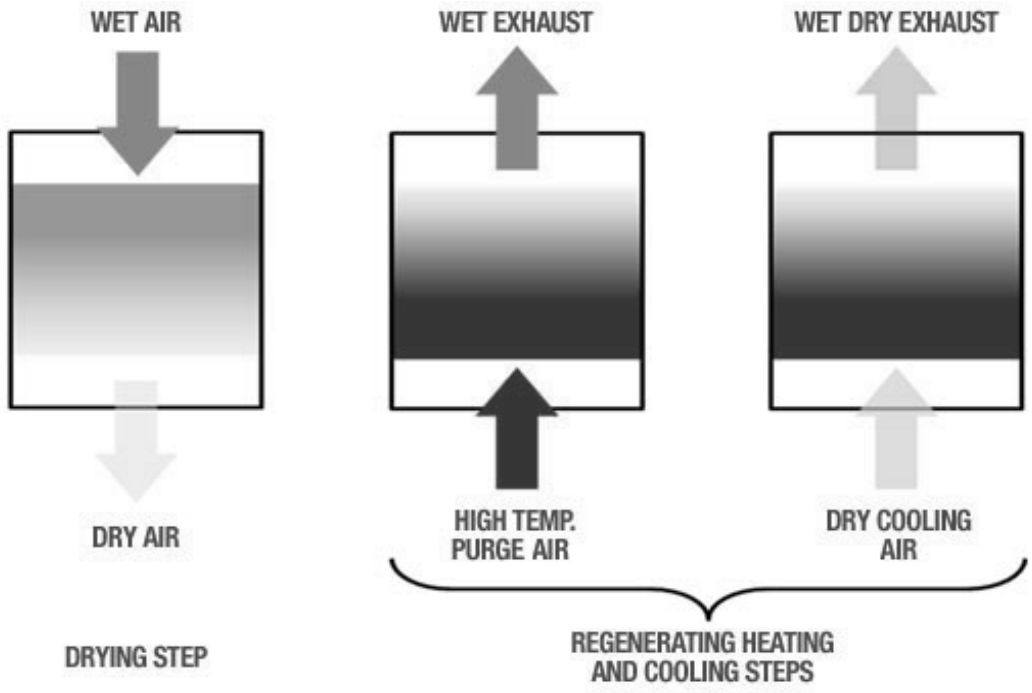

Figure 2.5 – Temperature Swing Adsorption (TSA) for removal of moisture

2.1.4. Adsorption isotherm models

Adsorption isotherms are developed to correlate adsorption equilibrium data for the adsorbent materials characterization and also for the design of the industrial adsorption gas process. Several isotherms have been established (Langmuir, Langmuir-Freundlich, Dubinin-Raduskevich, etc) for VOC – activated carbon systems. The amount of gas adsorbed depends on the pressure, temperature and the interaction between the gas and the solid surface as adsorbent. The adsorbed gas reduces the pressure and results in increase of total volume enclosed in the solid [10]. The plot between mass/volume with the pressure/relative pressure is called adsorption isotherm [IUPAC, 1985] [10].

The simulation of adsorption processes requires adsorption experimental thermodynamic data which can be obtained with difficulties. Adsorption isotherm models have been developed to represent the adsorption equilibrium data in mathematical forms with different theories behind it. The isotherm models are generally derived from the fundamental equation of Gibbs isotherm [11].

Several isotherm models have been established such as Langmuir, Langmuir Freundlich and Dubinin-Radushkevich (DR) to model the adsorption phenomena [11-12].

During dynamic adsorption, the temperature rise at different sections of the adsorbent bed depends on the properties of Volatile Organic Compounds (VOCs), on the characteristics of the adsorbent, and also on the interactions between the VOCs and the adsorbent. The increase in temperature in the adsorbent bed is caused due to the integral amount of adsorption heat. The increase in temperature in the adsorbed bed will decrease the adsorption capacity [13-22].

While constructing a mathematical equilibrium expression for adsorption isotherm, the following factors were considered as important: [23]

- The enthalpy of adsorption;
- The pore size distribution function of the adsorbent;
- The ability of adsorbate to condense within the pore of certain size;
- The adsorbate affinity itself which would have an impact on the thickness of the adsorption layer.

The theories behind the isotherm models have already been extensively discussed in the literature [24-34]. Here the classical models of adsorption are Langmuir isotherm; Langmuir – Freundlich and the Dubinin Radushkevich (DR) isotherm model are summarized from the literature [24-34]. The well known Langmuir model (see equation 2.1) is based on the hypothesis that the adsorbed phase is constituted of a monolayer of adsorbed molecules, the adsorbent surface is energetically homogeneous, there is no interaction between molecules, each adsorbed molecule is located on one adsorption site and each adsorption site could receive only one molecule, and the adsorbed phase is a perfect phase. According to the Van't Hoff law, the affinity coefficient could be expressed as a function of the adsorption enthalpy and the temperature. The equation 2.2 represents the Langmuir-Freundlich isotherm and it has one more additional parameter compare to classical Langmuir model (equation 2). This additional parameter (n) gives more flexibility for the model.

$$q_e = \frac{q_m\, b \exp\left(\frac{H}{RT}\right) C_e}{1 + b \exp\left(\frac{H}{RT}\right) C_e} \qquad (2.1)$$

$$q_e = \frac{q_m\, b \exp\left(\frac{H}{RT}\right) C_e^{1/n}}{1 + b \exp\left(\frac{H}{RT}\right) C_e^{1/n}} \qquad (2.2)$$

q_e is the adsorbed amount (mol kg^{-1}), q_m is the adsorbed amount at saturation, *i.e.* for infinite concentration, H is the adsorption enthalpy variation ($J.mol^{-1}$), T is the temperature (K), R is the perfect gas constant, and C_e is the experimental concentration at the thermodynamic equilibrium ($mol.m^{-3}$).

The Dubinin-Radushkevich (DR) isotherm model is based on the potential theory developed by Polányi and the pore volume filling theory by Dubinin (see equation 2.3).

$$q_e = \frac{W_0}{V_m} . \exp\left(-\left(\frac{RT}{E} \ln\left(\frac{p_s}{p_e} \right) \right)^2 \right) \qquad (2.3)$$

W_0 is the microporous volume that can be filled by adsorbate ($cm^3\ g^{-1}$), V_m is the molar volume of the adsorbed phase ($cm^3\ mol^{-1}$), E is the characteristic energy, *i.e.* the adsorption potential of the couple adsorbent-adsorbate ($J\ mol^{-1}$), and p_s is the vapor saturation pressure of the adsorbate (Pa).

2.2. Regeneration of Volatile Organic Compounds (VOCs)

2.2.1. Definition of regeneration and its mechanism

Regeneration is defined as the process followed by adsorption to remove the organic vapors from the adsorbent either by raising the temperature or decreasing pressure or other driving force such as vacuum [34]. In general, regeneration is of two steps: desorption and drying [35-36]

Drying is a required step particularly in the case of steam regeneration, because there is a possibility of condensed water in the bed; then the condensed water can be removed by passing the hot dry air through the bed. The drying step could be neglected in the case of absence of moisture in the bed. The factors influencing the effectiveness of regeneration are: (i) the degree of purification; (ii) the adsorbent stability, (iii) the degree of recovery of adsorbed components and (iv)energy consumption [35-36].

2.2.2. Types of regeneration

There are two main types of regeneration of VOCs [37-39] which are as follows:

- Thermal Regeneration – by hot nitrogen / steam as heating fluids (TSA)
- Combination of vacuum – hot nitrogen regeneration (VTSA)

2.2.3. Steam regeneration

Steam is readily available in industries and produced by using boiler units at relatively low cost. Steam regenerates very well hydrophobic organics like chlorinated solvents and they are separated by gravity after condensation. Steam is less preferred to hydrophilic contaminants like alcohols, aldehydes, and ketones. If the steam is used for these kinds of VOC, then they are separated by distillation and so it makes the total cost higher [40]. Steam has been proven to be very effective and economical to regenerate activated carbons and hydrophobic zeolites [40]. The temperature distribution along the bed is uniform unlike using purge gas (like nitrogen) for regeneration [40].

The high heat of condensation makes the bed hot and by allowing dry air, it can remove the residual moisture, but still there is some water left in the activated carbon [40]. The temperature is being critical to maintain in steam regeneration and it is a challenge because to remove the some rested moisture from the bed by passing the dry air. Also the time for regeneration has to be optimized, because regeneration time directly links to the energy consumption and it can limit the economics [41]. Regeneration time is defined as the time required for the effluent concentration to reach 1% of feed gas concentration [38].

Drying is one of the most energy intensive steps after the regeneration cycle [36]. The bed has to be made sure that it does not contain any moisture and it involves mainly on the heat loss gradually by passing the dry air at ambient temperature [36]. But it can be overcome by heating the bed constantly and passing the dry air through the bed [36]. The selection of the regeneration temperature depends upon the heat capacity of the adsorbent and the boiling point and solvency of adsorbate [36]. The regeneration of organic compounds (O-chlorobiphenyl, tetrachloroethylene, carbon tetrachloride, p-dichlorobenzene and methyl ethyl ketone) from Ambersorb 563 adsorbent by using steam at 160 °C has been consistent for six cycles [41]. During the drying process after steam regeneration, the strategy of maintaining the heat stored in the bed by an external heat exchanger will help the dry air to remove the moisture in short period of time [42]. Figure 2.5 shows the cycle of steps in recovery of adsorbed molecule [36]. The regeneration of the chloro-organic derivatives are very efficient with steam at 140 °C and the number of cycles of adsorption and desorption does not influence the adsorption capacity [3].

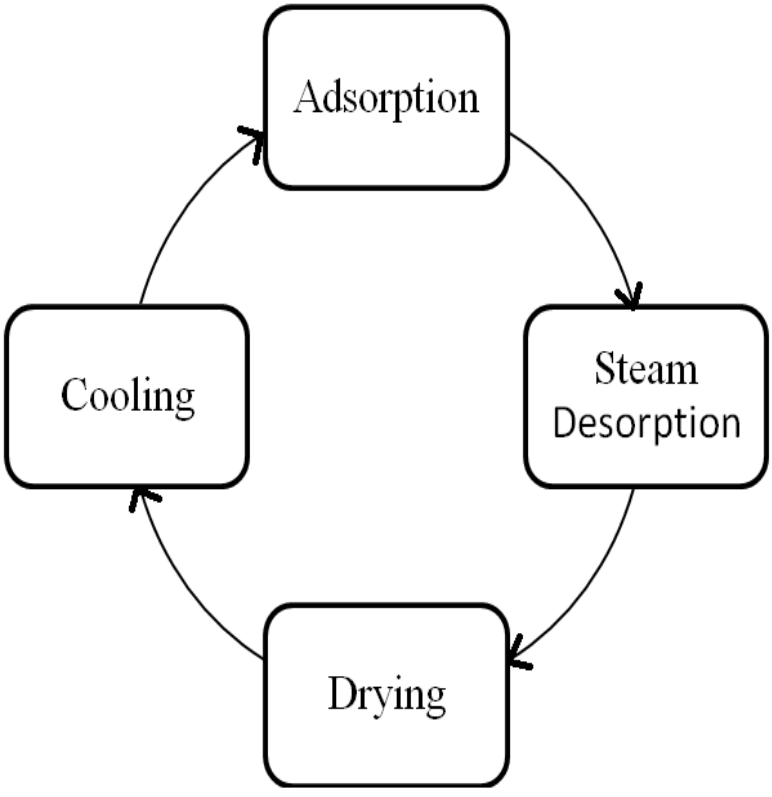

Figure 2.5 - Cycle of adsorption, steam regeneration, drying and cooling

The amount of steam depends on the interaction between the VOCs and the activated carbon [40]. The criteria for selecting the steam mass flow rate depends on the bed pressure drop and is generally kept same as during adsorption step [40]. But the minimum flow rate is essential to reduce the partial pressure of the VOCs in vapor phase and transfer solvent out of the bed [40]. Steam consumption can be expressed in different forms as follows [40]:

- Grams of steam / Grams of VOC desorbed;
- Grams of steam / Grams of adsorbent regenerated;
- Number of bed volumes of steam consumed to regenerate single bed of spent adsorbent

The criteria for finding the mass flow rate of steam are presented as [40]:

- The ratio of mass of steam per mass of adsorbent is in the range of 0.84 and this value can be used in the calculations
- The ratio of steam / VOCs should be at least three

Drying is an important step after the steam regeneration, because the moisture left in the bed can dramatically affect the adsorption capacity and the operational performances [36]. When the bed is hot right after the regeneration, the ambient air is passed through the bed and so that drying is faster at the beginning [36].

To conclude, steam consumption depends on the amount of the carbon, the amount of adsorbed VOC, the reactor dimensions, and adsorbent – VOC interactions. Environmental Protection Agency (EPA, United States) [1996] derived the equation 2.4 for the annual cost of steam (Cs).

$$C_s = 3.5 \text{ x } 10\text{-}3.\ M_{voc}.\ T_o.\ P_s \qquad (2.4)$$

Where, C_s = Steam cost ($\$.yr^{-1}$); T_o = System operating hours ($h.yr^{-1}$); M_{voc} = VOC inlet loading ($kg.hr^{-1}$); P_s = current steam price ($\$.tons^{-1}$). The cost of the steam (P_s) is taken as 120 % of current fuel price. Cost of steam varies with the VOC type, loading concentration and flow rates.

2.2.4. Nitrogen regeneration

The temperature of hot nitrogen is usually in the range of 135 - 160 °C depending upon the VOC to be regenerated. Nitrogen flow rates design is deduced from the literature review based on the amount of flow rates, the flow velocity and dimensions of the bed [19]. In the case of cyclohexanone, nitrogen regeneration had higher regeneration efficiencies in comparison with steam regeneration [35]. Nitrogen regeneration had always kept the bed dry and so the adsorption capacities would not be affected once after the regeneration [35]. The occurrence of bed fires was highly unlikely in the case of nitrogen regeneration compared with the steam regeneration [35].

High temperature regeneration range (700 – 1000 °C) would increase the cost and as well damage the activated carbon leads to decrease in adsorption capacity in the next cycle. In each cycle after regenerating at higher temperatures will lead to 5 – 15% of loss of adsorption capacity and the specific surface area, so it makes the adsorbent useless after several cycles. So the regeneration requires low temperature range (110 – 400 °C) [3]. Thermal regeneration using nitrogen at elevated temperature (140 °C) on the synthesized activated carbon with meso porous silicon supports proved the potential of effective regeneration without affecting the carbon properties [43]. The regeneration is done based on different temperature (75, 120, 130, 140 °C) for different flow rates of mixture of CO_2 and polyethylenimine to optimise the regeneration conditions [43]. Indirect heating by internal heat exchanger in the column and cooling strategy helped in reducing the regeneration time and high purity of VOCs recovered [42]. But the investment cost of heat exchanger, structural heat exchanger design, and energy consumption would be high [42]

Hot nitrogen regeneration had been advised for regenerating poly-ethylenimine based adsorbents, because of formation of urea linkages. These linkages had affected the adsorption capacity in successive cycles [43]. The regeneration studies on Toluene and Acetone were performed using nitrogen as purge gas on the activated carbon BPL at different temperatures (120, 150, 200°C) and different superficial velocities showed significant variation in regeneration of acetone and toluene [44]. Acetone had weaker interaction on the activated carbon than the toluene interactions [44]. Also Toluene has a significantly high boiling point than acetone, so it needs more energy requirement than acetone [44].

2.2.5. Comparison of Steam vs Nitrogen regeneration

Table 2.2 – Comparison - Steam vs Nitrogen Regeneration [35, 45]

Steam Regeneration	Nitrogen Regeneration
Production of steam is readily available in industries and so it is cheaper	It cost 40 – 50 % higher than a steam generation system
Less equipments, less complexity in operation if the steam is readily available in industrial unit	More equipments, more complexity in operation
Maintenance cost is lower	Maintenance cost is high
Recovery efficiencies can be lower in case of presence of moisture	Recovery efficiencies can be high because N_2 will not affect the bed in case of cooling
Drying is intensive and adds regeneration time and energy	Drying is not intensive, because of no moisture
Possible hydrolysis of regeneration	Weak transformation of the regenerate

2.2.6. Combined vacuum-hot nitrogen regeneration

The use of vacuum regeneration followed by thermal regeneration is more relevant than vice versa in terms of achieving final regeneration percentage [37,46,47]. During the vacuum regeneration, a small velocity of nitrogen 0.05 $m.s^{-1}$ and a pressure of 0.04 bars are used [37,46,47].

2.3. Simulation model for adsorption and regeneration cycles

The adsorption-desorption process was described by first deriving the mass and energy balances for each step, accounting for the axial dispersion of mass and heat. Radial velocity, temperature and concentration gradients were assumed as negligible. The main equations and their respective assumptions used are described below [8,19,21,37].

Mass balance

The following are the assumptions for fluid dynamics and properties of the systems [8,19,37]

- Uniform bed voidage ;
- Negligible pressure drop through the fixed bed;
- Constant superficial velocity of the gas-phase;
- Lumped dispersion mechanisms;
- Gas-phase density and specific heat equal to those of air;
- Densities and heat capacities of the different phases independent of temperature;

The following are the assumptions for the mass transfer in the system:

- Carrier gas in adsorption is negligible;
- No radial mass transfer in the column

The partial mass balance equation expresses that the change in the concentration of the VOC in the gas phase along the column results from its transport in the gas flowing and from the accumulation of the adsorbate in the solid phase:

$$-D_L \frac{\partial^2 C_i}{\partial z^2} + \frac{\partial (vC_i)}{\partial z} + \frac{\partial C_i}{\partial t} + \frac{1-\varepsilon}{\varepsilon} \rho_p \frac{\partial q_i}{\partial t} = 0 \qquad (2.5)$$

q_i – VOC concentration in the adsorbed phase, $mol.kg^{-1}$; C_i –VOC concentration in the gas phase, $mol.m^{-3}$; ε – bed porosity; ϱ_p – bulk adsorbent density, $kg.m^{-3}$; D_L – axial mass dispersion coefficient, $m^2.s^{-1}$; v – superficial velocity, $m.s^{-1}$

Linear driving force model (LDF)

The adsorption and desorption rates are described according to the Linear Driving Force (LDF) model [8,19,37]. According to this model, the mass transfer kinetics is represented as a function of a global mass transfer coefficient K, weighting a potential difference between the actual amount of VOC adsorbed qi and the amount that would be obtained at the equilibrium qi*:

$$\frac{\partial q_i}{\partial t} = K.(q_i^* - q_i) \qquad (2.6)$$

q_i – adsorbed VOC concentration, $mol.kg^{-1}$; K – global mass transfer coefficient, s^{-1}; qi^* - adsorbed VOC concentration at the equilibrium with the gas phase, $mol.kg^{-1}$;

The global resistance to the mass transfer embodies the partial resistances to the transfer of the gas at the external surface of the particles and within the intra-granular porous volume. Assuming a combination in series of the external and internal mass transfer resistances, the following expression can be proposed [4]:

$$K = \gamma \exp\left(\frac{0.45\,\Delta H_{ads}}{RT}\right) \qquad (2.7)$$

γ - adjustable coefficient (s^{-1}); D_S - surface diffusivity ($m^2.s^{-1}$) ; ΔH_{ads} - heat of adsorption ($J.mol^{-1}$)

The effective diffusion coefficient takes into account the various elementary diffusion mechanisms which control the migration of the organic component to the adsorption sites (porous, Knudsen, and surface diffusion). It is here considered as one adjustable parameter, which remains unchanged whatever the sense of migration of the molecules, towards or backwards the adsorption sites.

Equilibrium model

The Linear Driving Force model requires the knowledge of the concentration distribution in the gas and in the solid phases at the equilibrium, at the operating temperature and pressure. The isotherm model used are Langmuir and multi-temperature Toth's equation [8,19,37].

Energy balance equation

The following are the assumptions involved in the energy balance of the system [8,19,37].

- Instantaneous local temperature equilibrium between gas and solid phases;
- Mean heat of adsorption, independent of the amount of VOC adsorbed;

- No radial heat transfer

The change in the enthalpy of the gas phase results from the heat transfers by convection and conduction with the solid particles and with the reactor walls:

$$-D_H \frac{\partial^2 T}{\partial z^2} + v\,\rho_g Cp_g \frac{\partial T}{\partial z} + \left(\varepsilon\rho_g Cp_g + \rho_{bed} Cp_s + \rho_{bed} C_{P_A} q\right)\frac{\partial T}{\partial t} = \rho_{bed}\left(-\Delta H_{ads}\right)\frac{\partial q}{\partial t} + 4\frac{h}{d_c}\left(T - T_0\right) \qquad (2.8)$$

D_H - coefficient of dispersion of heat ($W.m^{-1}.K^{-1}$); T - temperature (K); ϱ_g - gas-phase density ($kg.m^{-3}$); Cp_g - gas-phase heat capacity ($J.kg^{-1}.K^{-1}$); Cp_s - solid-phase heat capacity ($J.kg^{-1}.K^{-1}$); Cp_A - adsorbed-phase heat capacity ($J.mol^{-1}.K^{-1}$); ΔH_{ads} - heat of adsorption ($J.mol^{-1}$); h - coefficient of heat transfer ($W.m^{-2}.K^{-1}$); T_0 - ambient temperature (K)

The heat transfer coefficient of gas to the adsorption wall (h) is calculated by the correlation Leva's correlation [48].

The adsorption enthalpy was derived according to the following statistical predictive model established [8, 21].

$$-\Delta H_{ads} = 103.2 + 1.16\alpha + 0.76\Delta H_{vap} - 3.87PI - 0.7\gamma - 26.19r_{mic} \qquad (2.9)$$

α - VOC polarisability 10^{-24} cm^3; ΔH_{vap} - latent heat of vaporisation $kJ.mol^{-1}$; *PI* - VOC ionisation potential (eV) ; γ - surface tension of the liquid solvent ($mN.m^{-1}$) - r_{mic}, adsorbent average micropore opening (nm).

Ergun equation

The Ergun equation was introduced in the model in order to describe the total pressure drops occurring in the system [8, 19,37].

$$\frac{\partial P}{\partial z} + 150.10^{-5}\left(\frac{1-\varepsilon}{\varepsilon}\right)^2 \frac{\mu}{d_p^2} v + 1.75.10^{-5}\left(\frac{1-\varepsilon}{\varepsilon}\right)\frac{\rho_g}{d_p} v^2 = 0 \qquad (2.10)$$

μ – dynamic viscosity, Pa.s; ϱ_p – bulk adsorbent density, $kg.m^{-3}$; d_p – equivalent particle diameter, m ; ε - bed voidage.

Numerical solving method

The model is composed of a set of fours partial differential equations (PDEs) describing the conservation laws: mass, energy and momentum transfer. The PDE set was first reduced to a set of ordinary differential equations (ODEs) using the method of lines - spatial discretization with finite differences [8, 37]

2.4. Factorial Experimental Design (FED) for optimization of regeneration

FED is a statistical analysis which helps to study the influence of the operating conditions on the desired responses to be measured [49]. FED also reduces the number of experiments when it comes to measure the influence of more than two factors [49]. Figure 1 shows the different combination of two different operating conditions (X_1, X_2) in an experiment and the signs (-, +) corresponds to minimum and maximum of the operating conditions [49]. The final response is measured as 'Y'. By using FED method in MINITAB, the analysis of variance (ANOVA) can be performed to obtain a response equation (Y) which is in linear form with the function of operating conditions (X_1, X_2) [49]. The main effect of each factor is computed by first subtracting the average of the results of maximum level (+) to the average of the results of the minimum level (-) and then divided by the total number of factors in the experiment [49]. The interaction effect ($X_1.X_2$) is computed by again subtracting the average of the results of maximum level combination to the minimum level combination [49]. For example, the product of an operating condition design (+, +) and (-, -) are considered as the maximum level combination.

$$Y = a_o + a_1.X_1 + a_2.X_2 + a_3.X_1.X_2 \qquad (1)$$

Y – Measured response; X_1, X_2 – operating conditions; a_0, a_1, a_2, a_3 – constants

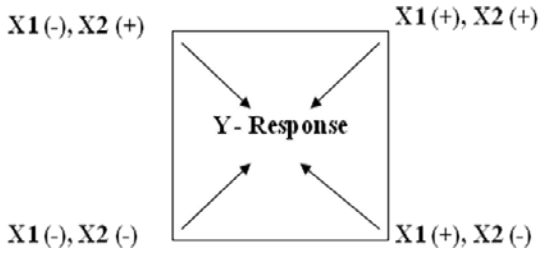

Figure 2.6 – Factorial Experimental Design (FED) representation

At the end of the analysis of variance in MINITAB software, the probability value p(f) has to be checked that it is less than 10% [49]. This shows that the the data obtained by the statistical analysis is significant with a confidence of interval 90% [49. If not, then the linear equation obtained in invalid [49]. If the statistical analysis is not successful, then a central point (0,0) in the operating conditions in an experimental design is chosen to measure the response. And then the error percentage on the response is estimated between the experimental and statistical results to consolidate the ANOVA equations.

2.5. Conclusion

A good approach to have an effective VOC regeneration from the literature review: (1) choosing a high performing activated carbon in terms kilograms of VOC adsorbed per kilogram of activated carbon; (2) knowing the solvent is soluble or non soluble in water. If the solvent is very soluble in water, then the nitrogen regeneration should be evaluated thoroughly with steam regeneration, because of account of additional cost of separation and purification in steam regeneration. On the contrary in nitrogen regeneration, there will be advantage of having only separation cost (as it is inert) and there is no need of drying step; (3) understanding and optimizing the influence of operating conditions on the regeneration performance and the operating cost is very critical.

With this approach, this research work had been developed in different steps such as (1) to characterize the activated carbon (such as BET surface area, micropore volume, bulk density and other properties); (2) to carry out the adsorption isotherms of VOCs on different activated carbons to choose the right activated carbon material; (3) the operating conditions are optimized by nitrogen regeneration and VTSA are optimized using FED to have high regeneration performance at an optimized cost; (4) to develop and improve the simulation model based on the experiments carried out in TSA and VTSA processes. All this approach had been carefully implemented in each dimension of this research work. The materials and methods, experimental setup and the results are discussed in length in the following chapters.

References

[1] EUR-lex. Access to European law. Directive 2004/42/ECof the European Parliament and of the Council, Apr 2004, http://eur-lex.europa.eu/en/index.htm, accessed: 19 Jun 2011

[2] U.S. Environmental Protection Agency. Office of Pollution Prevention and Toxics (OPPT). Dichloromethane fact sheet - EPA 749-F-94-018, Aug1994, http://www.epa.gov/chemfact/f_dcm.txt, accessed: 19 Jun 2011

[3] K.S. Hwang, D.K. Choi, S.Y. Gong, S.Y. Cho, Adsorption and thermal regeneration of methylene chloride vapor on activated carbon bed, Elsevier – Chemical Eng. and Pro. 46 (1998) 1111 -1123

[4] European Parliament. Health and Environment. Dichloromethane to be banned in paint-strippers. REF: 20090113IPR46095, Jan 2009, http://www.europarl.europa.eu, accessed : 19 Jun 2011

[5] M. Worrall, AMNEC Inc., Case studies on capturing organic vapors from non-condensable gases using activated carbon technology, Jan 1998

[6] The Brownfields and Land Revitalization Technology Support Center [BTSC], U.S. EPA, Argonne National Laboratory, and the U.S. Army Corps of Engineers) – Definitions, http://www.brownfieldstsc.org

[7] C.L. Cavalacante et al., Industrial Adsorption Separation Processes: Fundamentals, Modeling and Applications and applications, Latin American Applied Research 2000; 30:357-64

[8] S. Giraudet, Exothermicity of adsorption of volatile organic compounds in fixed activated carbon beds: modelling and simulation valdiation of experimental work, PhD dissertation, EMN, France, 2006

[9] EPA Technical Bulletin Report, "Choosing an Adsorption system for VOC"; Clean Air Technology Centre (CATC), May 1999

[10] T. Jayabalan, Study of oxidation of carbon materials, Ph.D. Dissertation, Ecole des Mines de Nantes, France, 2008

[11] Jürgen, S. Reiner, Gas Adsorption Equilibria, Springer publications, USA, 1994

[12] D.M. Ruthven, Principles of adsorption and adsorption processes, John Wiley & Sons: New-York, Univ of New Brunswick: Fredericton, USA, 1984

[13] P. Pré, F. Delage, P. Le Cloirec. A model to predict the adsorber thermal behavior during treatment of volatile organic compounds onto wet activated carbon. Environ Sci Technol 2002; 36:4681-88

[14] F. Delage, P. Pré, P. Le Cloirec. Mass transfert and warming during adsorption of high concentrations of VOCs on an activated carbon bed: experimental and theoretical analysis. Environ Sci Technol 2000; 34:4816-21

[15] P. Pré, F. Delage, P. Le Cloirec. Modeling the exothermal nature of V.O.C. adsorption to prevent activated carbon bed ignition. In: Fundamentals of Adsorption 2001; 700-7

[16] E. Fiani, L. Perier-Cambry, G. Thomas. Non-isothermal modelling of hydrocarbon adsorption on a granulated active carbon. J Therm Anal Cal 2000; 60:557-70

[17] L. Yong, K. Sumathy. Comparison between heat transfer and heat mass transfer models for transportation process in an adsorbent bed. Int J Heat Mass Transfer 2004; 47:1587-98

[18] L. Luo, M. Bailly. Gestion de la thermique dans les procédés d'adsorption de gaz, Rev Gén Therm 1996; 35:693-7

[19] J.H. Yun, D.K. Choi, H. Moon. Benzene adsorption and hot purge regeneration in activated carbon beds. Chem Eng Sci 2000; 55:5857-72

[20] H.J. Bart, R. Germerdonk, P. Ning. Two dimensional non-isothermal model for toluene adsorption in a fixed-bed adsorber. Chem Eng Processing 1996; 35:57-64

[21] S. Giraudet, P. Pre, H. Tezel, P. Le Cloirec. Estimation of adsorption energies using physical characteristics of activated carbons and VOCs molecular properties. Carbon. 2006; 44: 1873-83

[22] D.P. Paulsen, F.S. Cannon. Polytherm model for methylisobutylketone adsorption onto coconut based granual activated carbon. Carbon. 1999; 37: 249-63

[23] G.O. Wood. Affinity coefficients of the Polanyi /Dubinin adsorption isotherm equations: a review with compilations and correlations. Carbon. 2001; 39:343–56.

[24] G.O. Wood. Review and comparisons of D/R models of equilibrium adsorption of binary mixtures of organic vapors on activate carbons. Carbon. 2000; 40:231-39

[25] C. Nguyen, DO DD. The Dubinin – Raduskevich equation and the underlying microscopic adsorption description. Carbon. 2000; 39:1327-336

[26] R.J. Dombrovski, C.M. Lastoskie, D.R. Hyduke. The Horvarth-Kawazoe method revisited. Colloids and Surfaces, A: Physicochemical and Engineering Aspects 2001;187-188:23-39.

[27] V.K. Dobruskin. Contribution of the edge effect to physical adsorption in micropores of activated carbons. Carbon 2002; 40:659-66.

[28] V.K. Dobruskin. Micropore structure of activated carbons and predictions of adsorption equilibrium. Carbon 2002; 40:1003-10.

[29] J. Wu, L.G. Hammarstrom, O. Claesson, I. Fangmark. Modeling the influence of physico-chemical properties of volatile organic compounds on activated carbon adsorption capacity. Carbon 2003;41:1322-5.

[30] A.M. Tolmachev, O.I. Trubnikov. Molecular models for vapor adsorption on microporous adsorbents. Carbon 2002; 40:1401-7.

[31] J.A. Schwarz, C.I. Contescu. Surfaces of nanoparticles and porous materials. Surfactant Sci Series, Marcel Dekker: New-York, USA, 1999

[32] Y. He, J.H. Yun, N.A. Seaton. Adsorption equilibrium of binary methane/ethane mixtures in BPL activated carbon: isotherms and calorimetric heats of adsorption. Langmuir 2004; 20:6668-78

[33] S. Giraudet, P. Pre, P. Le Cloirec. Modeling the Heat and Mass Transfer in Temperature Swing Adsorption of Volatile Organic compounds on to Activated Carbons. Env. Sci. and Tech 2009; 43:1173 – 179

[34] L.K. Wang, N.C. Pereira, Y.T. Hung. Air pollution control engineering. Humana press, Totowa, New Jersey. Volume 1, 2004

[35] R.C. Nattkemper, Nitrogen Vs Steam Regeneration in activated carbon systems, American Carbon Society, Imation Corp., Camarillo, CA 93012, Jul 1997

[36] J. Gu, N. M. Faqir, H.J. Bart, Drying of an Activated Carbon Column after Steam Regeneration. Wiley Publications - Chemical Eng. and Tech. 1999, 22:859-64

[37] J.F. Nastaj, B. Ambrożek, J. Rudnicka, Simulation studies of a vacuum and temperature swing adsorption process for the removal of VOC from waste air streams, Elsevier – Interna. Comm. of heat and mass transfer. 2006; 33: 80 - 6

[38] R.H. Zanitsch, R.T. Lynch, Carbon Adsorption Handbook, Selecting a Thermal Regeneration System for Activated Carbon, Calgon Carbon Corporation, 1997

[39] R.T. Yang, Adsorbents: fundamentals and applications, John Wiley & Sons pub., New Jersey, 2003

[40] J. Kuntzel, R.Ham, T.Melin. Steam regeneration of hydrophobic zeolites, Chemie Ingenieur Technik, 1999; 7:71 - 76

[41] J.S.J. Van Deventer, B.S. Camby, The influence of Regeneration conditions on the adsorptive behavior of activated carbon, Mineral Engg., 2003

[42] J. Bonjour, J.B. Chaflen, F. Meunier, TSA process with indirect cooling and heating, I& EC research, 2002, 41:5802-811

[43] T.C. Drage, A. Arenillas, K.M. Smith, C.E. Snape, Thermal stability of polyethylenimine based carbon dioxide adsorbents and its influence on selection of regeneration strategies, Microporous and Mesoporous Materials, 2008, 116:504-12

[44] J. Kim, S. Lee, M. Kim, J. Lee, C. Lee, Sorption equilibrium and thermal regeneration of acetone and toluene vapours on an activated carbon, I&EC Research, 2007, 46:4584-594

[45] S.G. Ramalingam, P. Pré, S. Giraudet, L. Le Coq, P. Le Cloirec, O.Baudouin, S.Déchelotte, Recovery comparisons - Hot Nitrogen Vs Steam regeneration of toxic dichloromethane from activated carbon beds in oil sands process, Journal of Hazardous Materials, 2012; 205-206:222-28

[46] T. Boger, A. Salden, G. Eigenberger, A combined vacuum and temperature swing adsorption process for the recovery of amine from foundry air, Elsevier - Chemical Eng. and Pro.,1997, 36:231-42

[47] S.G. Ramalingam, J. Saussac, P. Pré, S. Giraudet, L. Le Coq, P. Le Cloirec, S. Nicolas, O. Baudouin, S. Déchelotte, A. Medevielle, Hazardous Dichloromethane recovery in combined temperature and vacuum pressure swing adsorption process, Elsevier – Journal of Haz. Materials 2011; 198:95-102

[48] R.H. Perry *et al.*, Perry's Chemical Engineers Handbook, McGraw-Hill, New York, 2007

[49] P.M. Berthouex., L.C. Brown, Statistics for Environmental Engineers, Second ed., Lewis Publishers, USA, 2002

3. Experimental and Modeling of adsorption isotherms

Adsorption isotherm equilibrium data are very essential in the dynamic simulation model [1-4]. These equilibrium data has been modeled to fit the different equilibrium isotherm models such as Langmuir, Langmuir-Freundlich and Dubinin Raduskevich for determining their corresponding coefficients [5-9]. So the isotherm equilibrium models are directly used in the dynamic simulation model.

3.1. Adsorption isotherm experimental and modeling procedure

3.1.1. Objectives

The objectives of performing the adsorption isotherm experiments are: (1) experimental modeling (by statistical analysis using R-STAT) of isotherm equilibrium data to find out the coefficient of different isotherm models; (2) establishing Multiple Linear Regression (MLR) models (by using statistical analysis software MINITAB) for the coefficients of the Langmuir and Dubinin Raduskevich isotherm models. The MLR models were developed based on the properties of the VOCs and the characteristics of the activated carbons; (3) these MLR models results are validated by comparing with the experimental results of the coefficients which are obtained by modeling with R-STAT; (4) these MLR models are then implemented in the dynamic adsorption simulation model called PROSIM. This implementation would enable the dynamic simulation PROSIM to be less complex and more efficient.

3.1.2. Selection of VOCs and Activated Carbons

The choice of 5 VOCs and 8 activated carbons was made to cover the wide range of critieria such as (1) nature of family of VOCs; (2) properties of VOCs; (3) the VOCs which are handled in chemical industries (for example as solvents / directly used in chemical reactions); (4) characteristics of the activated carbons; (5) mode of activation of activated carbons; (6) raw material of activated carbons; (7) manufacturer of the activated carbons. Table 3.1 shows the selected VOCs and their physical properties which were essential to establish the MLR models. The selected VOCs are (1) acetone; (2) dichloromethane; (3) ethyl formate; (4) ethanol and (5) toluene.

Chapter 3 – Experimental and modeling of adsorption isotherms

The physicochemical properties of VOCs are used in the dynamic simulation model and also in the modeling section of adsorption isotherms [10].

3.1 – Physicochemical properties of volatile organic compounds

Compounds	Family nature	Molecular weight	Ionization Potential	Polarisability	Dipole moment	Surface tension	Parachor
		(g mol^{-1})	(eV)	(10^{-24} cm^{-3})	(Db)	(mN.m)	$cm^{-3}.g^{0.25}.s^{-0.5}.mol^{-1}$
Dichloromethane	Chloro	84.93	11.32	5.4	1.55	27.89	147.9
Toluene	Aromatic	92.14	8.86	12.3	0.37	27.9	244.6
Ethanol	Alcohol	46.07	10.47	5.4	1.69	22	128.3
Ethyl Formate	Ester	74.08	10.61	8.0	1.9	23.18	177.6
Acetone	Ketone	58.08	9.71	6.4	2.88	23.46	162.8

3.1.3. Characteristics of activated carbon

(a) Mercury Porosimetry

In 1921, Wasburn introduced the technique of using mercury with pressure to determine the macro and meso pore volumes of activated carbons. The pressured mercury fills the meso and macro pores in the activated carbon and mercury has the ability to form a contact angle more than 90° with the most carbons. From this technique, the bulk density, total pore volume and the surface area distribution are measured [11-12].

Apparent density can be defined as the weight of the solid divided by the volume of the solid included with the internal pores of the solid. True density is defined as the ratio of weight of the solid divided by the volumes of the solid with exclusion of volume of pores and internal voids. All the experiments are carried out by the using Micrometrics Auto pore IV 9500 mercury porosimeter analyzer. There are basically two types of analysis carried out and they are high pressure analysis and low pressure analysis. The pressure applied is inversely proportional to the size of the pores. The pressure and the diameter ranges for high pressure and low pressure analysis are as follows:

Low pressure Analysis:

Diameter range: 200 – 3.6 μm

Pressure: 0 – 4 bar

High Pressure Analysis:

Diameter range: 8 – 200 μm

Pressure: 1 – 2230 bar

(b) Nitrogen Adsorption Analysis

The primary idea of passing the nitrogen gas is to fill the micropores in the activated carbon and the amount adsorbed depends on the pressure, temperature and the interaction of adsorbate – adsorbent. The characteristics of the activated carbons such as BET surface area, micro pore volume (by Horvath-Kawazoe method) are measured by performing nitrogen adsorption isotherm at 77 K [13]. The microporous volume is calculated for the size of pore less than 2 nm [13]. The Table 3.2 summarizes their characteristics.

Table 3.2 – Characteristics of activated carbons

Producer	Commercial name	Raw Material	Activation Mode / agent	Bulk Density	Micro pore Volume	Meso+ macropore volume	BET Surface Area
				($mg.l^{-1}$)	($cm^3.g^{-1}$)	($cm^3.g^{-1}$)	($m^2.g^{-1}$)
Pica	BC 120	Wood	Chemical/H_2SO_4 (H_2O)g	0.26	0.82	0.36	1687
Norit	GF 40	Olive Stone	Chemical/H_2SO_4 (H_2O)g	0.38	0.80	0.38	1881

Ceca	ACV 404	Coconut	Physical/$H_2O_{(g)}$	0.53	0.54	0.60	1256
Pica	NC 100	Coconut	Physical/$H_2O_{(g)}$	0.30	0.54	0.48	1617
Pica	ACM 404	Coal	Physical/$H_2O_{(g)}$	0.42	0.44	0.55	1063
Chemviron	BPL	Coal	Physical/$H_2O_{(g)}$	0.50	0.40	0.44	955
Ceca	ACM 204	Coal	Physical/$H_2O_{(g)}$	0.59	0.34	0.38	698
Pica	NC 60	Coconut	Physical/$H_2O_{(g)}$	0.47	0.43	0.31	1028

The above all experiments for determining the characteristics of the activated carbon have been repeated for three times to have the consistency of error percent less than 10%.

3.1.4. Adsorption isotherm measurements and error propagation

The volumetric apparatus used to perform measurement is described by Figure 3.1. The activated carbon must be dried at 120 °C for 48 hrs for the moisture remove before experiments. 0.2 g of each activate carbon is put in ten glass reactors of 2.1 L size. A known volume of VOC was injected in glass reactors in the range of 20-400 μL. After equilibrium is reached, a part of the gas phase was sampled and analyzed using a gas chromatograph to establish the VOC gas phase concentration (C_e). The adsorbed amount of VOC was determined by mass balance according to equation 3.1 where C_0 is the injected VOC concentration, V is the volume of the reactor containing the AC, and m is the adsorbent mass [14].

$$q_e = \frac{(C_0 - C_e)V}{m} \qquad (3.1)$$

The above procedure has been followed for the 5 VOCs – 8 activated carbon systems to establish the isotherm equilibrium data at 293, 313, 333, and 353 K. So there are totally 120 isotherms have been performed, in which 60 isotherm equilibrium data have been taken from the previous research work [15].

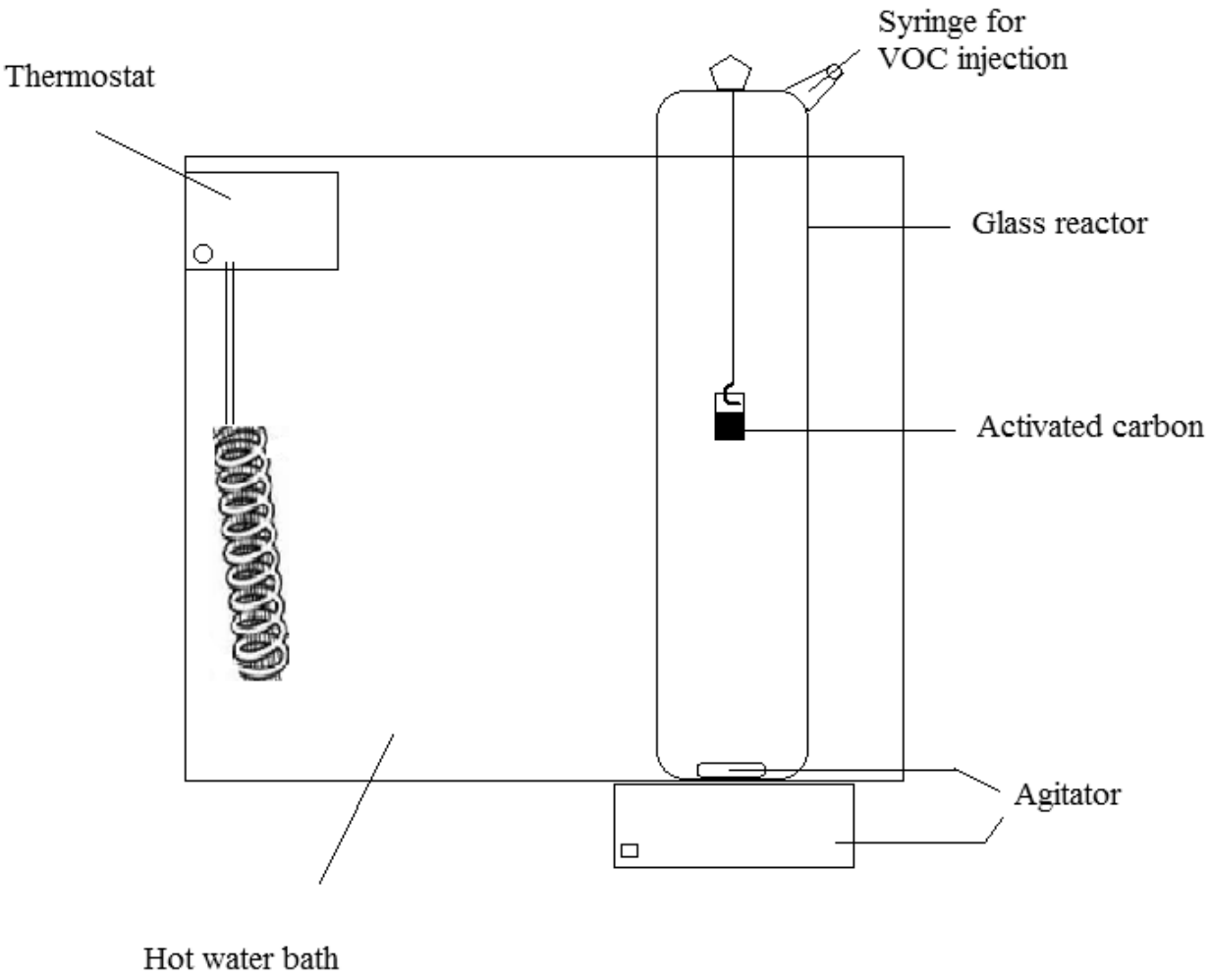

Figure 3.1 – Adsorption isotherm experimental setup

The error bars for the isotherm measurement are calculated by using the classical error propagation method [15]. Figure 3.2 summarizes the procedure for the calculation of the errors on the measurement of adsorption capacity (q_e) at equilibrium. The errors were based on the accuracy of: (1) mass of activated carbon (m); (2) measurement of equilibrium concentration (C_e); (3) volume of the reactor (V_{tank}) [15].

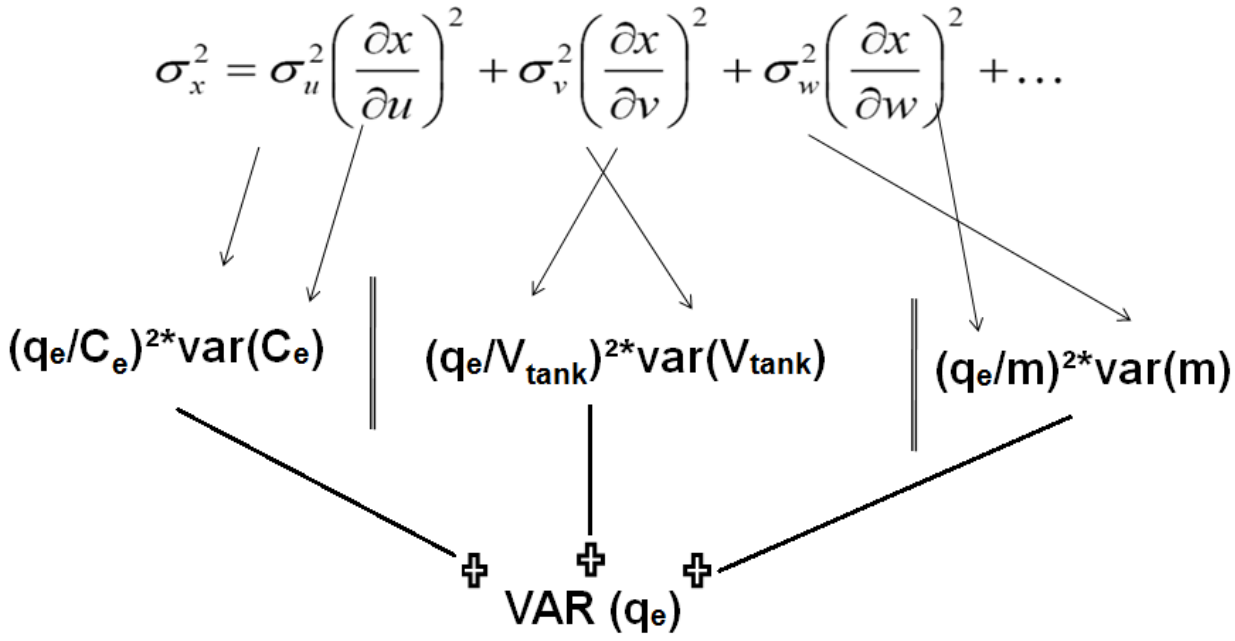

Figure 3.2 – Error propagation method on adsorption isotherm measurements

3.1.5. Selection of adsorption equilibrium models

In Table 3.3, the classical models of adsorption are Langmuir isotherm; Langmuir – Freundlich and the Dubinin Radushkevich (DR) isotherm model are summarized [15]. The choice of these three isotherm models are based on: (1) an empirical model (Langmuir and Langmuir-Freundlich isotherm model); (2) pore filling model (DR isotherm model).

Table 3.3 – Summary of adsorption isotherm models

Model	Equation	Adjustable parameters
Langmuir	$q_e = \frac{q_m b \exp\left(\frac{H}{RT}\right) C_e}{1 + b \exp\left(\frac{H}{RT}\right) C_e}$	q_m, b, H

Langmuir-Freundlich	$q_e = \frac{q_m\, b \exp\left(\frac{H}{RT}\right) C_e^{1/n}}{1 + b \exp\left(\frac{H}{RT}\right) C_e^{1/n}}$	q_m, b, H, n
Dubinin – Raduskevich	$q_e = \frac{W_0}{V_m}.\exp\left(-\left(\frac{RT}{E}\ln\left(\frac{p_s}{p_e}\right)\right)^2\right)$	W_O, E

q_e is the adsorbed amount (mol kg^{-1}), q_m is the adsorbed amount at saturation, *i.e.* for infinite pressure, H is the adsorption enthalpy variation (J mol^{-1}), T is the temperature (K), n – constant parameter of the model, and c_e is the experimental concentration at the thermodynamic equilibrium ($mol.m^{-3}$),W_0 is the hypothetical microporous volume that can be filled by adsorbate ($cm^3\ g^{-1}$), V_m is the molar volume of the adsorbed phase ($cm^3\ mol^{-1}$), E is the characteristic energy, *i.e.* the adsorption potential of the couple adsorbent-adsorbate (J mol^{-1}), and ps is the vapor saturation pressure of the adsorbate (Pa).

3.1.6. Modeling procedure to determine the coefficients of adsorption isotherm models

The equilibrium data of the 120 isotherm experiments (which includes 5 VOCs and 8 activated carbon systems) were modeled (by using Gauss-Newton method in RSTAT, a statistical analysis programming) to find out the coefficients of different isotherm models [15-17]. With the coefficients obtained by R- STAT modeling, the adsorption capacities at equilibrium (qe) for each equilibrium data of all the VOC – activated carbon were calculated. These experimental results of 'qe' were compared with the results of 'qe' calculated by the equation 2. The student's t-test had been performed on the 'qe' (by modeling with RSTAT) and the 'qe' (by equation 3). The statistical results were significant under 95% confidence of interval [17]. All the coefficient values of different isotherm models are enlisted in the annexes section for different activated carbon – VOC systems. These values are going to be used in the dynamic simulation of adsorption and regeneration cycles.

3.1.7. Multiple Linear Regression (MLR) procedure for establishing the coefficients of isotherms based on the properties of the VOCs and activated carbons

MLR is a standard procedure that enables to understand the most significant variables (from the characteristics of activated carbon and properties of activated carbon) on the measured response [17]. The discrimination of less significant variables makes the MLR model more statistically reliable and also it could be applied to a wide range of VOC – activated carbon systems. The MLR models had been established by using the statistical package MINITAB. The MLR models for the different coefficients of DR and Langmuir isotherm models are going to be established as a function of the properties of VOCs and the characteristics of the activated carbons [15]. The F-test had been used on each of the parameters in the MLR model to test the statistical significance of the model under 95% confidence of interval. Finally, the calculated value from MLR model (for example, H_{MLR}) will be compared with the value obtained from the modeling of experimental value (H_{Exp}) by plotting a following graph (Figure 3.3) to check the linear regression validity of the MLR model [15].

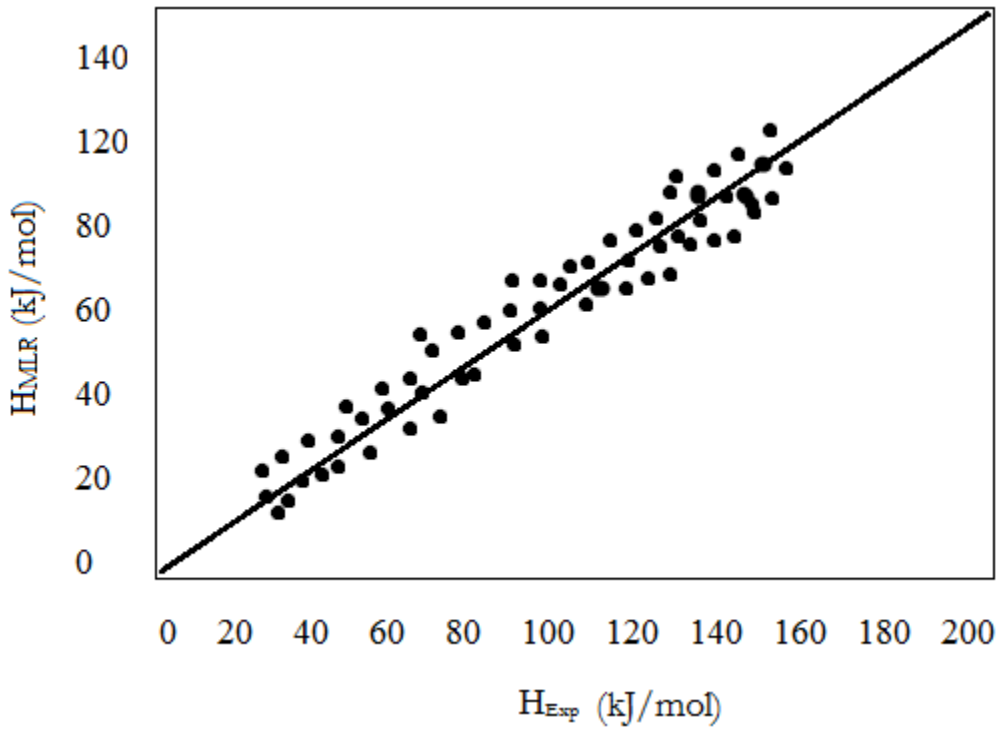

Figure 3.3 – Plot of MLR model values Vs Experimental values

3.2. Results and Discussion

3.2.1. Error bars on the adsorption isotherm

The error bars on the measurement of adsorption is calculated by the classical error propagation method. The accuracy of isotherm measurement decreases as a function of increase in concentration of different reactors in an isotherm experiment. This effect is due to the higher deviation of equilibrium concentration measurement (while 3 times sampling in the Gas Chromatography, GC), in the reactor which has the highest equilibrium concentration. For example, the error deviation (while 3 times sampling) in the reactor of 10 µl injected VOC (first point in the figure 3.5) is much less than the error deviation in the 400 µl injected VOC (last point in the figure 3.5). This is because of the area measure (volts x time) in the GC measurement for high concentration has a larger deviation than for a smaller concentration. The average of the concentration at equilibrium had been taken to have a balance on the error of uncertainty. The results from modeling are fitted to the actual experimental date (without the error bar consideration). Two examples of error bars on adsorption isotherm measurements are shown in the following figures 3.4 and 3.5. The error bar tendency has not varied independent of VOC and the activated carbon used in the isotherm experiment.

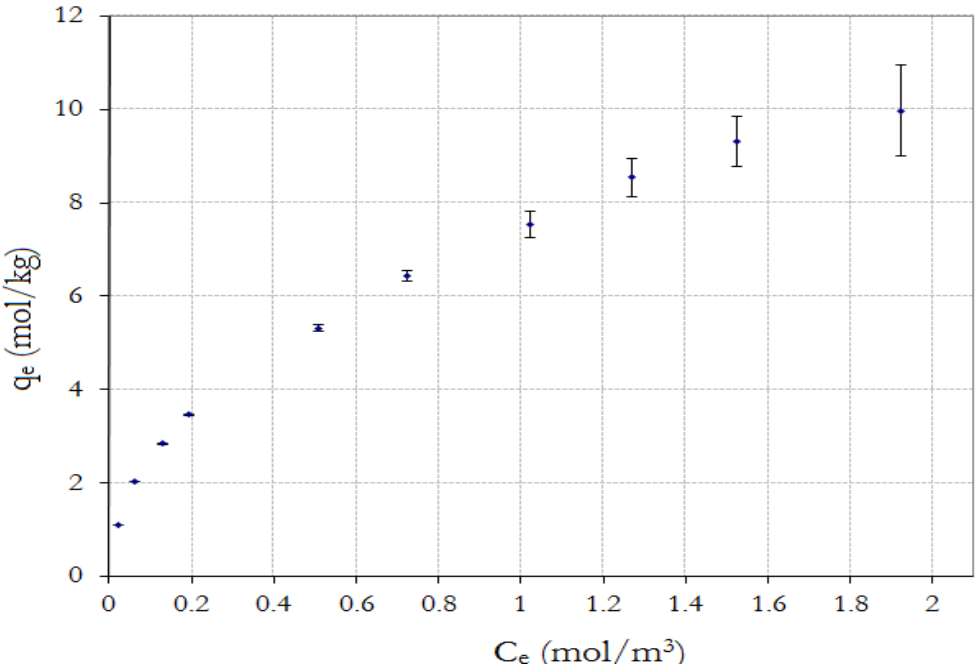

Figure 3.4 – Error bars on the adsorption isotherm of Dichloromethane – ACV404 system at 20°C

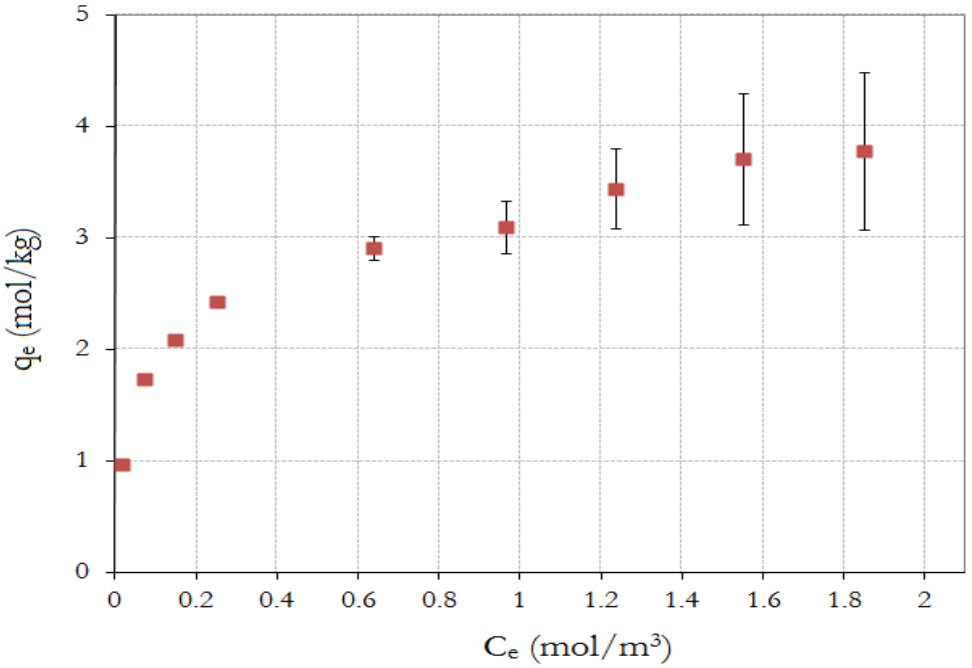

Figure 3.5 – Error bars on the adsorption isotherm of Acetone – ACM204 system at 20°C

3.2.2. Influence of temperature on adsorption isotherm

Figures 3.6, 3.7 show the influence of temperature on the adsorption capacity of ethanol and toluene in activated carbons. The adsorption capacity is a function of temperature, and as expected that at low temperature, better adsorption capacities are obtained [15].

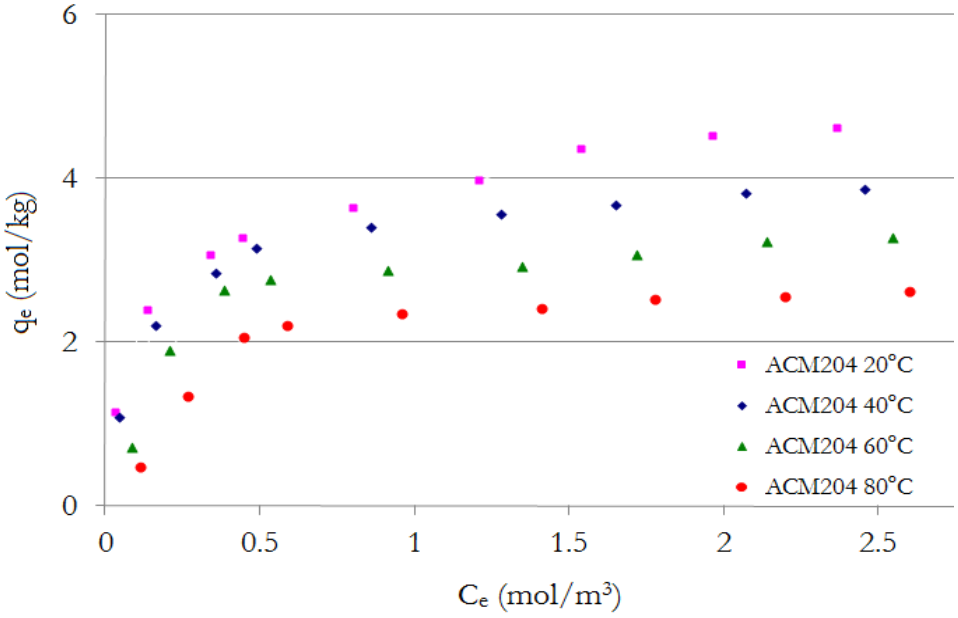

Figure 3.6 – Influence of temperature on adsorption isotherm of Ethanol – ACM204 system

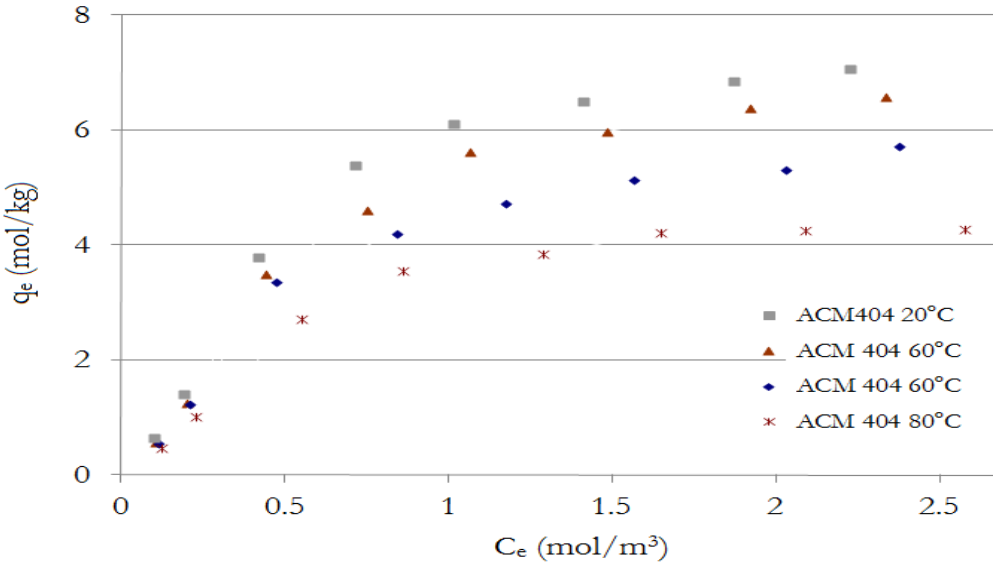

Figure 3.7 – Influence of temperature on adsorption isotherm of Toluene – ACM404 system

3.2.3. Influence of properties of activated carbon on adsorption isotherm

Figures 3.8, 3.9 show the influence of activated carbon on the adsorption capacities of VOCs. As expected that the activated carbons which possess higher BET specific surface area, micropore volume have higher adsorption capacity [15].

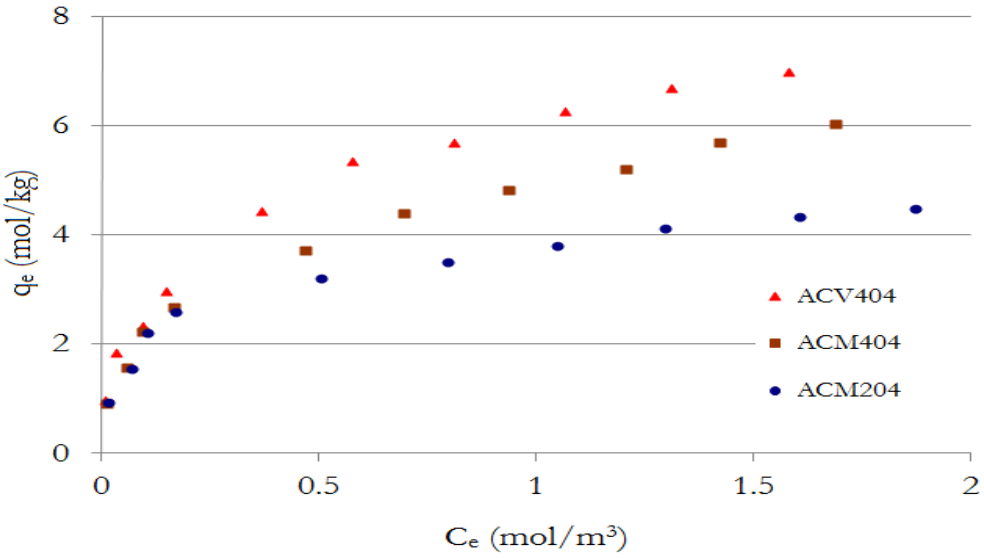

Figure 3.8 – Influence of properties of activated carbons on adsorption of Ethyl formate at 20°C

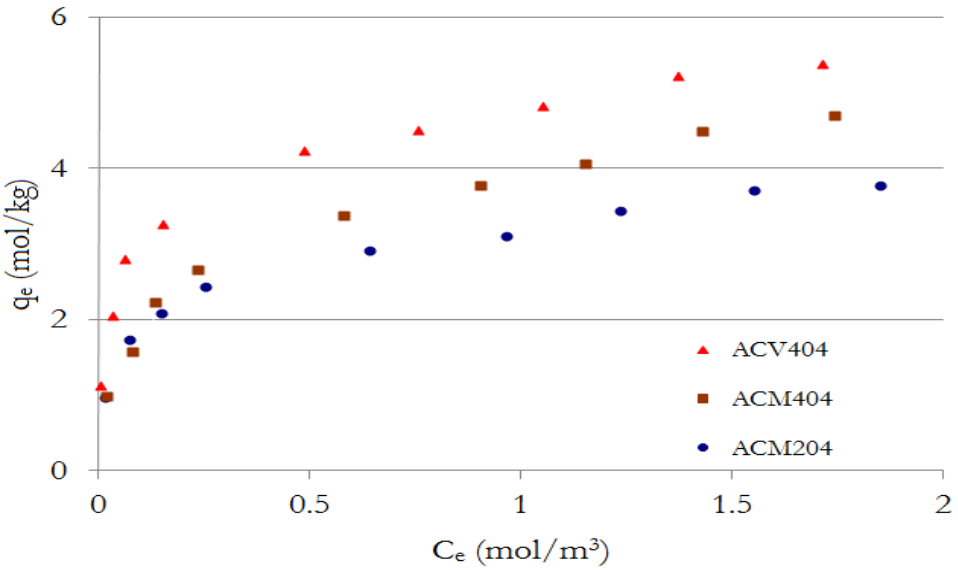

Figure 3.9 – Influence of properties of activated carbons on isotherm of Acetone at 20°C

3.2.4. Influence of VOC on adsorption isotherms

The influence of VOC on the adsorption isotherm (from the reactor injected volume of 400 µl) of activated carbon ACV404 is shown in the Figure 3.10. The order of adsorption capacity of the VOC depending upon the family of the VOCs and independent of the activated carbon tested is Chlorinated organics > Aromatics > Alcohol > Ester > Ketone [15].

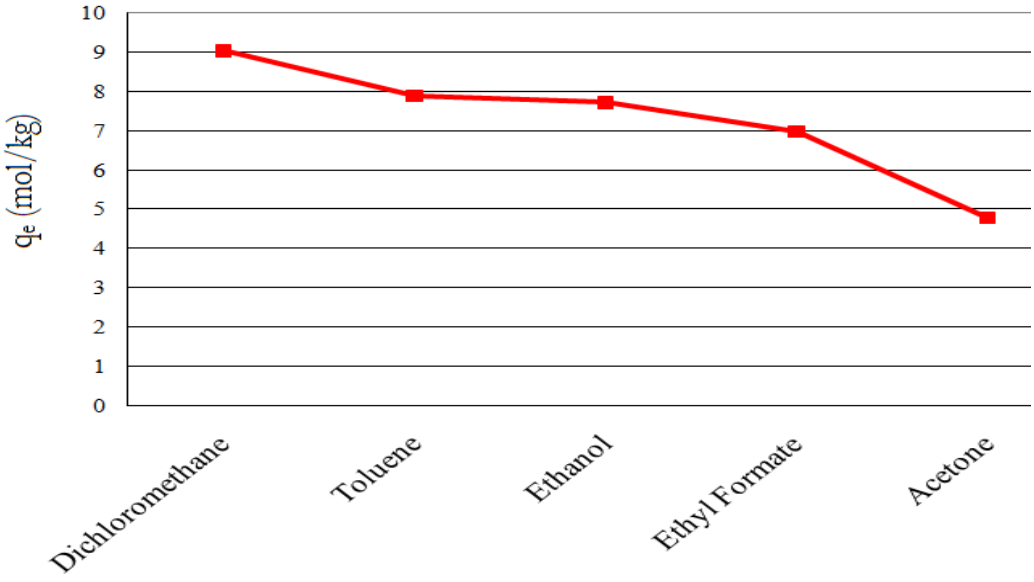

Figure 3.10 – Influence of properties of VOC adsorption on ACV404 at 20°C

3.2.5. Modeling results of coefficients of adsorption isotherms by Gauss Newton method

The coefficients of the different isotherm model (such as Langmuir, Langmuir-Freundlich and Dubinin-Raduskevich) were found by using Gauss Newton method. The Gauss Newton method reduces the error (to the minimum) between the experimentally measured values of adsorption isotherm and the calculated values of adsorption isotherm. The calculated values of adsorption isotherm points are significant under 95% confidence of interval with the experimental isotherm measurements by student t-test. In the following section, an example of comparison between the calculated values of adsorption isotherm points (Cal.q_e) and the experimental value of adsorption isotherm measurements (Exp.q_e) to check the linearity of the model. The adsorption isotherm results and the coefficients of VOC – activated carbon systems (acetone/ethyl formate/ dichloromethane – NC 60/NC 100/ BC120/ BPL /GF 40) [15] are included in the entire process of isotherm modeling and the MLR model.

(a) Langmuir isotherm model coefficients.

In the figure 3.11 (Dichloromethane adsorption systems), the values of calculated adsorption isotherms are having a very good agreement with the experimental adsorption isotherms.

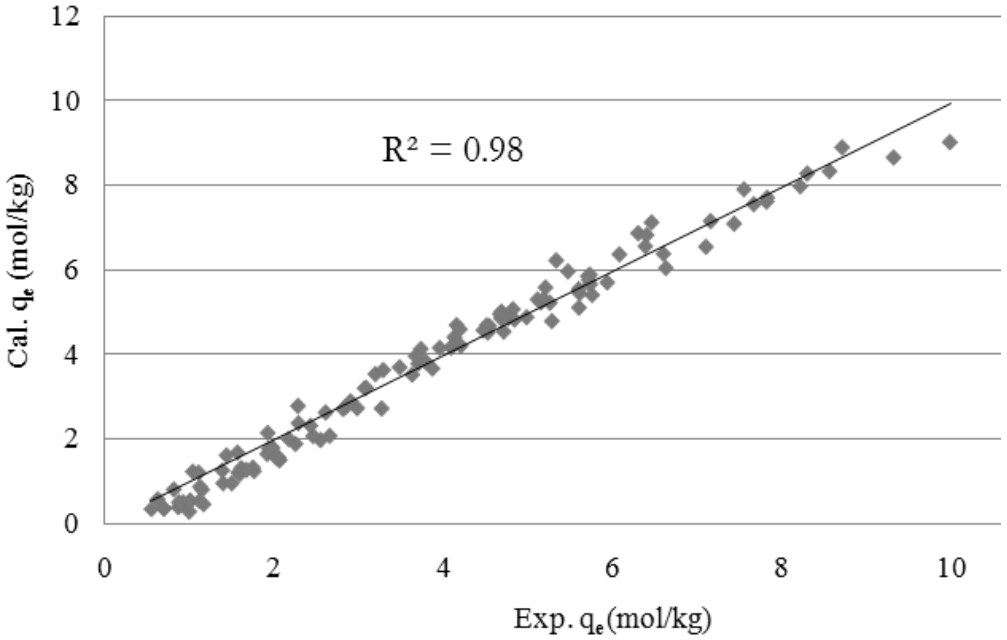

Figure 3.11 – Validity of Langmuir isotherm model for Dichloromethane – activated carbon systems

The validity of the calculated q_e for all VOC – individual activated carbon systems are shown in the following tables 3.4, 3.5 and 3.6.

Table 3.4 – Summary of experimental results of coefficients of Lagmuir isotherm model

VOC	CA	R^2_{adj}
Ethyl Alcohol	ACM 204	0.93
Ethyl Alcohol	ACM 404	0.99
Ethyl Alcohol	ACV 404	0.97
Dichloromethane	ACM 204	0.98
Dichloromethane	ACM 404	0.98
Dichloromethane	ACV 404	0.98
Ethyl Formate	ACM 204	0.92
Ethyl Formate	ACM 404	0.95
Ethyl Formate	ACV 404	0.95
Acetone	ACM 204	0.92
Acetone	ACM 404	0.98
Acetone	ACV 404	0.95
Toluene	ACM204	0.94
Toluene	ACM404	0.95
Toluene	ACV404	0.98

(b) Langmuir-Freundlich isotherm model coefficients:

The Langmuir-Freundlich isotherm model works better than the Langmuir model, because it has an additional parameter (n) which gives greater flexibility to the validity of the model. One of the the example of the validity fitting for the model is shown in the following figure 3.12. The disadvantage of the model is that it has the most number of coefficients and there could be difficulties in computing them.

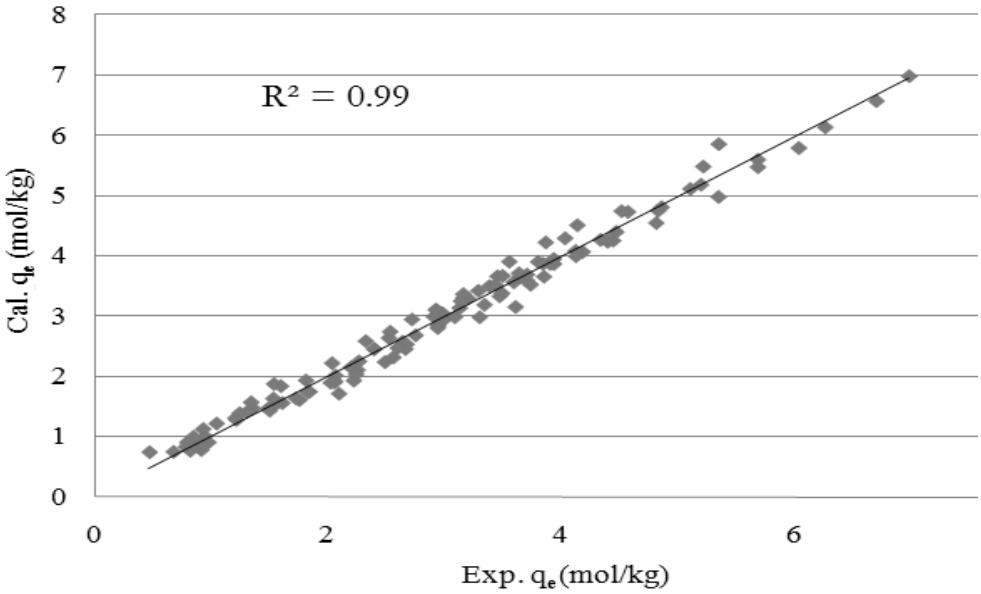

Figure 3.12– Validity of Langmuir-Freundlich isotherm model for Ethyl formate – activated carbon

Table 3.5 – Summary of experimental results of coefficients of Langmuir-Freundlich model

VOC	CA	R^2_{adj}
Ethyl Alcohol	ACM 204	0.99
Ethyl Alcohol	ACM 404	0.99
Ethyl Alcohol	ACV 404	0.99
Dichloromethane	ACM 204	0.99
Dichloromethane	ACM 404	0.99
Dichloromethane	ACV 404	0.99
Ethyl Formate	ACM 204	0.99
Ethyl Formate	ACM 404	0.99
Ethyl Formate	ACV 404	0.99
Acetone	ACM 204	0.97
Acetone	ACM 404	0.98
Acetone	ACV 404	0.97

Toluene	ACM204	0.95
Toluene	ACM404	0.96
Toluene	ACV404	0.98

(c) Dubinin-Raduskevich (DR) isotherm model coefficients:

Here is an example of the validity fitting for DR isotherm model in the figure 3.13. The DR isotherm model results (calculated by using R-STAT modeled on isotherm coefficients of DR isotherm model) are statistically less significant with the raw experimental results of adsorption isotherms in comparison to the results of Langmuir and Langmuir-Freundlich isotherm models.

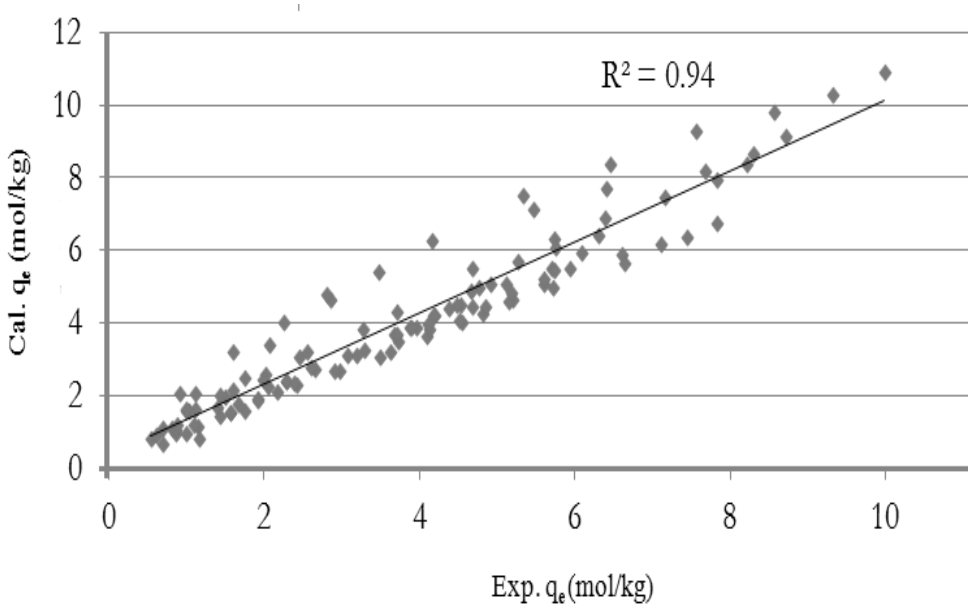

Figure 3.13 – Validity of DR isotherm model for Dichloromethane – activated carbon systems

Table 3.6 – Summary of experimental results of coefficients of DR isotherm model

VOCs	ACs	R^2_{adj}
Acetone	ACM 204	0.96
Acetone	ACM 404	0.92

Acetone	ACV 404	0.97
Dichloromethane	ACM 204	0.96
Dichloromethane	ACM 404	0.92
Dichloromethane	ACV 404	0.95
Ethyl Formate	ACM 204	0.95
Ethyl Formate	ACM 404	0.93
Ethyl Formate	ACV 404	0.92
Ethyl Alcohol	ACM 204	0.96
Ethyl Alcohol	ACM 404	0.91
Ethyl Alcohol	ACV 404	0.90

The DR model is not valid for toluene – activated carbon system. The reason is because that the saturation pressure of toluene was not varying in the temperature range (293 – 353 K) unlike in the other case of VOCs (ie. acetone, ethanol, ethyl formate and dichloromethane have similar tendency) as shown in the figure 3.14. The saturation pressure is a function of temperature and it directly influences the amount of VOC vapors formed inside the reactor. Since the amount of toluene vapors had not varied significantly like in the cases of other selected VOCs, so it is not evident to have one characteristic adsorption energy value (E) for the adsorption isotherms operating at a wide temperature range (293 – 353 K).

And also given the limitation that the DR model cannot have different micropore volume for different temperature and independent of VOC filling (as it represents strongly the characteristics of the activated carbon), it limits the DR model for toluene's case in this temperature range (293 – 353 K).

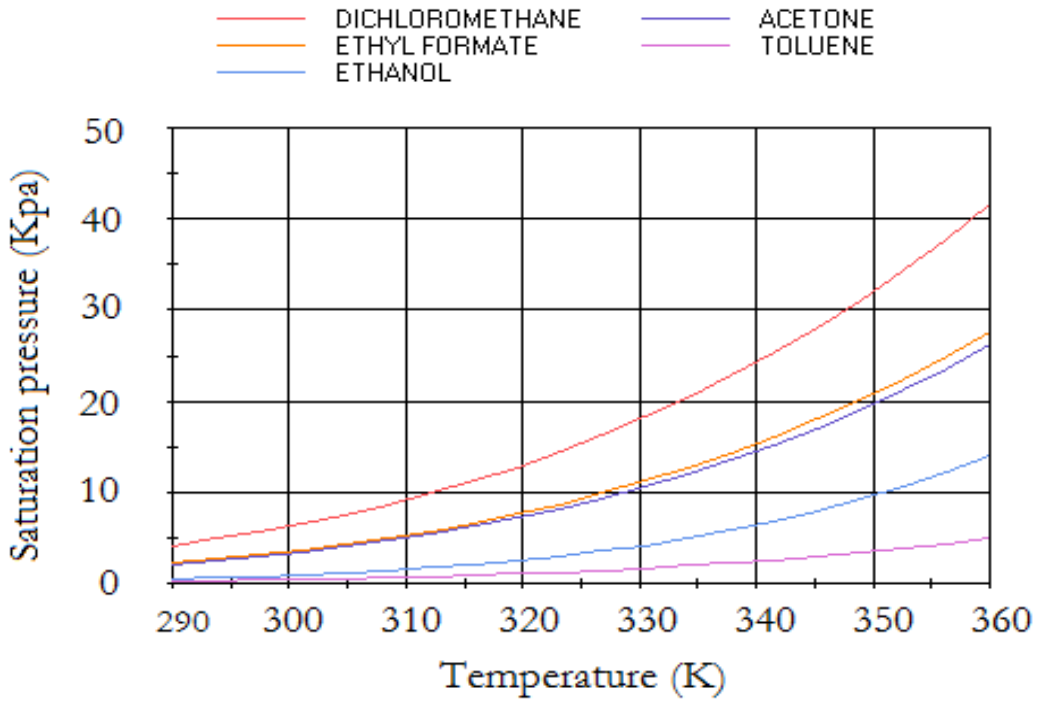

Figure 3.14 – Saturation pressure variation of VOCs with temperature

So to conclude in general, the reliability of the adsorption isotherm model for VOC-activated carbon system is in the form of descending order Langmuir-Freundlich > Langmuir > DR model [15].

3.2.6. Multiple Linear Regression (MLR) equation for characteristic energy in Dubinin Raduskevich isotherm

	α	Vμ	Ps	Vm	rμ	Pa	BET	H vap
α	1.00							
Vμ	0.14	1.00						
Ps	0.72	0.16	1.00					
Vm	0.37	0.07	-0.17	1.00				
rμ	0.25	0.39	0.24	0.21	1.00			
Pa	0.49	0.09	-0.01	0.99	0.25	1.00		
BET	0.15	0.24	0.14	0.13	0.55	0.15	1.00	
H vap	-0.65	-0.19	-0.75	-0.42	-0.36	-0.55	-0.22	1.00

Table 3.7 – Choosing parameters for the DR-MLR characteristic energy (E) MLR model

The properties of the VOCs and the characteristics of the activated carbons were taken as variables in the MINITAB statistical software [15,18,19,20]. Table 3.7 shows the linear regression between the parameters. All the symbols of the different parameters and their corresponding units in table 3.7 are given in the nomenclature section. In case of two parameters sharing stronger value of R^2, one has to be eliminated based on its less importance to the MLR model to be developed [18-20]. Therefore in the case of DR model, the parameters such as micropore volume (W_o), saturation pressure (Ps), parachor (Pa), and specific surface area (BET) have been chosen to form the MLR model.

The measured response adsorption characteristic energy [E] was also taken in the MINITAB statistical software. The MLR model of the response was established as a function of variables by regression analysis. The best MLR model (in terms of accuracy) for the characteristic adsorption energy [E] in the DR isotherm model is expressed as equation 3.2. The MLR model is dimensionless (normalized) because the variables had been normalized to avoid the art effect on each variable.

Adsorption characteristic energy [E] with R^2 value = 0.94

$$E = 0.61.W_o - 1.39.BET + 0.45.Ps – 0.33.Pa \qquad (3.2)$$

The coefficient [E] of MLR model was calculated using the quantitative equation 3.2 for each VOC – activated carbon system and these calculated results were statistically significant (under 95 % confidence of interval by f-test) with the experimental values obtained by modeling with Gauss Newton method in R-STAT. The quantitative MLR model which is used to calculate the characteristic adsorption energy is expressed as equation 3.3

$$E = 9.96 + 6.92.W_o - 0.005.BET + 0.05.Ps + 0.03.Pa \qquad (3.3)$$

A very good agreement between the calculated characteristic adsorption energy values (E_{MLR}) and the modeled characteristic adsorption energy values (E_{Exp}) from the isotherm experimental data had been observed by plotting the as shown in the Figures 3.15 and the value of R^2 is 0.94. Based on the large set of 120 adsorption isotherm experiments, the statistical MLR model had been established for the characteristic adsorption energy [E]. This MLR model had been validated with the experimental values which were obtained by using R-STAT software. This MLR model

represents 4 VOCs of different families and also the 8 activated carbons and hence the model is rich and diverse in terms of different VOCs and activated carbons. This MLR model will be implemented in the dynamic adsorption simulation model PROSIM and so it will make the simulation tool PROSIM simpler and more efficient (by not dealing with isotherm equilibrium data). The variables such as BET, micropore volume, saturation pressure and parachor had emphasized the influence of adsorbate-adsorbent interactions as shown in equation 3.3 [18-20]. These interactions were often described as the most influential parameters for the adsorption mechanisms of DR isotherm model. Despite of the limitation that the MLR model is not valid for toluene activated carbon system, it will be very a useful option of covering the equilibrium isotherm data of 4 VOCs – 8 activated carbon systems with a simpler predictor MLR equation in the dynamic simulation tool PROSIM.

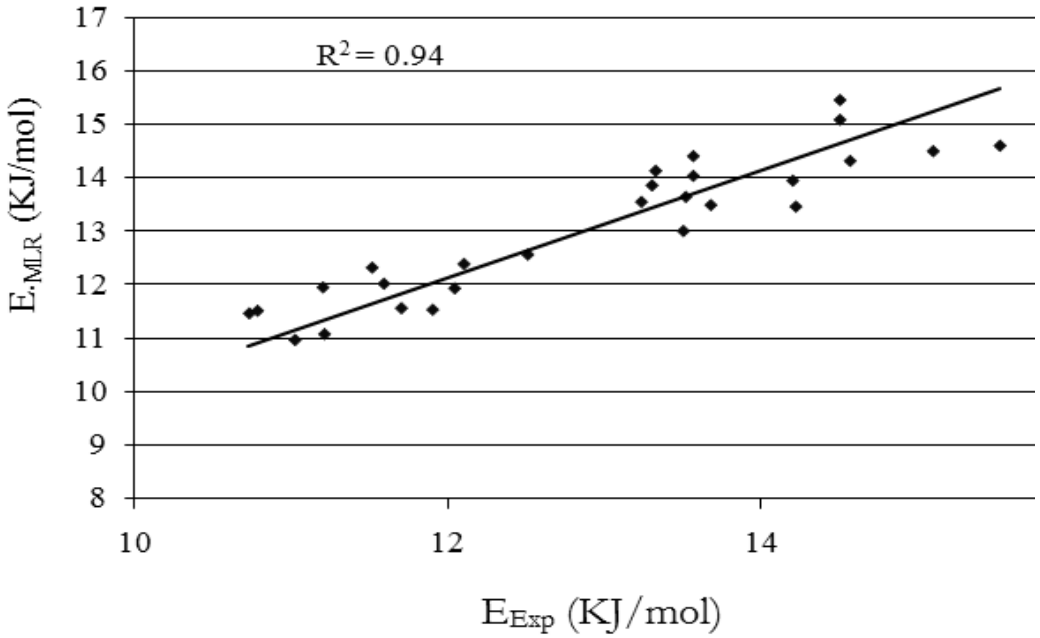

Figure 3.15 – Characteristic adsorption energy [E] of DR model

3.2.7. Multiple Linear Regression (MLR) equation for enthalpy of adsorption in Langmuir isotherm

A similar approach of choosing the parameters had been followed for the Langmuir model. The parameters are shown in the table 3.8. The enthalpy of adsorption (H) along with the physical

properties of VOCs and the characteristics of the activated carbon had been taken in the Minitab software for performing MLR analysis [15].

	α	IP	BET	H vap	Vm	Vμ	μ	V tot	Ps	Mw	Pa	rho	rμ
α	1.00												
IP	0.69	1.00											
BET	0.15	0.01	1.00										
H vap	-0.65	-0.12	-0.22	1.00									
Vm	0.37	-0.38	0.13	-0.42	1.00								
Vμ	0.12	0.01	0.17	-0.18	0.10	1.00							
μ	-0.49	-0.94	0.06	-0.21	0.45	0.05	1.00						
V tot	0.09	0.01	0.67	-0.13	0.07	0.86	0.03	1.00					
Ps	0.72	0.69	0.14	-0.75	-0.17	0.12	-0.40	0.08	1.00				
Mw	0.94	0.82	0.14	-0.66	0.06	0.11	-0.59	0.08	0.90	1.00			
Pa	0.49	-0.28	0.15	-0.55	0.99	0.12	0.40	0.89	-0.01	0.20	1.00		
rho	-0.18	-0.02	-0.84	0.26	-0.15	-0.84	-0.07	-0.80	-0.17	-0.16	-0.18	1.00	
rμ	0.25	0.02	0.80	-0.36	0.21	0.24	0.10	0.50	0.24	0.23	0.25	-0.84	1.00

Table 3.8 – Choosing parameters for the enthalpy of adsorption (H) of Langmuir model

There are several MLR models resulted from the analysis based on different combination of variables. The best MLR model for the enthalpy of adsorption [H] in terms of accuracy and agreement with the experimental values is expressed as equation 3.4.

Enthalpy of adsorption [H] with R^2 value = 0.93

$$H = 0.082 - 0.186.\alpha + 1.21\ r_{\mu} - 0.459.BET + 0.319.Pa \qquad (3.4)$$

The MLR quantitative model (equation) 3.4 is dimensionless (normalized) because the variables had been normalized to avoid the art effect of each variable. The coefficient [H] of MLR model was calculated for each VOC – activated carbon system and so that they were compared with the experimental values obtained by experimental modeling of equilibrium isotherm data points. This comparison had been done by plotting the experimental values Vs the value obtained from the MLR model as shown in the Figure. 3.16.

The coefficient [H] of MLR model was calculated using the quantitative equation 4 for each VOC – activated carbon system and these calculated results were statistically significant (under 95 % confidence of interval by f-test) with the experimental values obtained by modeling with Gauss Newton method in R-STAT. The quantitative MLR model which is used to calculate the characteristic adsorption energy is expressed as equation 3.5

$$H = 0.29 - 2.42.\alpha + 75.5\, r_{\mu} - 0.02.BET + 0.07.Pa \quad (3.5)$$

The agreement between the calculated enthalpy of adsorption values (H_{MLR}) and the experimental enthalpy of adsorption values (H_{Exp}) is shown in the Figure 3.16 and the value of R^2 is 0.93. The F-test on each parameter had been tested against the responses (E) and all the parameters are statistically significant under 95% confidence of interval. But the problem with the model is that there are not data in the middle of the figure and that concerns the consistency of the model, whereas it is consistent in DR model.

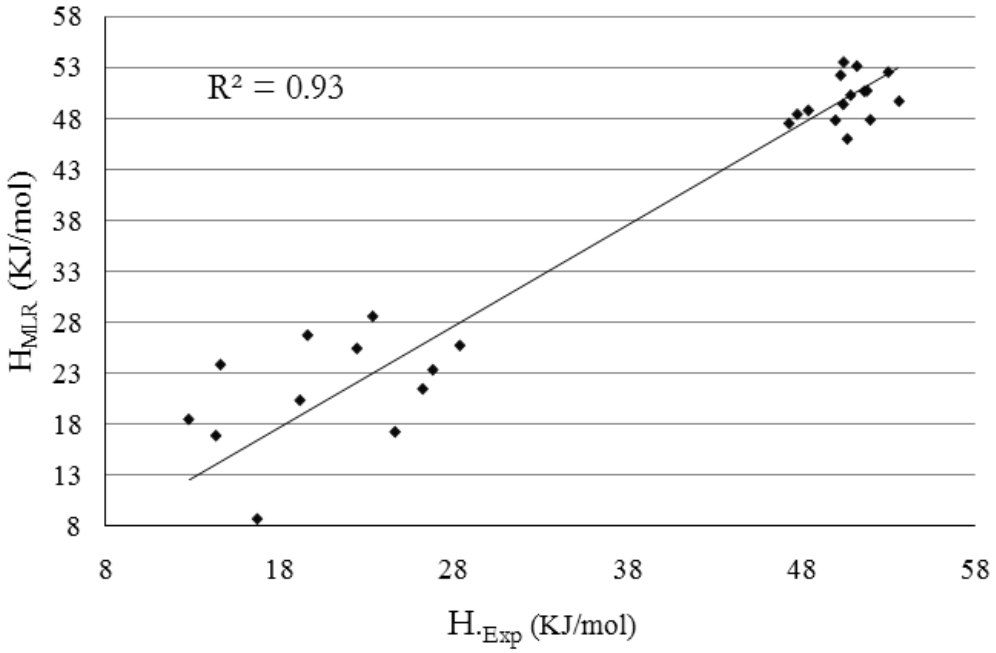

Figure 3.16 – Enthalpy of adsorption [H] of Langmuir MLR model

A similar approach has been tried for the other coefficients of Langmuir isotherms to establish MLR model. But it has been unsuccessful because of the very bad consistency to predict the coefficients.

3.3. Conclusions

The concentration range (1 - 170 $g.m^{-3}$) which had been chosen in the adsorption isotherm experiments covers a wide range which represents the typical situation in food, chemical and hydrocarbon industries. The adsorption isotherm coefficients to predict the adsorption capacity

have undergone rigorous statistical tests to consolidate the reliability of each VOC – activated carbon system. The goal of establishing these huge set of isotherm data are to use them in process simulation PROSIM. Even though the DR- MLR model for the characteristic adsorption energy (E) for toluene-activated carbon systems has failed to work because of the reasons given in the discussion, the DR- MLR characteristic energy model would reduce the necessary to perform the adsorption isotherm experiments. The other values such as micropore volume (from nitrogen analysis), the saturation pressure and molar volume (from VOC properties) are already available. So by having this MLR model in the simulation tool, it will make the simulation efficient and simple.

References

[1] K.S. Hwang, D.K. Choi, S.Y. Gong, S.Y. Cho. Adsorption and thermal regeneration of methylene chloride vapor on an activated carbon bed. Chem Eng Sci 1997; 52:1111-23

[2] D.P. Paulsen, F.S. Cannon. Polytherm model for methylisobutylketone adsorption onto coconut based granual activated carbon. Carbon. 1999; 37: 249-63

[3] S. Giraudet, P. Pre, P. Le Cloirec. Modeling the Heat and Mass Transfer in Temperature Swing Adsorption of Volatile Organic compounds on to Activated Carbons. Env. Sci. and Tech 2009; 43:1173 – 179

[4] A.M. Tolmachev, O.I. Trubnikov. Molecular models for vapor adsorption on microporous adsorbents. Carbon 2002;40:1401-7

[5] P. Pré, F. Delage, P. Le Cloirec. A model to predict the adsorber thermal behavior during treatment of volatile organic compounds onto wet activated carbon. Environ Sci Technol 2002; 36:4681-88

[6] J. Wu, L.G. Hammarstrom, O. Claesson, I. Fangmark. Modeling the influence of physico-chemical properties of volatile organic compounds on activated carbon adsorption capacity. Carbon 2003;41:1322-5.

[7] S. Giraudet, P. Pre, H. Tezel, P. Le Cloirec. Estimation of adsorption energies using physical characteristics of activated carbons and VOCs molecular properties. Carbon. 2006; 44: 1873-83

[8] G.O. Wood. Affinity coefficients of the Polanyi /Dubinin adsorption isotherm equations: a review with compilations and correlations. Carbon. 2001; 39: 343–56.

[9] G.O. Wood. Review and comparisons of D/R models of equilibrium adsorption of binary mixtures of organic vapors on activate carbons. Carbon. 2000; 40:231-39

[10] R.H. Perry *et al.*, Perry's Chemical Engineers Handbook, McGraw-Hill, New York, 2007

[11] T. Jayabalan, Study of oxidation of carbon materials, Ph.D. Dissertation, Ecole des Mines de Nantes, France, 2008

[12] D.M. Ruthven, Principles of adsorption and adsorption processes, John Wiley & Sons: New-York, Univ of New Brunswick: Fredericton, USA, 1984

[13] E.W. Washburn, Note on method of determining the distribution of pore sizes in a porous material. Proc.Nat. Acad. Sci 1921, 7: 115 -16

[14] J. Keller, R. Staudt, Gas Adsorption Equilibria, Universitat Siegen. Springer, USA, 1994

[15] S. Giraudet, Exothermicity of adsorption of volatile organic compounds in fixed activated carbon beds: modelling and simulation valdiation of experimental work, PhD dissertation, EMN, France, 2006

[16] J.H. Maindonald, Using R for Data Analysis and Graphics, Introduction, code and commentary, R- Stat, http://cran.r-project.org/doc/contrib/usingR.pdf, 2008

[17] P.M. Berthouex, and L.C. Brown, Statistics for Environmental Engineers, Lewis Publishers, USA, 2002

[18] C. Nguyen, DO DD. The Dubinin – Raduskevich equation and the underlying microscopic adsorption description. Carbon. 2000; 39:1327-336

[19] V.K. Dobruskin. Contribution of the edge effect to physical adsorption in micropores of activated carbons. Carbon 2002; 40:659-66

[20] V.K. Dobruskin. Micropore structure of activated carbons and predictions of adsorption equilibrium. Carbon 2002; 40:1003-10

4. Experimental and Modeling of dynamic Vacuum Temperature Swing Adsorption (VTSA)

Experimental and simulation studies on VTSA process to recover organic vapors had been initiated to identify the advantage and limitations of the VTSA process over the normal TSA process [1-2]. And the influence of operating conditions has not been investigated in depth to estimate the combined vacuum temperature regeneration efficiency and the operating costs [1-2]. In addition, there are not many studies that compares the dynamic experimental and the simulation results of combined vacuum temperature regeneration [1-2].

4.1. Objectives

The objectives of the VTSA are: (1) to study the influence of operating conditions on the recovery efficiency and operating costs by using Factorial Experimental Design (FED); (2) to find the time for which vacuum regeneration can be applied to achieve maximum recovery efficiency and reduce the operating costs, (3) to achieve the cooling benefits of the activated carbon bed after hot nitrogen regeneration, and also to perform the simulation for the experimental results. The aim of the study is to develop the simulation tool for VTSA process which has consists of VOC – AC system based on all the experimental work.

4.2. Dichloromethane – CECA ACM404 system

4.2.1. Characterization of Activated Carbon

The activated carbon CECA – ACM 404 is a coal based physically activated carbon. For all the characterization methodologies and results of the ACM 404, the chapter 3 could be referred [4-6].

4.2.2. Properties of dichloromethane

ACROS Organics supplied 99% pure dichloromethane for the experiments and the properties of dichloromethane (CH_2Cl_2) could be referred in chapter 3 [4].

4.3. Adsorption isotherm equilibrium model

The value q_i* in the linear driving force model (LDF) was computed from the modified Langmuir isotherm model, taking into account the temperature effect on the equilibrium data. The parameters of the Langmuir equation were derived from the experimental data measured for the system (dichloromethane – ACM 404) at 20, 40, 60 and 80 °C [7]. Since, the isotherms are performed at different temperature, it is important to include the temperature parameter in the isotherm model as shown in equation 4.1. The R-Stat statistical software was used to check the significance of the computed parameters using an interval of confidence of 95% by student t-test [8]. The results are summarized in table 4.1.

$$q_i^* = \frac{q_{m0}\exp(\frac{q_{m1}}{T})k_0\exp(\frac{k_1}{T})P_i}{1+k_0\exp(\frac{k_1}{T})P_i} \qquad (4.1)$$

Table 4.1 – Langmuir isotherm coefficients

Langmuir model coefficients - Dichoromethane – ACM404 system			
qm_0 (mol.kg^{-1})	Qm_1 (T^{-1})	k_1 (T^{-1})	k_0 (atm^{-1})
2.695	239.21	2723.24	0.01441

4.4. Experimental

Figure 4.1 shows the experimental setup of ACM404 (activated carbon) – dichloromethane (VOC) system. The adsorption column used is made of stainless steel and the dimensions are 1.5 m in length, 0.05 m of internal diameter and 1.5 cm thickness. The thermal conductivity value (λ) of the adsorption column's wall (stainless steel = 16 W.m^{-1}.K^{-1} at 25 °C) was taken from the database which had been implemented in the simulation package. A thermocouple is placed in the activated carbon bed at 105 cm to record temperature data. The first step was the adsorption of dichloromethane on ACM404, and then followed by regeneration step which is a combination of hot N_2 and vacuum. In the system, a continuous gas-phase sampling of VOC concentration using Flame Ionization Detector (FID) was present in figure 4.1. FID was used to measure the exit

concentration of dichloromethane from the column and it was calibrated before the adsorption experiments. For the calibration curve, different volume samples (from 10 – 400 μl) are injected into a glass balloon of 1L volume [4]. The mass of VOC is calculated by multiplying density of VOC and volume of VOC injected in the glass balloon. Once having the value of VOC mass, the concentration ($g.m^{-3}$) is calculated by the ratio of mass of VOC to the volume of the glass balloon. Hence, a linear calibration curve of concentration of VOC ($g.m^{-3}$) Vs FID response (volts) could be established for the dynamic experiments.

For the regeneration step, a system of heating cable was arranged around the pipeline to heat the nitrogen externally before entering the column. It was done to avoid the heat loss of hot nitrogen with atmosphere before entering the column for regeneration.

4.4.1. Adsorption step

The adsorption step of dichloromethane on ACM 404 was achieved with the operating conditions as mentioned in Table 4.2. A constant flow rate of 0.0257 $g.sec^{-1}$ of dichloromethane was passed through the evaporator which is at 35°C. A small flow rate of nitrogen (0.05 $NL.sec^{-1}$) was passed through the evaporator to carry the dichloromethane which is in vapor form. The small flow rate of nitrogen was diluted with another nitrogen stream of 0.56 $NL.sec^{-1}$, thus forming a concentration of 50 $g.m^{-3}$ of dichloromethane in the gas stream (dichloromethane + nitrogen) which is entering the column for adsorption. The gas which is at 0.56 $NL.sec^{-1}$ was sent from the bottom of the column which was packed with 1.222 kg of ACM404 (activated carbon) as shown in the Figure 4.1.

Table 4.2 – Pilot specifications and adsorption step operating conditions

Adsorption column size	1.5 m x 0.05 m
Superficial adsorption gas velocity	0.28 $m.s^{-1}$
Concentration CH_2Cl_2	50 $g.m^{-3}$
Pump flow rate CH_2Cl_2	0.0257 $g.sec^{-1}$
Total gas flow rate (N_2 + CH_2Cl_2)	0.56 $L.sec^{-1}$

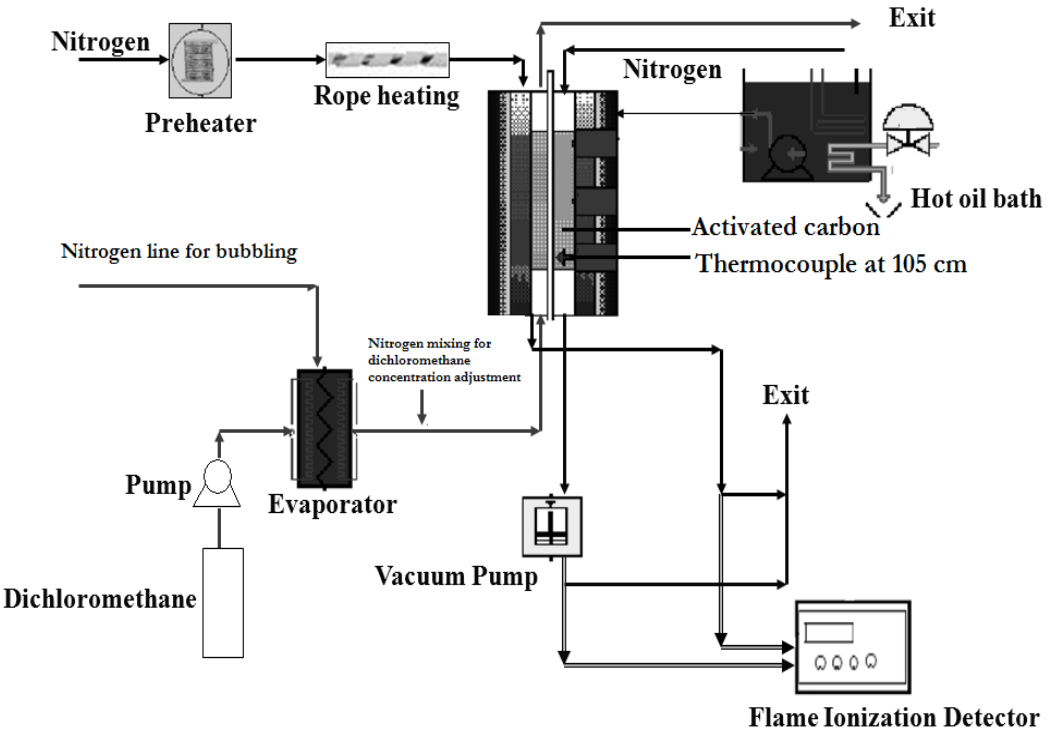

Figure 4.1 – VTSA Pilot plant scheme

There is a thermocouple present at 105 cm in the activated carbon bed. As the thickness of steel column is very large (1.5 cm) and so there was not significant heat transfer by the hot nitrogen to the activated carbon bed during the hot nitrogen regeneration step. So the column was heated along by hot oil bath at 80°C for 40 minutes. The nitrogen for regeneration from the pre-heater was then passed on to rope heating to avoid heat loss before entering the column.

4.4.2. Regeneration step

After the adsorption step, the regeneration was performed with the combination of thermal (hot N_2) and vacuum regeneration. Six regeneration experiments had been designed by changing the operating conditions (during the first step of nitrogen regeneration) such as temperature of hot nitrogen [85°C, 93 °C], flow rates of nitrogen [0.07 $NL.sec^{-1}$, 0.14 $NL.sec^{-1}$], and intermediate regeneration percentages [55%, 75%]. FED has been be used to study the effect of nitrogen temperature (T); flow rate of nitrogen (V_f); and intermediate regeneration (I_R) on the responses such as recovery percent (F_R) and the operating costs (OP_c) [3]. The procedure and the limitation of FED

are given detailed in the literature review section. The three operating conditions which change during thermal regeneration step are: (1) nitrogen temperature, (2) flow rate of nitrogen; and (3) intermediate regeneration percentage (I_R). Intermediate regeneration percentage (I_R) is defined as the percentage for which vacuum regeneration is applied just after hot nitrogen regeneration to achieve maximum recovery efficiency at optimized cost. Intermediate regeneration was chosen as 55% (-) and 75% (+) for analyzing the vacuum regeneration effect.

Figure 4.2 shows the different steps and the operating conditions in the combination of hot nitrogen and vacuum regeneration.

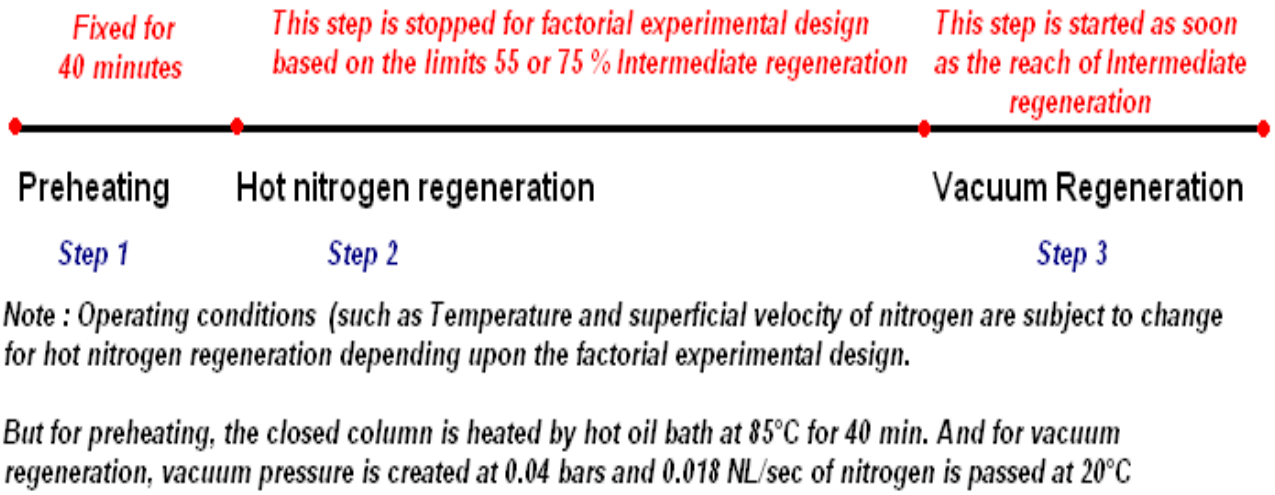

Figure 4.2 – Different steps in combination of hot nitrogen and vacuum regeneration

During the second step of regeneration which was the vacuum regeneration, the operating conditions had been fixed at 0.04 bars by passing 0.018 $NL.sec^{-1}$ of nitrogen at room temperature. The total regeneration time was fixed in all the six cases as 180 min, which includes 40 min of the hot oil bath along the column. All these operating conditions were summarized in Table 4.3.

Table 4.3 – VTSA Regeneration - operating conditions

Exp.	Step 1 : Thermal Regeneration (Hot N_2)				Step 2 : Vacuum Regeneration	
	T_{N2} (°C)	Flow N_2 ($NL.s^{-1}$)	Time (min)	I_R (%), step1	Flow N_2 ($NL.sec^{-1}$)	Time (min)
1	93	0.14	100	75	0.018	40
2	85	0.14	105	75	0.018	35
3	93	0.14	50	55	0.018	90
4	85	0.14	55	55	0.018	85
5	93	0.07	108	55	0.018	72
6	85	0.07	121	55	0.018	59

4.4.3. Factorial Experimental Design (FED)

FED has been implemented to study the effects of set of factors on the responses; (1) to estimate the magnitude of the effects contributed by the factors; (2) and to develop a mechanistic model. In FED, say X_1 and X_2 are two different factors and the response (output) was measured as say Y. The FED analysis was performed by with MINITAB software by using analysis of variance (ANOVA) method [3].

At the end of the ANOVA, it gives a model in the form of the following equations 4.2 and 4.3.

$$F_R = a_o + a_1.T + a_2.I_R + a_3.T.I_R \qquad (4.2)$$

$$OP_€ = b_o + b_1.T + b_2.V_f + b_3.T.V_f \qquad (4.3)$$

F_R –Recovery efficiency; $OP_€$ - Operating costs; T – Temperature of nitrogen factor; I_R – Intermediate regeneration factor; V_f – Volumetric flow rate of nitrogen factor

4.4.4. Estimation of recovery efficiency and operating costs

The recovery efficiency was estimated from the integration of the regenerated mass ($g.l^{-1}$) with time (min) and then multiplied by corresponding flow rate of nitrogen. The multiplication of different flow rates is because the values of nitrogen flow are different in hot nitrogen and vacuum regeneration. The operating costs for the regeneration step was calculated by the summation of energy costs of all the heating equipments (pre-heater, rope heating, hot oil bath, and vacuum pump) and the consumption of nitrogen during the regeneration step. The parameters required for the cost analysis were tabulated in the Table 4.4 [9]. Equations 4.4, 4.5 and 4.6 are used to calculate the recovery efficiency, operating cost for regeneration and recovery speed.

Table 4.4 – Inputs for operating costs estimation

Power of vacuum pump (kW)	0.396
Power of hot oil bath (kW)	2
Power of pre-heater (kW)	0.3
Power of rope heating (kW)	0.2
Cost of Nitrogen (€.m^{-3}), supplier – Air Liquide	0.18
EDF Electricity Tariff (€.MWh^{-1}) in France	60

Recovery efficienty (%) = [Regenerated VOC] (g). [Adsorbed VOC] $^{-1}$ (g^{-1}) (4.4)

Operating cost (€ cents) = Heating costs (€ cents) + Cost of N_2 (€ cents) (4.5)

Recovery speed = Total mass of VOC regenerated (g). [Regeneration time] $^{-1}$ (min^{-1}) (4.6)

4.5. Simulation model development and validation

4.5.1. Simulation arrangement

As per the experimental setup, the VTSA process arranged in the PROSIM simulation tool and it is shown in the figure 4.3. Stream 1 represents the adsorption step of the dichloromethane coming at a concentration 50 $g.m^{-3}$. Stream 2 represents the hot nitrogen regeneration until to achieve the intermediate regeneration according to the FED. Stream 3 represents the vacuum pressure regeneration and it is applied once the intermediate regeneration is achieved by hot nitrogen regeneration. Stream 4 is the purge nitrogen at the end of the regeneration to cool the bed once after the regeneration. Stream 5 is the exit for the concentration measurement in different steps of the VTSA process. In the case of TSA process, the stream 3 will be absent in the simulation interface [10-11].

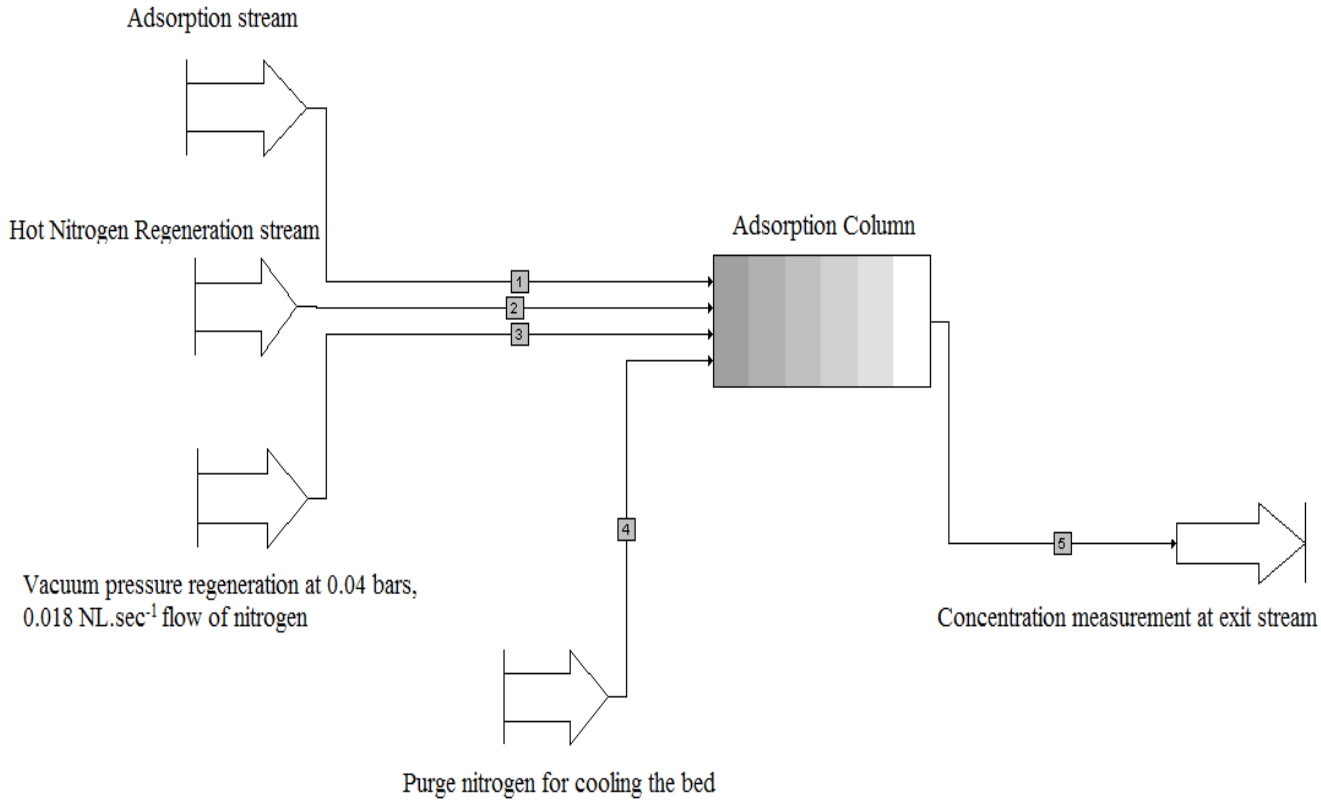

Figure 4.3 – VTSA process - PROSIM simulation setup

4.5.2. Different data entry sections in the simulation interface

In the figure 4.4, the architecture of the simulation model calculation is summarized. It composed of the input parameters, model equations and the output parameters of the simulation interface. The order of the input parameters that are given in different sections of the simulation interface such as: (1) characteristics of activated carbon; (2) physico-chemical properties of different VOCs from the library of thermodynamic properties; (3) details on feed streams during adsorption and regeneration steps; (4) constituents of the isotherm equilibrium data from modeling results; (5) mass and heat transfer models to calculate or even adjust the corresponding coefficients; (6) adsorption column dimensions; (7) initializing operating condition parameters of adsorption and regeneration (such as time of adsorption and regeneration, temperature of hot nitrogen, flow rate of hot nitrogen, vacuum pressure, time and temperature of hot oil bath, etc); (8) method of numerical analysis

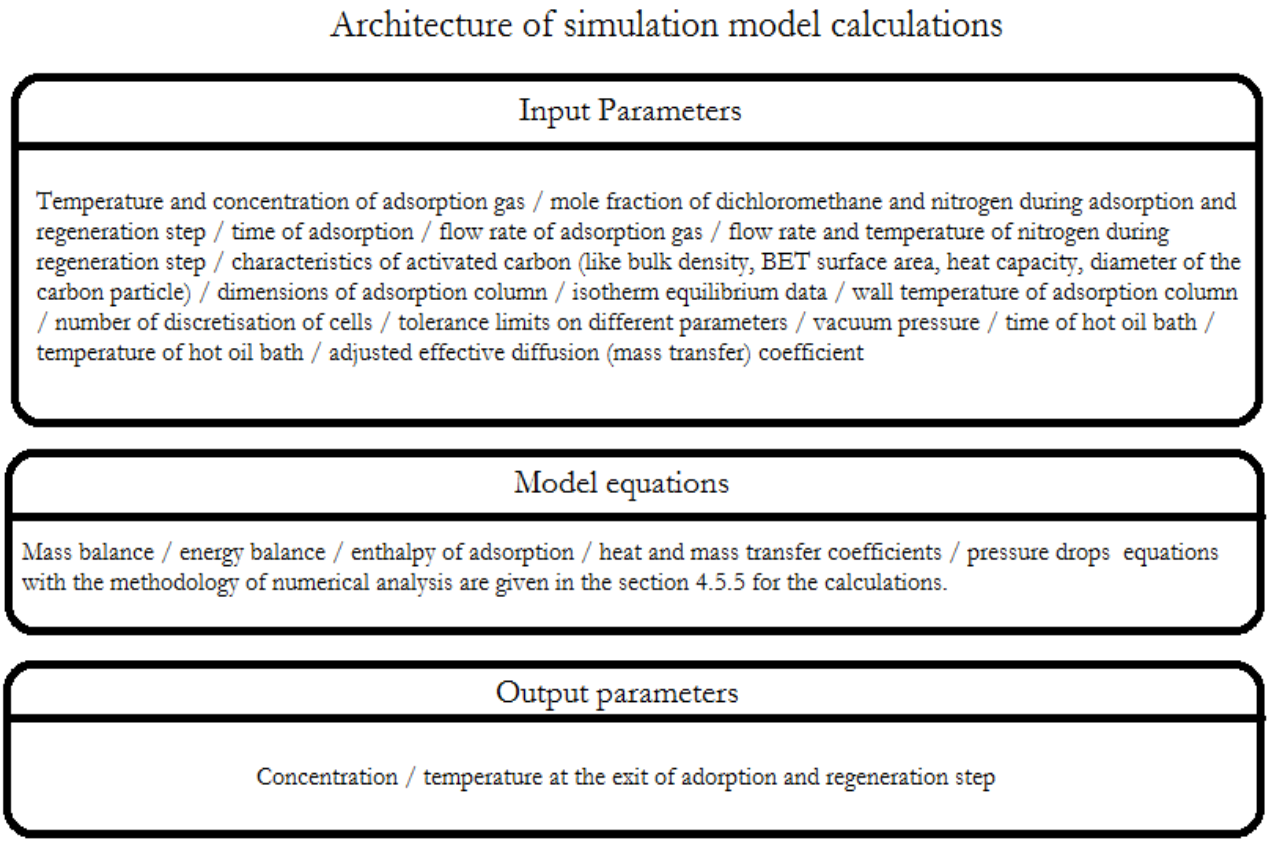

Figure 4.4 – Architecture of the simulation model calculations

Figure 4.5 shows a snapshot of the simulation interface with some details of the input parameters in the column section and the characteristics of the activated carbon.

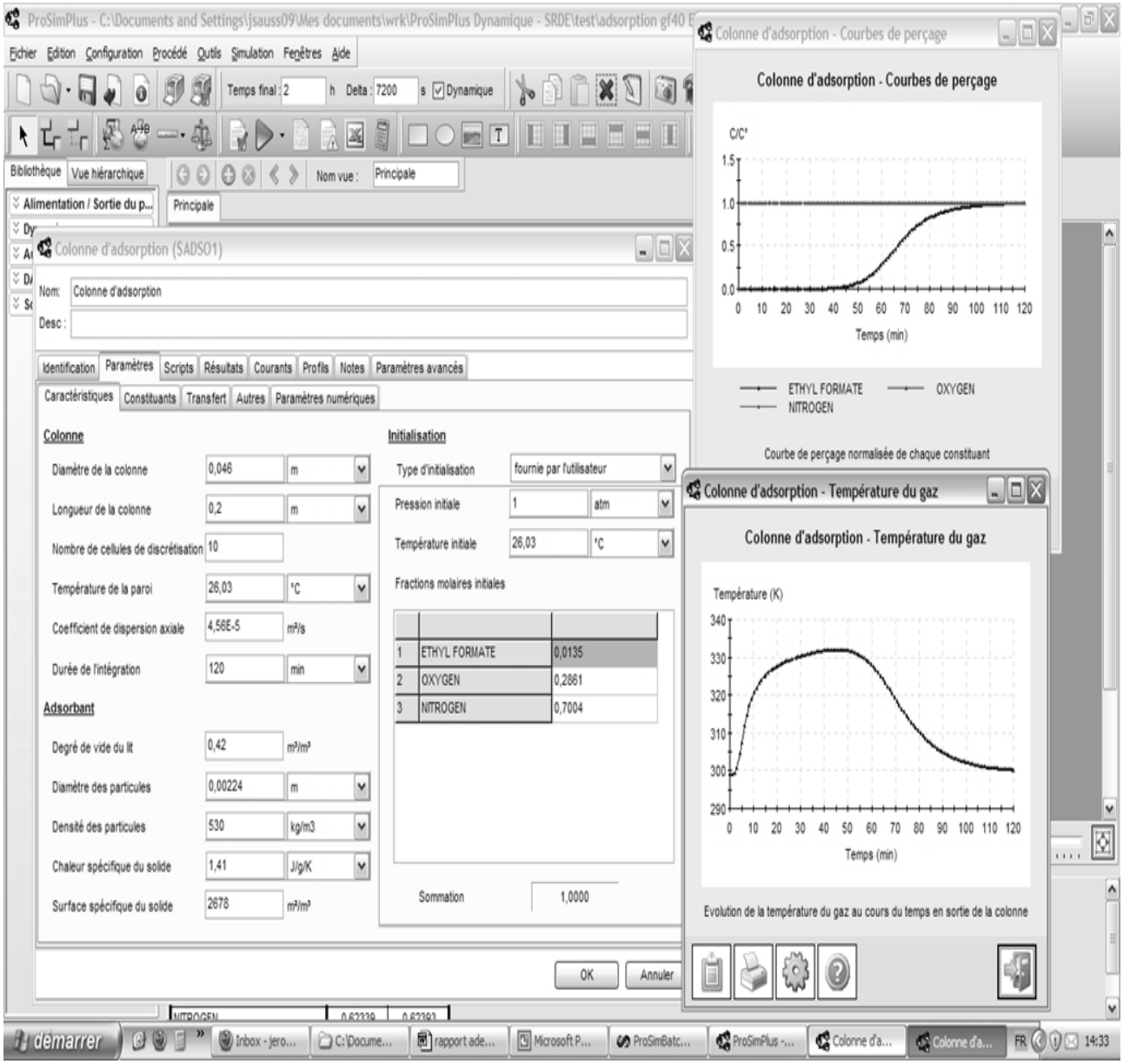

Figure 4.5 – Different data entry sections in the simulation interface

The simulation model is developed in order to have minimum adjustable parameters in the model. The entry data like physico-chemical properties of VOCs, characteristics of activated carbon,

dimensions of the column, isotherm equilibrium data, operating conditions of adsorption and regeneration are fixed in the beginning of the simulation.

The external mass transfer coefficient (K_f) was computed from the correlation from Petrovic and Thodos [12]. The heat transfer coefficient of the gas to adsorbent (h^p) is calculated by the Satterfield correlation [12] and the heat transfer coefficient of gas to the adsorption wall (h^w) is calculated by the correlation Leva's correlation [12].

4.5.3. Adjustable variable in the simulation model

The effective diffusion coefficient between gas to solid (D_{gl}) takes into account the various elementary diffusion mechanisms which control the migration of the organic component to the adsorption sites (porous, Knudsen, and surface diffusion). The effective diffusion coefficient could be very difficult to obtain theoretically for different VOC – activated carbon because of its complex mechanism and it had been already explained in the literature review. It is here considered as the only one adjustable parameter, which remains unchanged whatever the sense of migration of the molecules, towards or backwards the adsorption sites. This value is adjusted in a way such that the simulation results have the least possible error with the experimental results of adsorption and regeneration.

4.5.4. Results analysis after the simulation execution

After entering the different data (listed in the section 4.5.2) and also initializing the data such as effective mass transfer coefficient, the simulation model is executed to run for the calculations with the numerical analysis method. Once the simulation is complete, it is possible to look for results such as breakthrough curve, VTSA regeneration profile, and temperature profiles of adsorption and regeneration. An example of results of breakthrough curve and temperature profile of dichloromethane – ACM404 system from the interface is shown in the figure 4.3. In addition to the results, the simulation interface is programmed to create automatic excel sheets of concentration and temperature profiles of the adsorption and regeneration cycles. This will be used for calculating the different results of the adsorption and the regeneration steps.

4.5.5. Development of simulation model equations

The adsorption-desorption process was described by first deriving the mass and energy balances for each step, accounting for the axial dispersion of mass and heat. Radial velocity, temperature and concentration gradients are assumed as negligible. The main equations and their respective assumptions used are described below [2, 4].

Mass balance and Linear Driving Force (LDF) equations

The mass balance and linear driving force are exactly the same which was presented in the literature review section. In the following section, the improvement of the simulation model will be presented. The global resistance to the mass transfer embodies the partial resistances to the transfer of the VOC at the external surface of the particles and within the intra-granular porous volume. Assuming a combination in series of the external and internal mass transfer resistances, the following expression can be proposed [1,2, 4]:

$$\frac{1}{K} = \frac{\rho_p V_m q_i^*}{K_f a_p y} + \frac{r_p}{5 D_{gl} a_p} \qquad (4.7)$$

K - global mass transfer coefficient, s^{-1}; K_f - external mass transfer coefficient $m.s^{-1}$; V_m - molar VOC volume, $m^3.mol^{-1}$; q_i^* - amount of VOC adsorbed at the equilibrium $mol.kg^{-1}$; a_p - ratio between the external surface and the volume of the particle, m^{-1}; y - VOC molar fraction in the gas ; r_p - particle equivalent radius, m; D_{gl} - global mass transfer coefficient $m^2.s^{-1}$.

The external mass transfer coefficient K_f was computed from the correlation from Petrovic and Thodos [12]. The effective diffusion coefficient takes into account the various elementary diffusion mechanisms which control the migration of the organic component to the adsorption sites (porous, Knudsen, and surface diffusion). It is here considered as one adjustable parameter, which remains unchanged whatever the sense of migration of the molecules, towards or backwards the adsorption sites.

Energy balances

The energy balances were derived for each phase, accounting for the changes in the enthalpy of the gas and of the solid phases. The energy balance is further developed to add the regeneration heat exchange term ($T - T_p$) in the equations 4.4 and 4.5. The following are the assumptions involved in the energy balance of the system.

- Instantaneous local temperature equilibrium between gas and solid phases;
- Mean heat of adsorption, independent of the amount of VOC adsorbed;
- Enthalpy of adsorption = Enthalpy of regeneration;
- No radial heat transfer

In the gas phase:

The change in the enthalpy of the gas phase results from the heat transfers by convection and conduction with the solid particles and with the reactor walls:

$$-\rho_g D_L \frac{\partial^2 H}{\partial z^2} + \varepsilon\rho_g \frac{\partial H}{\partial t} + \varepsilon \frac{\partial(v\rho_g H)}{\partial z} + \frac{4}{d_c}\left[\frac{1}{h^p} + \frac{dc.\mathrm{e}}{(dc+e).\lambda}\right]^{-1}(T - T_w) + (1-\varepsilon)\frac{6h^p}{d_p}(T - T_p) = 0 \qquad (4.8)$$

T – gas temperature, K; H – enthalpy of gas phase, $J.kg^{-1}$; T_p – temperature of solid phase, K; ϱ_g – density of gas phase, $kg.m^{-3}$; Cp_g – specific heat capacity of gas phase, $J.kg^{-1}.K^{-1}$; h^w – heat transfer coefficient of wall, $W.m^2.K^{-1}$; h^p – heat transfer coefficient with solid, $W.m^2.K^{-1}$; d_c – diameter of the column, m; v – superficial gas velocity, $m.s^{-1}$; D_L – diffusivity ($D_H = \varrho_g .Cp_g.D_L$), $m^2.s^{-1}$; D_H – axial heat dispersion coefficient, $J.m^{-1}.s^{-1}.K^{-1}$

The heat transfer coefficient of the gas to adsorbent (h^p) is calculated by the Satterfield correlation [12] and the heat transfer coefficient of gas to the adsorption wall (h^w) is calculated by the correlation Leva's correlation [12].

In the solid phase:

In the solid phase, the change in the specific heat of the solid phase is computed taking into account the calorific capacities of the virgin carbon adsorbent and of the liquid adsorbed organic solvent. The generation term expresses the amount of heat, either released during the exothermal adsorption process or transferred during the desorption step:

$$(\rho_p Cp_p + \rho_p Cp_a q_i)\frac{\partial T_p}{\partial t} + \frac{6h^p}{d_p}(T_p - T) + \Delta H_i \rho_p \frac{\partial q_i}{\partial t} = 0 \qquad (4.9)$$

T – temperature of gas, K; T_s – temperature of solid, K; ϱ_p –bulk adsorbent density, $kg.m^{-3}$; ΔH_i – enthalpy of adsorption/desorption of the compound i, $J.mol^{-1}$; Cp_a – specific heat capacity of adsorbed phase, $J.kg^{-1}.K^{-1}$; Cp_p – specific heat capacity of the adsorbent, $J.kg^{-1}.K^{-1}$.

The enthalpy of adsorption is an important measure to understand the exothermal nature of the VOC adsorption and it could cause bed fires [13-16]. The adsorption enthalpy was derived according to the following statistical predictive model established [4]. It has been already discussed in the literature review section. As a first approximation, the integral enthalpy of desorption was assumed in absolute value to be equal to the one computed for the adsorption. This assumption may however be discussed as some experimental work reported in the literature, indicate some significant lowering in the desorption energies compared to the adsorption ones.

Ergun equation

The Ergun equation was introduced in the model in order to describe the total pressure drops occurring in the system [1-2]. It has been already described in the literature review section.

Numerical solving method

The model is composed of a set of fours partial differential equations (PDEs) describing the conservation laws: mass, energy and momentum transfer. In addition, constitutive equations were introduced in the model in order to express the rates of heat and mass transfers, as well as the equilibrium concentration distribution and the integral adsorption enthalpy. The PDE set was first reduced to a set of ordinary differential equations (ODEs) using the method of lines, which itself

was solved using the method of Gear [1,2, 4]. The discretization of the cells in the adsorption column is changed between 3 and 50. The model was implemented in the PROSIM software environment, which provides with the numerical method subroutines required to solve the equation set.

4.6. Results and Discussion

4.6.1. Results and discussion of adsorption step

The breakthrough curve of dichloromethane adsorption on ACM404 was measured during adsorption cycle and it was shown in the figure 4.6. Breakthrough curves represent the concentration of VOC (dichloromethane) start to rise in the exit of the column and it was measured by the FID. The amount of dichloromethane adsorbed was calculated by estimating the first momentum of the breakthrough curve. And the adsorption capacity can be calculated by the ratio of the mass of dichloromethane adsorbed to the mass of ACM404 (activated carbon). The adsorption capacity calculated by this method was found to be 31 % from the adsorption cycle. The breakthrough time was determined based on 10 % of the concentration of dichloromethane, which is set for adsorption in the inlet stream. The breakthrough time is 188 min as shown in the figure 4.6.

The dynamic adsorption capacity value (3.7 $mol.kg^{-1}$) was verified if it is close to the value of the equilibrium adsorption capacity value (3.9 $mol.kg^{-1}$). The dynamic adsorption capacity value was calculated by the ratio of dichloromethane in 'moles' to the mass of activated carbon in 'kg' and these values are taken from the dynamic adsorption experiments which generates the breakthrough curves. The equilibrium adsorption capacity was calculated by the ratio of dichloromethane in 'moles' to the mass of activated carbon in 'kg' and these values are taken from the equilibrium adsorption isotherm experiments which are conducted at 20, 40, 60, and 80°C. The error deviation between the dynamic and equilibrium adsorption capacity was found to be 5 %.

The simulation model PROSIM was executed to compare the results of the experimental and simulated break through curve, temperature profile (placed at 105 cm in the activated carbon

bed) and it is shown in the figures 4.6, 4.7. The simulation model results had a good agreement with experimental results and it has showed in figures 4.6 and 4.7. The mass transfer coefficient between the gas-solid (D_{gl}) is adjusted in the simulation model and the value is $0.008 m^2.s^{-1}$. The calculation of the adsorption capacity for the simulations having 3 and 50 discretization cells has remained the same value of 31%.

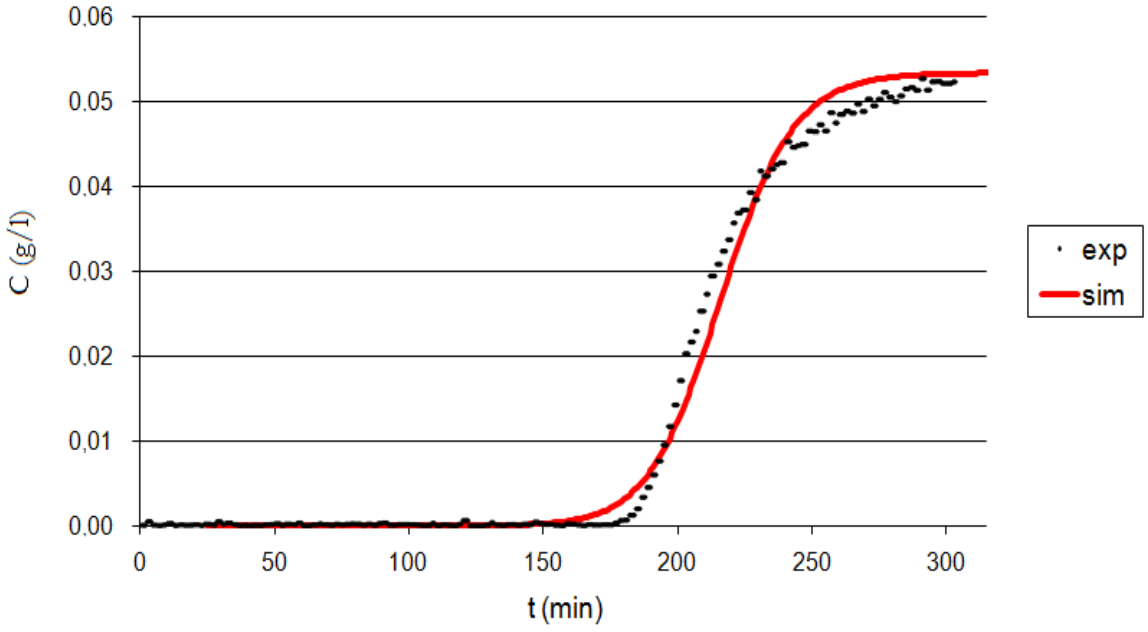

Figure 4.6 – Experimental and simulation breakthrough curves comparison

In figure 4.6, there was a slight deviation between the experimental and the simulation breakthrough curve and it could be explained because of the mass transfer coefficient between the simulation and experimental results. But the discrepancy percentage on the basis of mass of dichloromethane between the experimental and simulation results is less than 2 % and it can be neglected. In figure 4.7, there has been also good agreement of the temperature profile between the experimental and the simulation results.

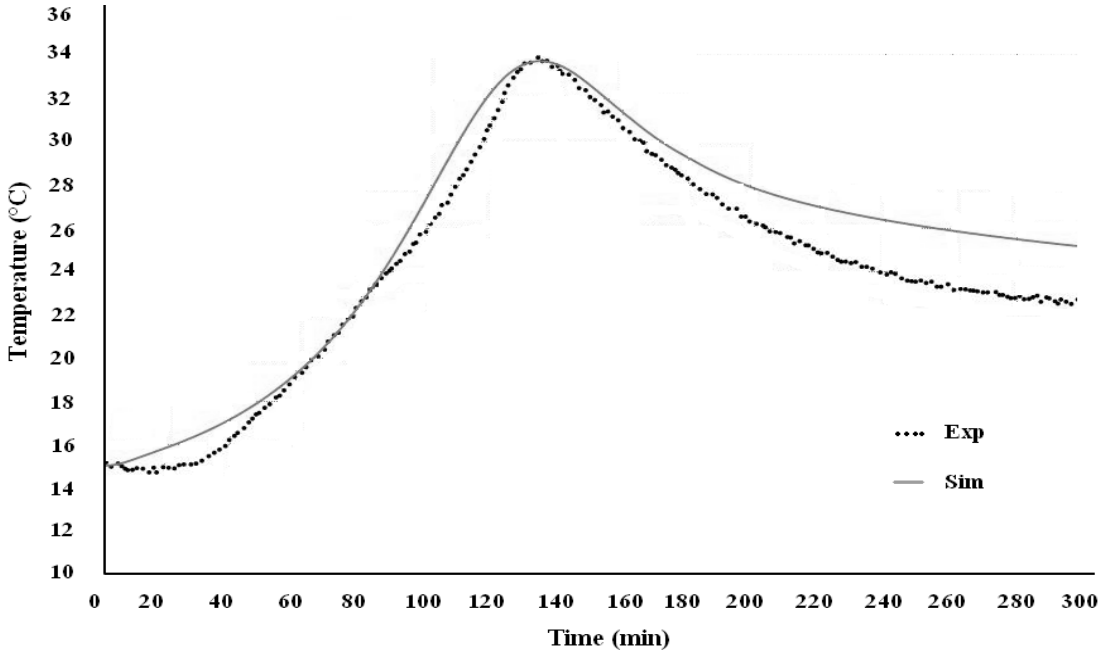

Figure 4.7 – Experimental and simulation adsorption temperature profile comparison

4.6.2. Results and discussion of regeneration step

In the regeneration profile (Figure 4.8), the first 40 minutes is the preheating of the column by hot oil bath by completely closing the column and then hot nitrogen is passed for regeneration. In figure 4.8, there is a clear shoot after hot nitrogen regeneration where the vacuum regeneration started. This jump occurs from the change in the flow rate of nitrogen (0.018 $L.sec^{-1}$) during the vacuum mode. The experimental regenerations and the corresponding simulation runs show that there was discrepancy of 10 – 12 % based on the calculated recovered dichloromethane mass. An example of regeneration temperature profile of the experiment and the simulation was shown in the Figure 4.8 and 4.9. The other results of regeneration profile at different operating conditions are given in the annexes. The validity (R^2) of the prediction of simulated regenerated dichloromethane mass to the experimental regenerated mass is 0.99 and it is shown in the figure 4.10. A similar graph is plotted between the average concentration of the simulation and the experiment and it is shown in the figure 4.11. It is interesting that the average concentration could be high, inspite of the low mass

of regeneration for example in regeneration trial 6 in table 4.5. This is due to the difference of flow rate of nitrogen used in the regeneration cycles.

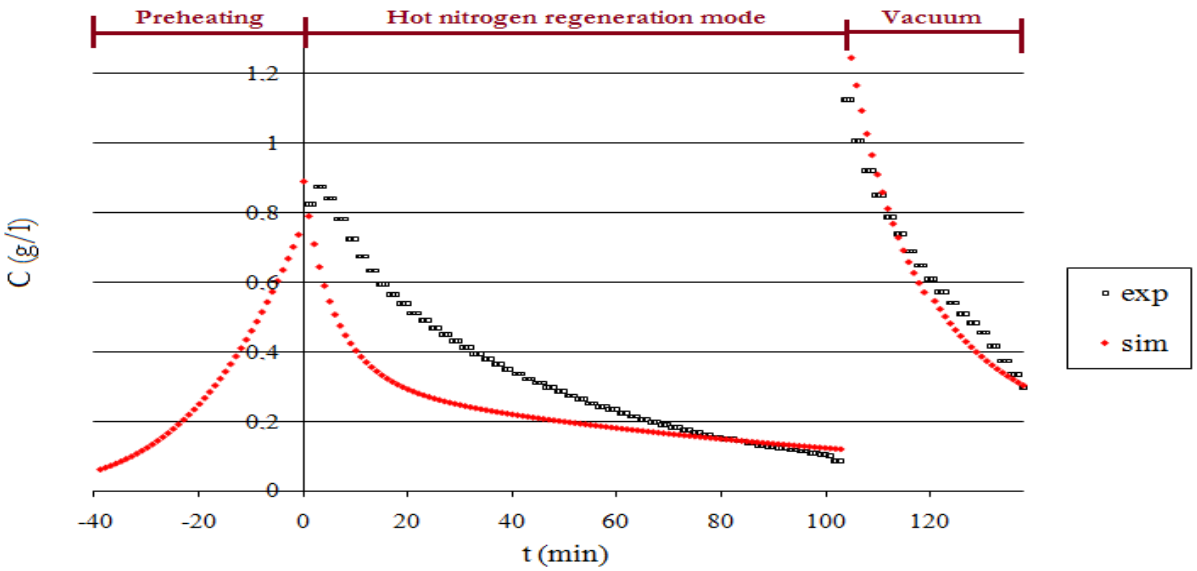

Figure 4.8 – Regeneration profiles corresponding to operating conditions in Table 7

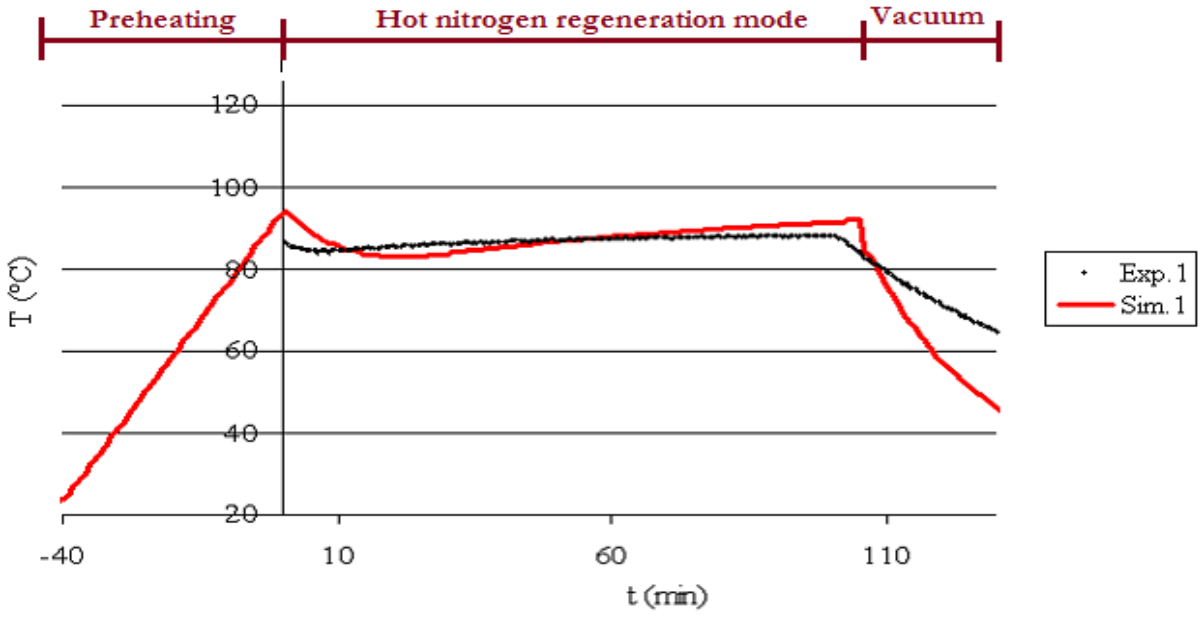

Figure 4.9 – Regeneration temperature profile at the exit of the column

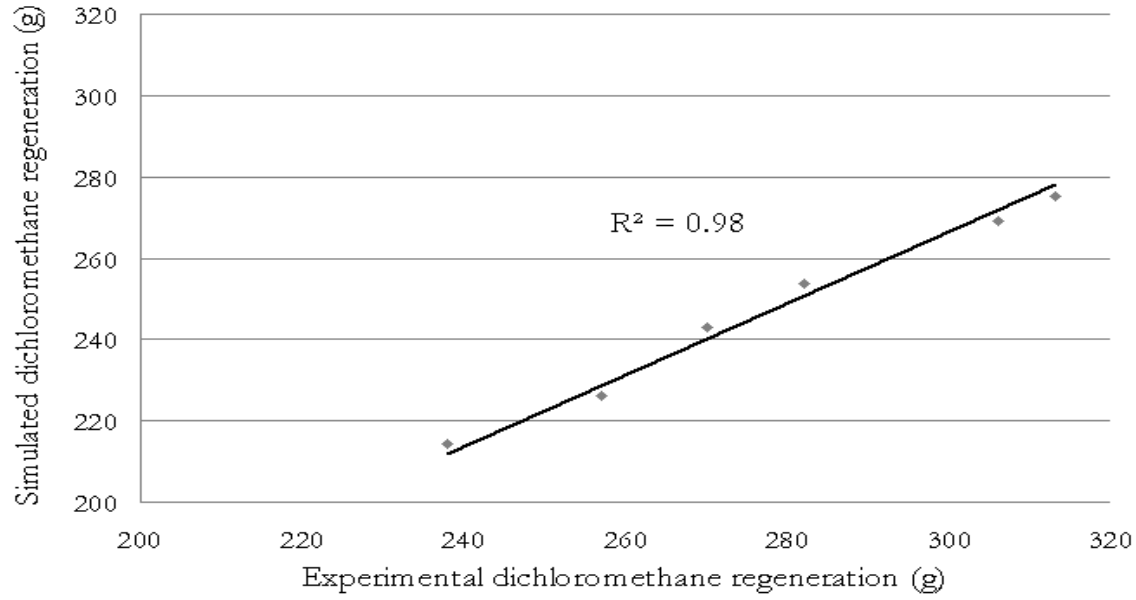

Figure 4.10 - Simulation and experimental results of regenerated mass of dichloromethane

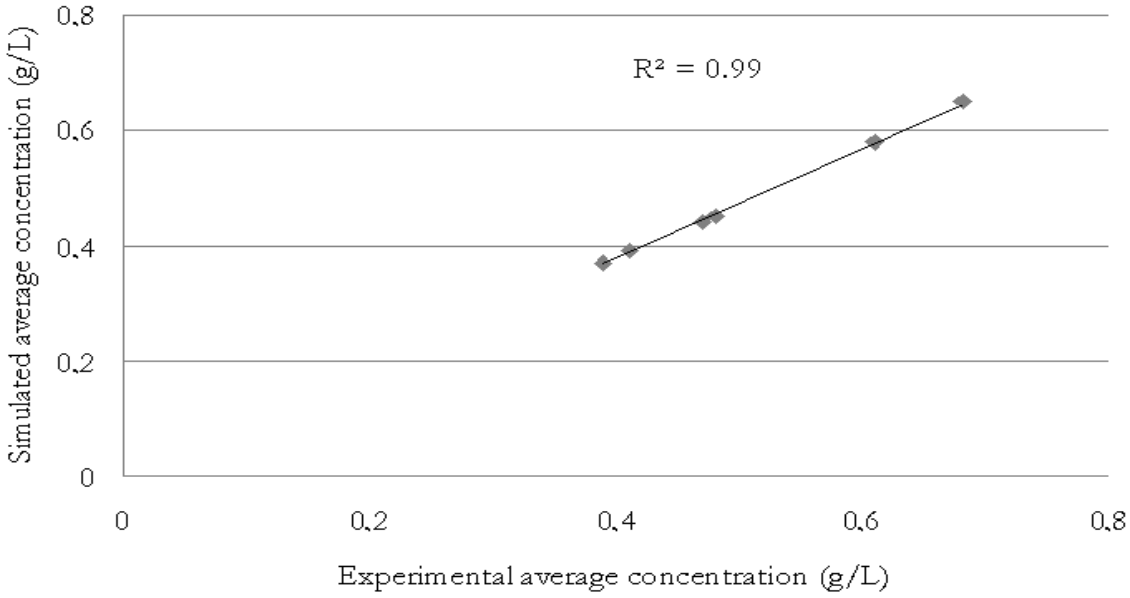

Figure 4.11 - Simulation and experimental results of average regenerated concentration of dichloromethane

4.6.3. Vacuum Cooling effect

Figure 4.8 illustrates that the vacuum regeneration (just after hot nitrogen regeneration) decreased the temperature difference of 33°C in the activated carbon bed. It will enable to save the cost and reduce the time of the cooling step and thus it proved the advantage of using vacuum regeneration in the combination mode.

4.6.4. Statistical analysis of regeneration results

The operating conditions (temperature of nitrogen, intermediate regeneration, and flow rate of hot nitrogen) of the six regeneration cycles and the corresponding FED responses which are measured as recovery efficiency (F_R) and operating costs ($OP_€$) are presented in the Table 4.5. The reason for two sets of 2x2 FEDs instead of just a 3x3 FED is that the flow rate of N_2 at 0.07 $L.sec^{-1}$ is too low to achieve the superior limit of intermediate regeneration of 75%. First set of FED – factors of temperature and intermediate regeneration (Table 4.5, experiments 1 to 4. And the second set of FED – factors of temperature and flow rate of N_2 (Table 4.5, experiments 3 to 6).

The influence of variation of each operating conditions on the recovery efficiency and operating costs were studied by using the FED. The variation of operating conditions such as temperature of nitrogen, intermediate regeneration, and flow rate of nitrogen have their inferior limit (-1) and superior limit (+1). Temperature of nitrogen = ($85_{[-1],}$ $93_{[+1]}$) in °C; intermediate regeneration = ($55_{[-1],}$ $75_{[+1]}$) in %; and flow rate of nitrogen = ($0.07_{[-1],}$ $0.14_{[+1]}$) in $L.sec^{-1}$.

Table 4.5 – Recovery efficiency and operating costs results

Exp.	Operating conditions FED Factors			FED Responses		Supplementary responses	
	T_{N2} (°C)	Flow N_2 ($NL.s^{-1}$)	I_R (%)	F_R %	$OP_€$ (€ cents)	$OP_€$ (€.kg^{-1})	Recovery ($g.min^{-1}$)
1	93	0.14	75	82	64	2.04	1.74
2	85	0.14	75	80	66	2.16	1.70

3	93	0.14	55	74	51	1.80	1.57
4	85	0.14	55	70	53	1.98	1.49
5	93	0.07	55	65	65	2.61	1.13
6	85	0.07	55	62	66	2.78	1.08

With the statistical package MINITAB, it was possible to check the statistical significance of the factors considered in the two sets of FED. The ANOVA were done for the two sets of FED by MINITAB and the solutions are presented as equations 4.10, 4.11, 4.12, and 4.13. The probability value p(f) from the analysis of variance is 8%. The effect of operating conditions such as T, I_R and V_f on recovery efficiency and operating costs could be visualized by comparing the significance of the coefficients of T, I_R and V_f from the equations 4.10, 4.11, 4.12, and 4.13.

It seems that the flow rate dominates the other factors in terms achieving high recovery efficiency and also significantly reducing the operating cost. The factor intermediate regeneration plays a critical role in achieving high recovery efficiency, but it increases the operating costs. The increase in the operating cost was justified by obtaining higher recovery efficiency and so that the number of successive regeneration cycles can be reduced. The interaction effect of temperature and the intermediate regeneration was very low in both cases of recovery efficiency and operating costs and it can be noticed from the value of coefficient of $T.I_R$ from equations 4.10 and 4.11. From equations 4.12 and 4.13, the interaction effects of temperature and flow rate (T.Vf) were not significant. The first FED set with temperature of nitrogen (T) and intermediate regeneration (I_R) as factors

$$F_R = 76.5 + 1.5.T + 4.5.I_R + 0.5.T.I_R \quad (4.10)$$

$$OP_{€\ cents} = 58.3 - 0.7.T + 6.3.\ I_R + 0.25.T.I_R \quad (4.11)$$

F_R – recovery efficiency; $OP_{€\ cents}$ - Operating Costs

The second FED set with temperature of nitrogen (T) and flow rate of nitrogen (V_f) as factors

$$F_R = 66.3 + 2.3.T + 5.8.V_f - 0.25.T.V_f \quad (4.12)$$

$$OP_{€\ cents} = 65 - 1.T - 13.V_f \quad (4.13)$$

Also, from the table 4.5, it is clear that the recovery efficiency (82%), average regeneration rate (1.74 $g.min^{-1}$) for regeneration 1 was the best operating conditions among the other conditions. The cost was slightly higher than regeneration 3, but it regenerates significantly more than the other experiments. This will also result in retaining good adsorption capacity in the successive adsorption cycle.

4.7. Conclusions

FED was an effective tool to understand how the operating conditions of regeneration influences in the objectives of achieving higher recovery efficiency at an optimized operating cost. The influence of flow rate of hot nitrogen has been significant in increasing the recovery efficiency and decreasing the operating cost [10-11]. The increase of intermediate regeneration has enabled to achieve maximum recovery efficiency at a shorter total regeneration time. By achieving higher recovery efficiency, it maintains the higher adsorption capacity for the successive cycles of adsorption. The temperature impact was slight (because of slight variation of temperature range 85 – 93 °C) in terms of achieving higher recovery efficiency and optimized operating cost. It could have been interesting, if the heating equipments of higher capacity could have been used, so that the temperature of nitrogen could reach up to 170°C during thermal regeneration mode. The effect of vacuum regeneration was proven in terms of (1) achieving further effective recovery of dichloromethane after the thermal regeneration mode; (2) cooling of activated carbon bed significantly. It could be more interesting to study the 3x3 FED factors effect (temperature of nitrogen, intermediate regeneration and the flow rate of nitrogen) in one design approach of experiments by increasing the capacity of heating equipments.

References

[1] T. Boger, A. Salden, G. Eigenberger. A combined vacuum and temperature swing adsorption process for the recovery of amine from foundry air, Elsevier - Chemical Eng. and Pro. 1997, 36: 231-42

[2] J.F. Nastaj, B. Ambrożek, J. Rudnicka. Simulation studies of a vacuum and temperature swing adsorption process for the removal of VOC from waste air streams, Elsevier – Interna. Comm. of heat and mass transfer. 2006; 33: 80 - 6

[3] P.M. Berthouex, and L.C. Brown, Statistics for Environmental Engineers, Lewis Publishers, USA, 2002

[4] S. Giraudet, Exothermicity of adsorption of volatile organic compounds in fixed activated carbon beds: modelling and simulation valdiation of experimental work, PhD dissertation, EMN, France, 2006

[5] D.M. Ruthven, Principles of adsorption and adsorption processes, John Wiley & Sons: New-York, Univ of New Brunswick: Fredericton, USA, 1984

[6] E.W. Washburn, Note on method of determining the distribution of pore sizes in a porous material. Proc.Nat. Acad. Sci 1921; 7: 115 -16

[7] J. Keller, R. Staudt, Gas Adsorption Equilibria, Universitat Siegen. Springer, USA, 1994

[8] J.H. Maindonald, Using R for Data Analysis and Graphics, Introduction, code and commentary, R- Stat, http://cran.r-project.org/doc/contrib/usingR.pdf, 2008

[9] GRL ARKEMA, Data sheets of tarrifs and equipment details of VTSA pilot plant, France, 2010

[10] J. Ho, D. Choi, H. Moon. Benzene adsorption and hot purge regeneration in activated carbon beds, Elsevier - Chemical Eng. Sci. 2000; 55: 5857 - 72

[11] K.S. Hwang, D.K.Choi, S.Y.Gong, S.Y.Cho. Adsorption and thermal regeneration of methylene chloride vapor on activated carbon bed, Elsevier – Chemical Eng. and Pro. 1998; 46: 1111 - 23

[12] R.H. Perry *et al.*, Perry's Chemical Engineers Handbook, McGraw-Hill, New York, 2007

[13] F. Delage, P. Pre, P. Le Cloirec; Mass transfert and warming during adsorption of high concentrations of VOCs on an activated carbon bed: experimental and theoretical analysis, Environ Sci Technol. 2000; 34: 4816 - 21

[14] P. Pre, F. Delage, P. Le Cloirec; Modeling the exothermal nature of V.O.C. adsorption to prevent activated carbon bed ignition, Fundamentals of Adsorption 2001; 7: 1172 – 85

[15] S. Giraudet, P. Pre, P. Le Cloirec; Modeling the Heat and Mass Transfer in Temperature Swing Adsorption of Voatile Organic compounds on to Activated Carbons, Environmental Science and Technology 2009; 43: 1173 - 79

[16] J. Wu, L.G. Hammarstrom, O. Claesson, I. Fangmark, Modeling the influence of physico-chemical properties of volatile organic compounds on activated carbon adsorption capacity. Elsevier – Carbon 2003; 41: 1322 – 25

5. Experimental and Modeling of Temperature Swing Adsorption (TSA)

Inspite of the high regeneration performance (82%) of the vacuum temperature swing adsorption process from the previous section, it has the limitation in terms of capital costs such as additional vacuum pump, hot oil bath, valves, different nitrogen supply lines, during hot nitrogen regeneration and vacuum regeneration, and complex controls of the process over Temperature Swing Adsorption (TSA). In the following section, the objectives of the TSA process, dynamic TSA experimental setup, and dynamic experimental and simulation results will be discussed.

5.1. Objectives

The objectives of this chapter are: (1) to evaluate and compare the performances and the operating costs of hot nitrogen for 3 VOCs (acetone, dichloromethane, and ethyl formate) and 3 activated carbons; (2) to validate the experimental results of adsorption and regeneration by simulation model PROSIM; (3) compare the regeneration performance of different families of VOCs – activated carbon system under same hot regeneration operating conditions by FED results of ANOVA equation [1]; (4) to evaluate the steam regeneration operating conditions for the VOCs – activated carbon systems

5.2. Selection of VOCs - activated carbon systems

The VOCs are selected based on the criteria (1) extremely hazardous causes cancer (Dichloromethane); (2) mostly used solvents in paint, oil /gas, chemical, pharmaceutical industries (Acetone and Ethyl formate). The activated carbons are selected based on: (1) the characteristics of activated carbon; (2) activation method and time (3) raw material (4) mean diameter of the carbon particle [ACV 404, ACM 404 = 4mm, BC 120 = 0.6mm].

5.3. Characterization of activated carbons

Three different activated carbons (such as ACV 404, ACM 404, and BC 120) are selected for this section of dynamic TSA process. They are selected in such to represent the diverse criteria such as: raw material; surface area; micropore volume; meso and macropore volume; activation method. All the characterization methodologies and results of the activated carbons could be referred in the chapter 3 [4-6].

5.4. Temperature Swing Adsorption (TSA) experimental setup

5.4.1. Adsorption step

Figure 5.1 shows the experimental setup of Temperature Swing Adsorption (TSA). It has an adsorption column with the dimension of 0.275m high x 0.05m internal diameter. Thermal couples are located at 3 various ports (at 2 cm, 19 cm and 25 cm from the top of the column) in the column to record the temperature data during adsorption and regeneration cycles. In the event to avoid heat losses, the column was insulated by 2 cm thick glass wool. During the adsorption step, 30 $g.m^{-3}$ of VOC concentration (acetone, dichloromethane and ethyl formate) are prepared by the VOC generating system (includes the two air streams, one for lifting the vapors of dichloromethane in the reservoir and the other for dilution, and enters the column at temperature = 25.8 °C). The flow meters which is used for connecting the adsorption column and the equipments is BROOKS mass flow controller 5851. The concentration of the VOC was measured and calibrated by using by a commercial Flame Ionization Detector (FID) called CAMBUSTION HFR-400FFID. For the calibration curve, different volume samples (from 10 – 400 µl) are injected into a glass balloon of 1L volume. The mass of VOC is calculated by multiplying density of VOC and volume of VOC injected in the glass balloon. Once having the value of VOC mass, the concentration ($g.m^{-3}$) is calculated by the ratio of mass of VOC to the volume of the glass balloon. Hence, a linear calibration curve of concentration of VOC ($g.m^{-3}$) Vs FID response (volts) could be established for the dynamic experiments. The superficial velocities of the adsorption gas corresponding to acetone, ethyl formate and dichloromethane are 0.24, 0.23 and 0.26 $m.s^{-1}$ respectively [2,6,7]. The temperatures in the activated carbon bed are monitored to observe the risks of bed fires during

adsorption and regeneration steps and also to compare with the simulation results of the TSA system [8-10].

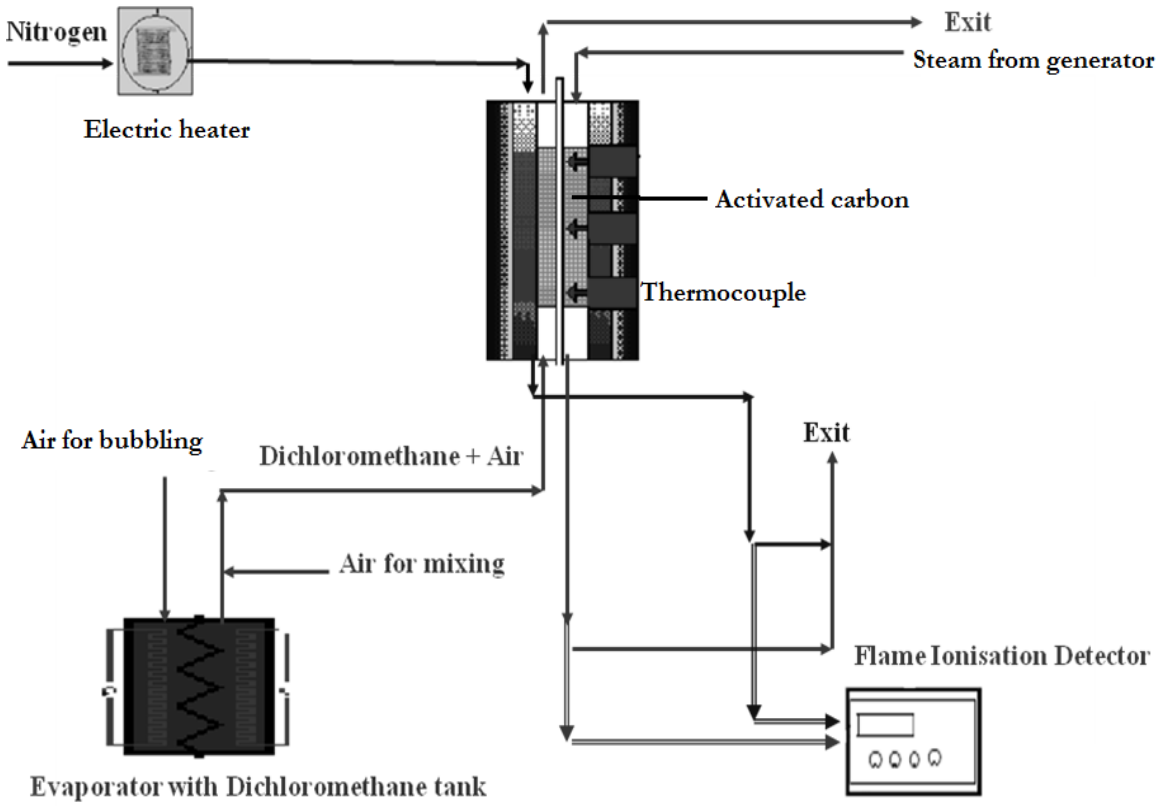

Figure 5.1 - Experimental setup of dynamic temperature swing adsorption pilot plant

5.4.2. Hot nitrogen regeneration TSA

Once after the adsorption step, the activated carbon is regenerated by hot nitrogen. The nitrogen is heated by a 2 kW electric heater. FED has allowed to construct 2x2 design by changing the operating conditions such as temperature of the nitrogen in the range [130 < T < 170°C] and the superficial velocity of the nitrogen in the range [0.10 < v < 0.17m.s^{-1}]. By doing Analysis of Variance (ANOVA) for the four experiments of regenerations with the statistical analysis software MINITAB, the regeneration efficiency (R_E) and the operating cost ($OP_€$) are measured as a function

of the operating conditions (T, v) by a mechanistic model. The operating cost was calculated on the basis of the nitrogen consumption (0.18€.m^{-3}, Supplier - Air Liquide) and the energy costs for heating nitrogen (60 €.Mwh^{-1}, French electricity tariff) [5]. Since the regeneration on three different families of VOCs has been performed with the same operating conditions, the results of ANOVA equation from FED will be very interesting to compare the regeneration performance and operating cost by using the microporous activated carbon.

5.4.3. Steam regeneration TSA

For the steam regeneration, a MAC STM series flow meter had been engaged to measure the volumetric flow rate of hot steam. The steam is generated by the commercial generator NEMO AURA Industrie Art.164.A and the maximum capacity of steam generation is 3 $kg.hr^{-1}$. The pressure of the hot steam at the entrance of the column could be adjusted to 2.7 bars. By adjusting the flow rate to 2.7 bars, the steam flow rate is equivalent to 0.833$g.s^{-1}$ at 140-200 °C [12].

Before starting the steam regeneration of dichloromethane, the flow of condensed steam was measured by the presence of activated carbon in the bed. The dichloromethane which was regenerated later will come along with steam (total flow). So the volume of the dichloromethane could be measured from the difference of the volume of total flow and condensed steam. And it had been also cross checked because of the insolubility of dichloromethane with water. This method of measuring dichloromethane has been implemented, because of the measuring troubles caused by the steam, which were condensed along the FID ports on the column and enters the opening of the FID. The operating cost of steam is calculated based on the tariff for water.

The operating cost was calculated on the basis of energy required for the steam (2722 KJ/kg of steam, NIST and the enthalpy value corresponds to the temperature (140°C) and pressure of the steam (2.7bars), electricity tariff in France (60€.Mwh^{-1}), cost of drying (drying time = 1 hour), and cost of water (used for the production of steam) in France (3€.m^{-3}) [5]. The heating cost during drying step had been calculated based on the amount of heat energy spent to eliminate the moisture in the bed by passing hot air.

5.5. Results and Discussion – experiments and simulations of TSA

5.5.1. Comparison of adsorption of dichloromethane on ACV404/ACM204/BC 120 systems

Here in this section, a comparison is drawn on the dichloromethane adsorption performance on the different activated carbons and also their corresponding simulation results.

Adsorption step of dichloromethane – ACV 404 system:

The dynamic adsorption capacity was calculated by the ratio of mass of dichloromethane adsorbed to the mass of activated carbon in the column. The mass of ACV404 is 250 g and so dynamic adsorption capacity was found to be 35 percent of the mass of dichloromethane adsorbed. It could also be represented as 4.02 $mol.kg^{-1}$. This dynamic adsorption capacity value could be compared with the equilibrium isotherm adsorption capacity at 20 °C to justify that there is not a significant deviation between the dynamic and the static state of adsorption. The value of equilibrium isotherm adsorption capacity was 4.2 $mol.kg^{-1}$ and so the error percentage was 4.3 %. The breakthrough time was calculated at the point, when the concentration at the exit of the column reaches 10 percent of the initial concentration (30 $g.m^{-3}$). So it was found to be 80 min. Figure 5.2 shows the breakthrough curve of the experimental (represented as Exp) and the simulation (represented as Sim) results.

From the Figure 5.2, it is clear that the simulation model predicts well the experimental points to give the similar breakthrough time and adsorption capacity. But there was dispersion at 90 min between the experimental and simulation points. From this point, the simulation model could under predict the mass transfer coefficient of the gas to the solid compared to the experimental points. The mass transfer coefficient of dichloromethane – ACV 404 system (D_{gl}) is adjusted as 0.009 $m^2.s^{-1}$. Figure 5.3 shows an example of the exit temperature profile (at the exit of the column 25cm) of the adsorption of dichloromethane on ACV 404. In general there was only a negligible temperature difference of 2°C between the simulation model and the experiment. The adsorption isotherm results of the three systems dichloromethane – ACV404/ACM204/BC120 are summarized in the annexes sections.

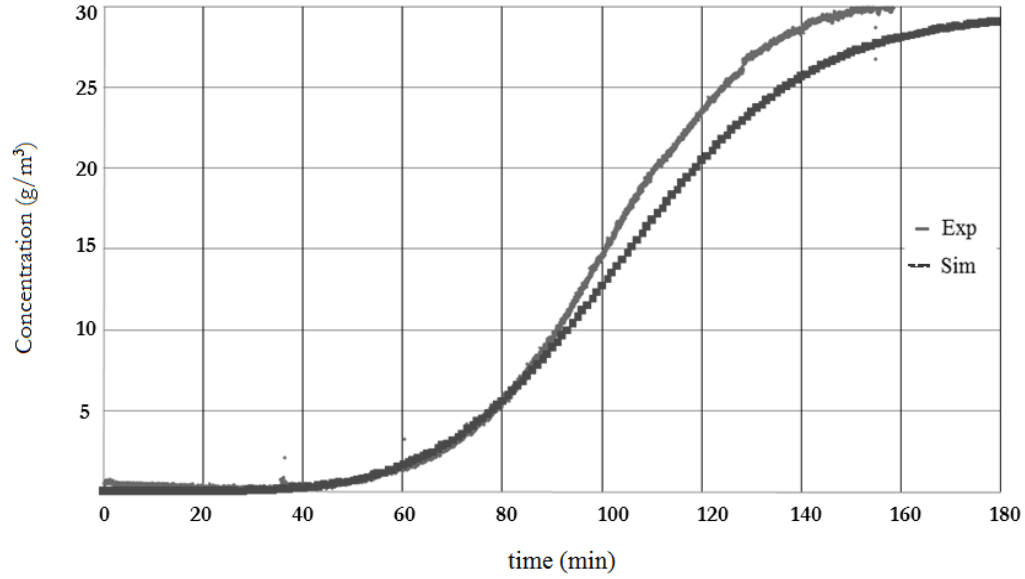

Figure 5.2 - Breakthrough curve of dichloromethane – ACV404: experiment and simulation

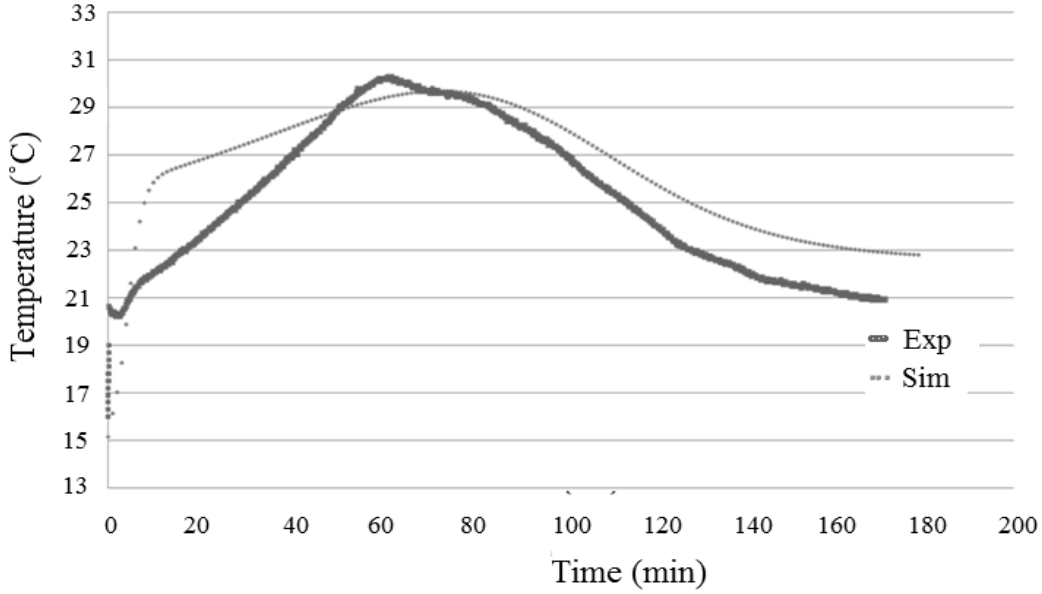

Figure 5.3 – Temperature profile of dichloromethane – ACV404: experiment and simulation

Adsorption step of dichloromethane – ACM 204 system:

The ACM 204 activated carbon is filled in the activated carbon and the mass of ACM 204 is 270 g. The adsorption capacity and the breakthrough time of the dichloromethane - ACM204 were found to be 22.1 percent / 2.6 mol.kg^{-1} and 44 min. The simulation results have a good agreement

with the experimental breakthrough profile and the temperature profile (Figures 5.4, 5.5). The mass transfer coefficient of dichloromethane – ACM 204 system (D_{gl}) is adjusted as 0.003 $m^2.s^{-1}$.

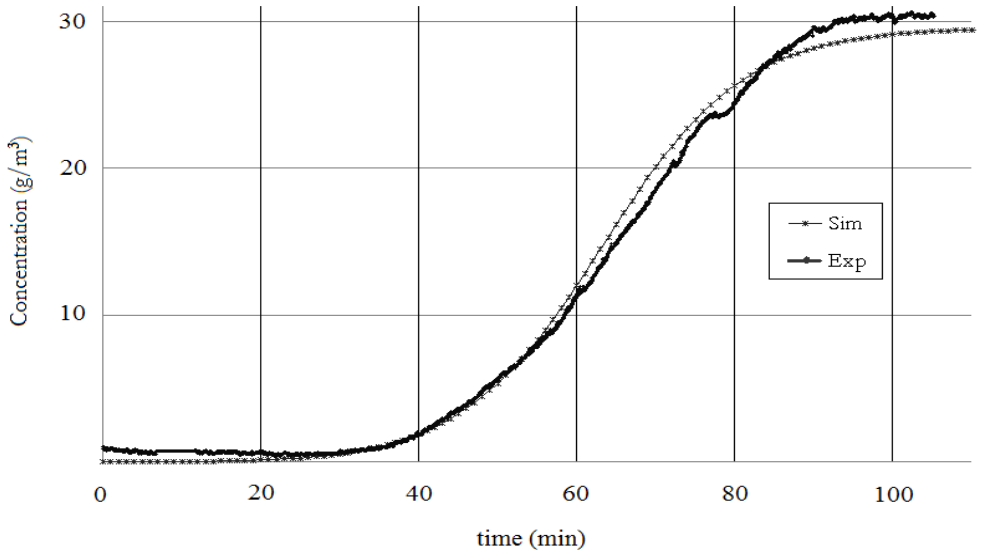

Figure 5.4 - Breakthrough curve of dichloromethane – ACM 204: experiment and simulation

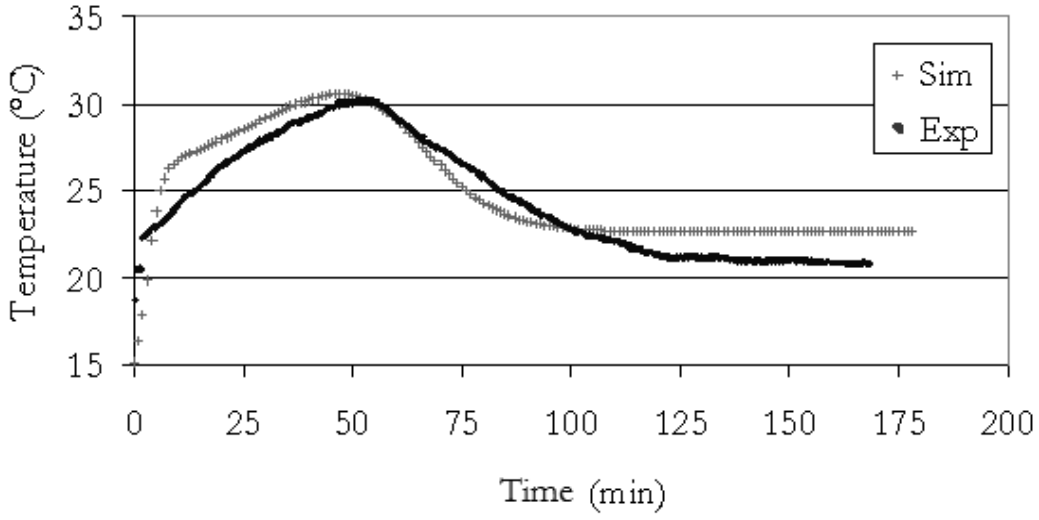

Figure 5.5 – Temperature profile of dichloromethane – ACM 204: experiment and simulation

Adsorption step of dichloromethane – BC 120 system:

The ACM 204 activated carbon is filled in the activated carbon and the mass of ACM 204 is 102 g. The mass filling of BC 120 is twice less than ACV404, because the bulk density of BC 120 (260 $kg.m^{-3}$) is almost twice less than their counter parts [ACV404 (530 $kg.m^{-3}$) and ACM204

(590kg.m^{-3})]. The adsorption capacity and the breakthrough time of the dichloromethane - ACM204 were found to be 36.1 percent / 4.24 mol.kg^{-1} and 34 min. The mass transfer coefficient of dichloromethane – BC 120 system (D_{gl}) is adjusted as 0.01 m^2.s^{-1}.

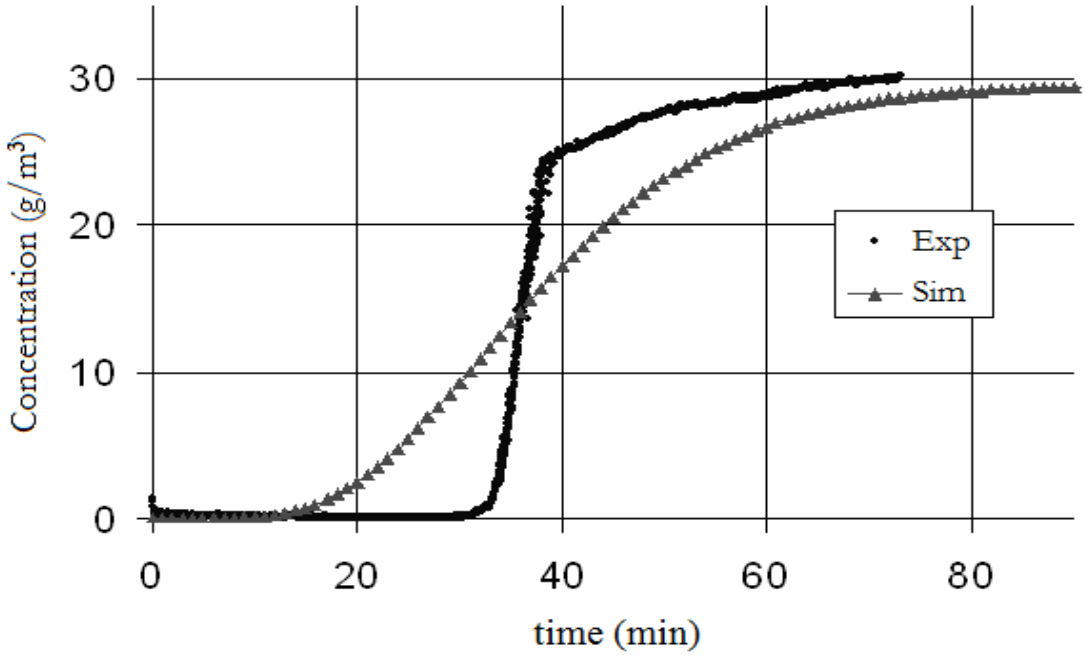

Figure 5.6 – Breakthrough curve of dichloromethane – BC 120: experiment and simulation

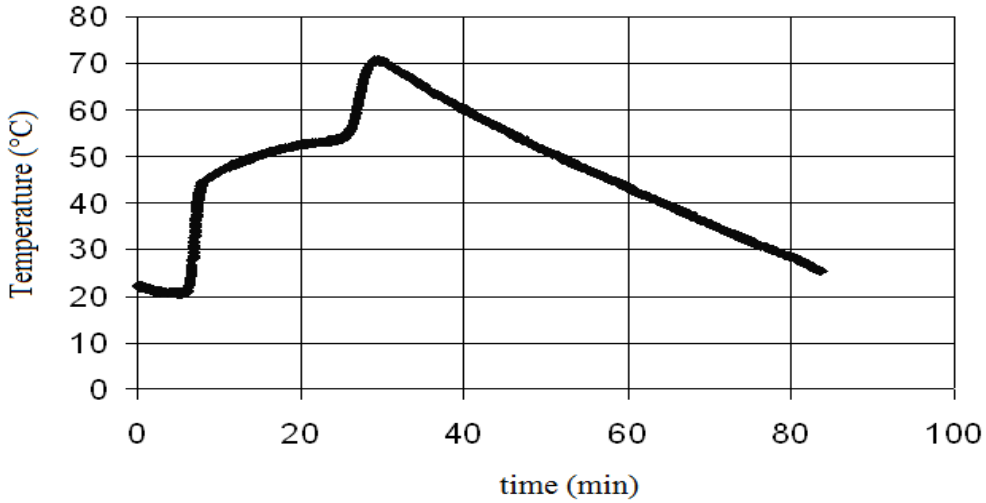

Figure 5.7 – Experimental temperature profile of dichloromethane – BC 120

From the breakthrough profile (Figure 5.6) of dichloromethane – BC 120, it there is a difficulty in predicting the breakthrough time, inspite of the fact the capacity of adsorption at complete saturation in both simulation and experiment remains the same. Inspite of all trial outs with in the simulation tool to change the mass transfer coefficient (D_{gl}), external mass transfer coefficient (K_f) and giving values for axial dispersion coefficient, still the simulation results has not represent the experimental profile. Similarly the problem in temperature is evident, because there are two jumps in the temperature profile, where as in the simulation it was like in the case of ACV 404 and ACM 204. The reasons could be: (1) the size of the particle (0.6 mm) could have caused more turbulence than the others (4 mm). So the mass transfer model could be invalid to show the sharp rise in the breakthrough curve; (2) BC 120 is chemically activated carbon and so the detail (different functional groups on the surface of BC120) is not included in the simulation tool. So it could be an explanation for the temperature profile. And these details are often very complicated to include in the simulation tool; (3) BC 120 is really micropores (Table 5.1) compared to its counterparts ACV404 and ACM204. This could be reason that the breakthrough rise momentum in BC120 is sharp and steep (Figure 5.6) than its counterparts.

To conclude, because of the low bulk density (will cause two times the capital cost for adsorption beds compared to using ACV 404) for dichloromethane – BC 120 system, ACV 404 could be preferred to BC 120 in this TSA application. ACV 404 is the outperforming material in terms of: (1) high adsorption capacity (4.2 $mol.kg^{-1}$); (2) high bulk density (530 $kg.m^{-3}$); (3) good simulation representation of experimental results of breakthrough curves and temperature profile.

5.5.2. Comparison of hot nitrogen regeneration results of dichloromethane from ACV404/ACM404/BC120 systems

Regeneration step of dichloromethane – ACV 404 system:

Table 5.1 summarizes all the operating conditions of the hot nitrogen regeneration experiments and the corresponding results such as regeneration efficiency (R_E), Operating Cost ($OP_€$). The regeneration efficiency was calculated by the ratio of mass of dichloromethane regenerated to the mass of the dichloromethane adsorbed. The average regeneration rate ($\sum R_R$) was calculated (Table 5.1) to represent as the average speed of regeneration during the cycle of 60 min.

The operating cost was calculated on the basis of the nitrogen consumption (0.18 €.m^{-3}, Supplier - Air Liquide) and the energy costs for heating nitrogen (60 €.Mwh^{-1}, French electricity tariff).

Table 5.1 – Regeneration operating conditions and results for dichloromethane – ACV 404 system

Regeneration Experiments	Operating Conditions		Regeneration %	Operating cost	Avg. Reg. Rate
	T (°C)	v (m/s)	R_E (%)	$OP_€$ (€/kg)	$\sum R_R$ (g.min^{-1})
Reg.1	170 (+)	0.17 (+)	84.8	3.44	1.30
Reg.2	170 (+)	0.10 (-)	58.9	3.31	0.88
Reg.3	130 (-)	0.17 (+)	66.9	4.35	1.00
Reg.4	130 (-)	0.10 (-)	48.2	4.04	0.72
Reg.5	150 (=)	0.14 (=)	66.5	3.68	0.99

The signs (+) and (-) in the Table 5.1 indicates the two ranges of the operating conditions for the FED and they were chosen based on the preliminary experiments. Since it was a 2x2 FED, there had been 4 regeneration experiments (Reg.1, Reg.2, Reg.3, and Reg.4) as shown in the Table 3. Regeneration experiment Reg.5 (=) (acts as a central point of the FED) had been performed to check the statistical validity of the mechanistic model obtained by performing ANOVA on the regeneration experiments Reg.1, Reg.2, Reg.3, and Reg.4. Regeneration time was always fixed at 60 min for all cycles. The mechanistic models for evaluating regeneration efficiency (R_E) and the operating cost ($OP_€$) obtained by doing an ANOVA with the MINITAB software were as follows:

$$R_{E\,\%} = 64.7 + 7.15.T + 11.15.v + 1.8.T.v \qquad (5.1)$$

$$OP_{€\,(€/kg)} = 3.79 - 0.41.T + 0.11.v - 0.05.T.v \qquad (5.2)$$

From the equation 5.1, it could be concluded that the superficial velocity of the nitrogen (v) has influenced more on achieving higher regeneration than the nitrogen temperature (T). The influence could be compared by the coefficient of the corresponding coefficients of the operating conditions (T, v) in equation 5.1. From the equation 5.1, it could be concluded that an increase in temperature of nitrogen could decreased the operating cost. This was due to the fact of increasing

the temperature had increased the regeneration of dichloromethane and decreased the regeneration time. The decrease in regeneration time has strictly implied less consumption of nitrogen. Regeneration experiment Reg.5 had the operating conditions in the central point of FED (T = 150 °C, v = 0.136 $m.s^{-1}$). The experimental results were compared with the mechanistic models and the error percentage of the mass o regeneration is 3.5 %. This shows that the mechanistic model was really statistically and realistically consistent with the range of operating conditions chosen. An example of simulation results of regeneration concentration and temperature profile is shown in the Figures 5.8 and 5.9.

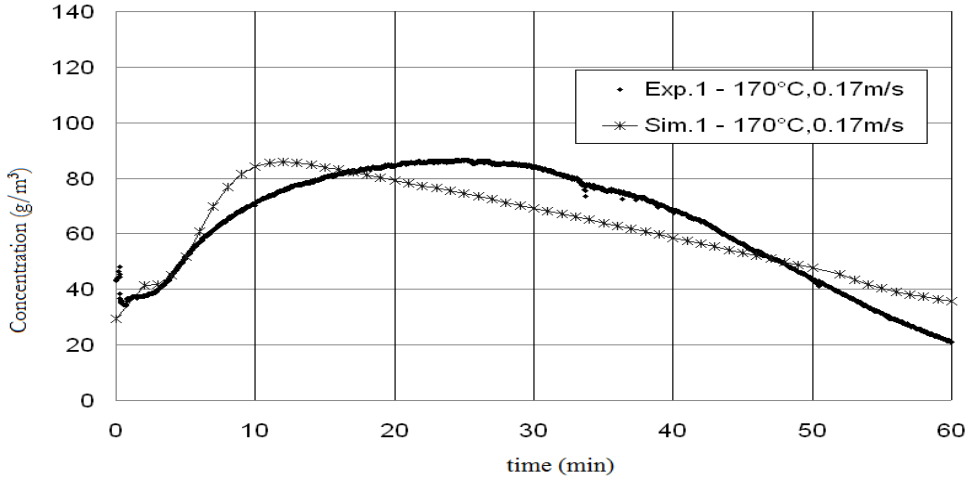

Figure 5.8 – Regeneration profile of dichloromethane – ACV 404: experiment and simulation

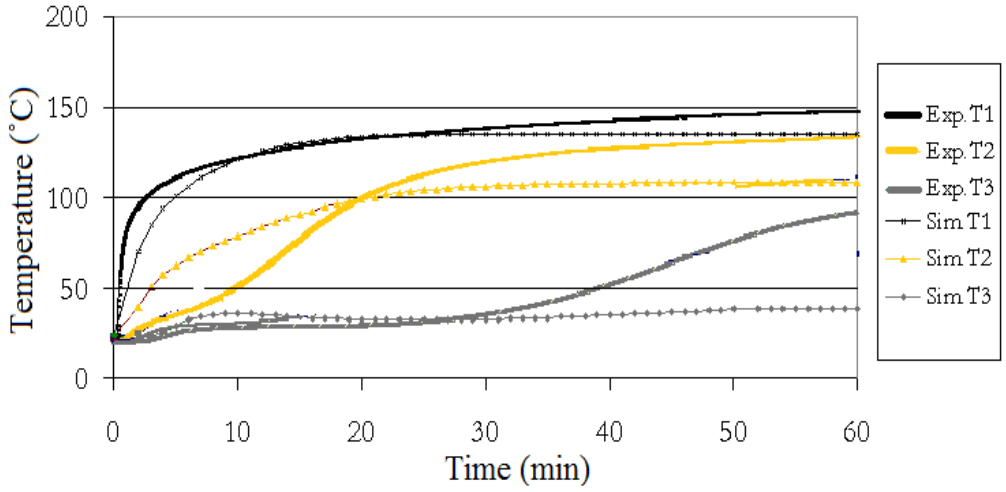

Figure 5.9 – Nitrogen regeneration temperature profile of Reg.1 at 170°C and 0.17$m.s^{-1}$

The average error percent of the mass of dichloromethane regenerated between the simulations and the experiments was 2.7 %. It had been noticed in Figure 5.8, there has been a delay in the regeneration concentration profile of the experimental in comparison with the simulation results. This was due to the fact of overestimation of the effective mass transfer coefficient of solid to gas (K) in the simulation model. The adjustable effective mass transfer coefficient (K) had been optimized to the best fit of the simulation curve.

There were T1, T2, and T3 thermocouples which have recorded at the 3 ports of the column (at x = 2, 19 and 25 cm). The simulation and the experimental readings are marked are 'Exp' and 'Sim' respectively in the above Figure 5.9. In Figure 5.9, the rise in temperature profile in the simulation was faster than in the experiment. This explains the delay in the regeneration concentration profile of the experiment in comparison with the simulation.

Regeneration step of dichloromethane - ACM 204:

The following table 5.2 summarizes the regeneration performance for dichloromethane – ACM204 system.

Table 5.2 – Regeneration operating conditions and results for dichloromethane – ACM 204 system

Regeneration Experiments	Operating Conditions		Regeneration %	Operating cost	Avg. Reg. Rate
	T (°C)	v (m/s)	R_E %	$OP_€$ (€/kg)	$\sum R_R$ (g.min^{-1})
Reg.1	170 (+)	0.17 (+)	76.7	5.81	0.75
Reg.2	170 (+)	0.10 (-)	61.3	4.86	0.60
Reg.3	130 (-)	0.17 (+)	66.4	6.70	0.65
Reg.4	130 (-)	0.10 (-)	51.1	5.83	0.50

The following are the ANOVA equations for the regeneration efficiency and the operating costs for the dichloromethane – ACM 204 system.

$$R_{E\,\%} = 63.9 + 5.12.T + 7.67.v + 0.02.T.v \quad (5.3)$$

$$OP_{€\,(€/kg)} = 5.8 - 0.47.T + 0.45.v - 0.02.T.v \quad (5.4)$$

The following figure 5.10 shows an example of experimental and simulation regeneration results of the dichloromethane – ACM 204 system. The regeneration concentration peaks at 55 $g.m^{-3}$ in the case of dichloromethane – ACM 204 system, whereas in the case of dichloromethane – ACV 404, the peak is observed at a concentration 90 $g.m^{-3}$ under the same operating conditions. This sign shows the superior regeneration performance of ACV 404 over ACM 204 and it could be justified because of the characteristics of the activated carbon.

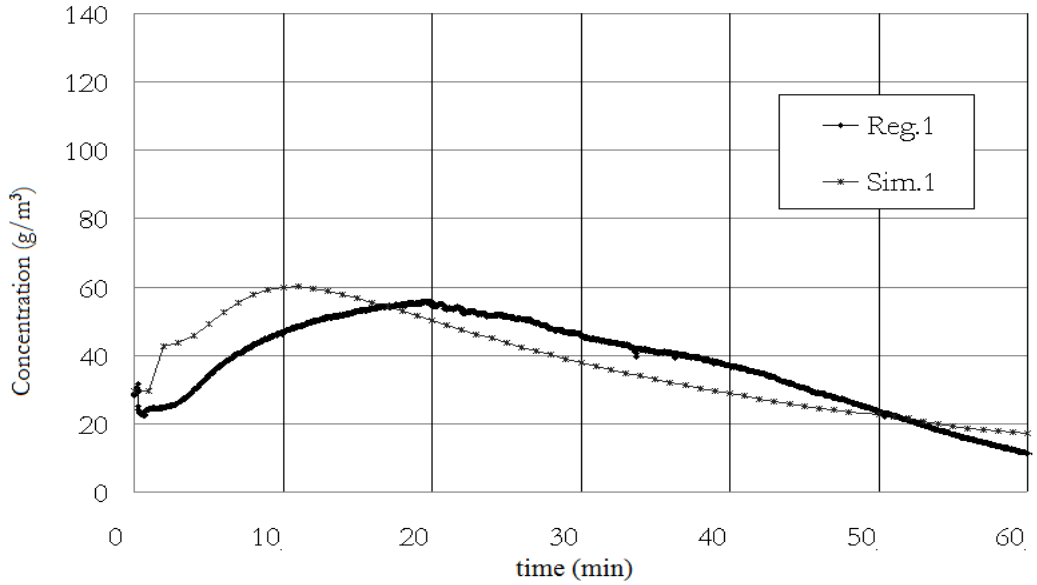

Figure 5.10 – Regeneration profile of dichloromethane – ACM 204: Reg.1 at 170°C and 0.17$m.s^{-1}$

Regeneration step of dichloromethane – BC 120:

The following table 5.3 summarizes the regeneration performance for dichloromethane – BC120 system. The regeneration efficiency is calculated at 20 min because of it low adsorption capacity compared to the ACV 404.

Table 5.3 – Regeneration operating conditions and results for dichloromethane – BC 120 system

Regeneration Experiments	Operating Conditions		Regeneration %	Operating cost	Avg. Reg. Rate
	T (°C)	v (m/s)	R_E %	$OP_€$ (€.kg^{-1})	$\sum R_R$ ($g.min^{-1}$)
Reg.1	170 (+)	0.17 (+)	93.6	2.10	1.72

Reg.2	170 (+)	0.10 (-)	80.0	1.48	1.47
Reg.3	130 (-)	0.17 (+)	88.4	2.22	1.63
Reg.4	130 (-)	0.10 (-)	62.1	1.90	1.14

The following are the ANOVA equations for the regeneration efficiency and the operating costs for the dichloromethane – ACM 204 system.

$$R_{E\,\%} = 81.0 + 5.78.T + 10.0.v - 3.2.T.v \quad (5.5)$$

$$OP_{€\,(€/kg)} = 1.93 - 0.14.T + 0.24.v + 0.075.T.v \quad (5.6)$$

The following figure 5.11 shows an example of experimental and simulation regeneration results of the dichloromethane – BC 120 ystem. The regeneration concentration peaks at 120 $g.m^{-3}$ in the case of dichloromethane – BC 120 system, whereas in the case of dichloromethane – ACV 404, the peak is observed at a concentration 90 $g.m^{-3}$ under the same operating conditions. In this case, the regeneration is calculated at 20 min and it is marked in the bold line. This calculation is because of the fact that at 20 min, a very good regeneration rate of 93.6 percent is achieved.

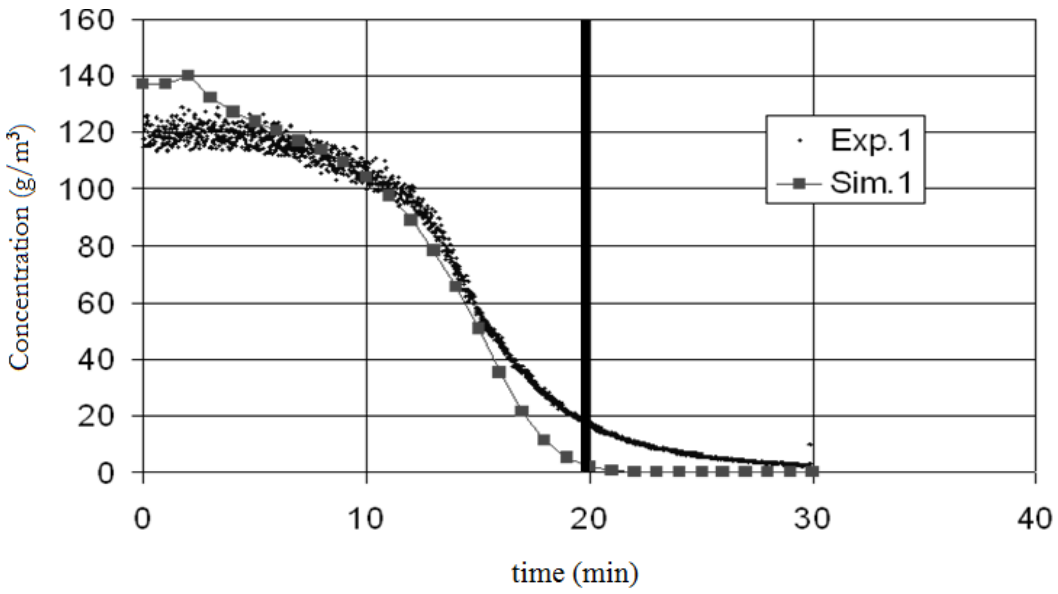

Figure 5.11 – Regeneration profile of dichloromethane – BC 120: Reg.1 at 170°C and 0.17$m.s^{-1}$

This sign could show the sharper regeneration performance of BC120 over ACV 404. The ability to conduct heat by chemically activated carbon (BC 120) increases significantly when the temperature increases, where as in physically it increases slightly [2]. It could be a reason, that BC 120 regenerates faster (in terms of regeneration efficiency) and less operating cost compared to ACV 404. But the amount of dichloromethane regenerated per activated carbon bed is twice less for the BC 120 (36 g at 30 min in Reg.1) of regeneration compared to ACV 404 (85 g at 60 min in Reg.1) in a same volume of adsorption bed. Inspite of the fact of less regeneration operating cost for dichloromethane – BC 120 system (2.10 €.kg^{-1} in Reg.1) over the dichloromethane – ACV 404 system, the capital cost (3.44 €.kg^{-1} in Reg.1), the capital cost for dichloromethane – BC 120 will be twice more than for the case of dichloromethane – ACV 404 in the account of adsorption column. This is because of the fact that the bulk density of ACV 404 is twice more than BC 120. And also the operation will be much simpler by using ACV 404, because of their higher bulk density, less need of adsorption beds, less need of hot nitrogen supply components.

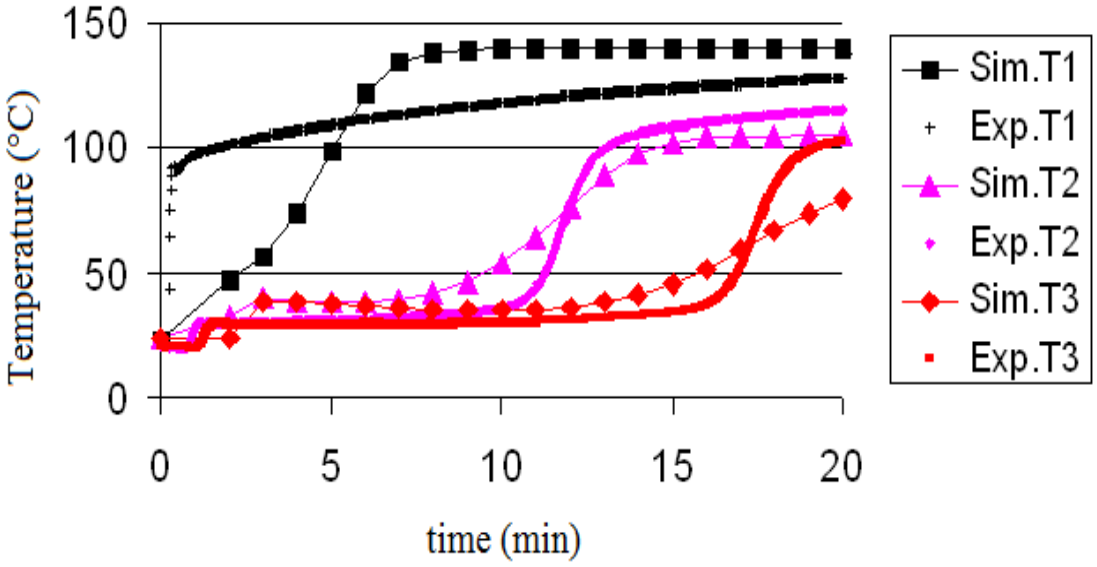

Figure 5.12 – Temperature profile of dichloromethane – BC 120: Reg.1 at 170°C and 0.17m.s^{-1}

In the temperature profile (Figure 5.12), it could be noticed that the simulation points lead the experimental points and it is an explanation for concentration lead in simulation compared to simulation results. From the adsorption and regeneration results, ACV 404 clearly showed its

superiority in terms of performance over ACM 204 and BC 120. The following section will involve different VOCs adsorption and regeneration from the activated carbon ACV 404.

5.5.3. Comparison of adsorption of acetone / dichloromethane / ethyl formate on ACV 404

The adsorption capacities of acetone, ethyl formate and dichloromethane are found to be 23.6, 30.3 and 35.6 % (based on mass of VOC adsorbed on the activated carbon ACV 404) respectively from the adsorption cycle. And the breakthrough time for acetone; ethyl formate and dichloromethane are found to be 53, 71 and 70 min and it is calculated from 10% of the initial concentration of VOC. Some examples of breakthrough curve and temperature profile of ethyl formate and acetone during adsorption have been presented in Figure 5.13, 5.14, 5.15, and 5.16. The simulation model PROSIM results were coherent with the experimental results and it is evident from the Figures 5.13 and 5.14. The error calculated on the mass of adsorption between the experiment and the simulation were always less than 4 % for all the VOCs involved. The mass transfer coefficients of ethyl formate – ACV 404 and acetone – ACV404 systems (D_{gl}) are adjusted as 0.003 and 0.001 $m^2.s^{-1}$ respectively. The adsorption isotherm results of the system acetone/dichloromethane/ethyl formate are attached in the annexes.

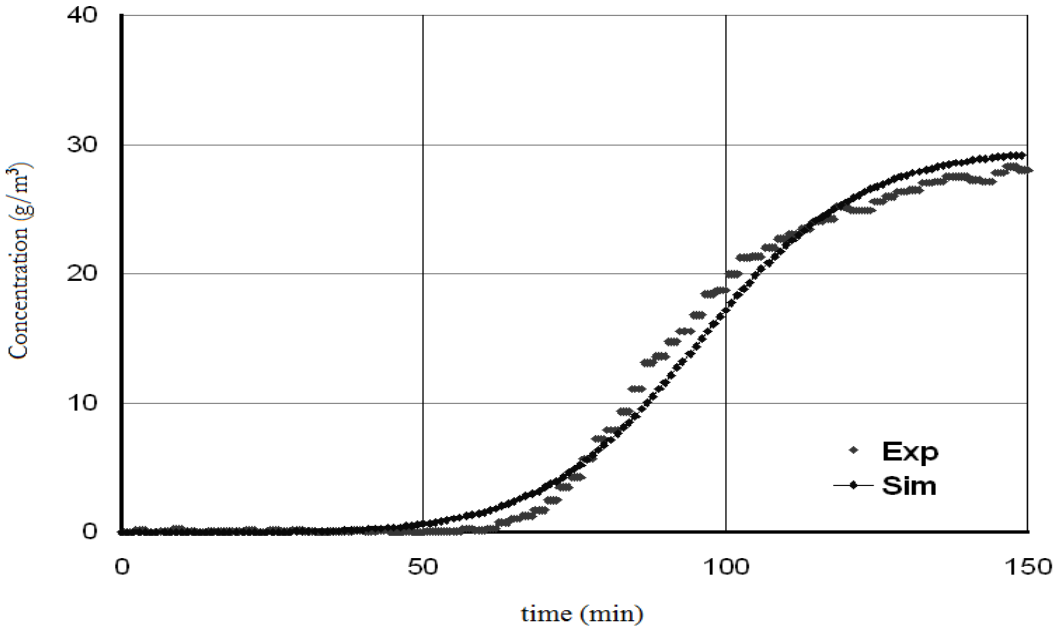

Figure 5.13 – Ethyl formate breakthrough profile of experiment and simulation

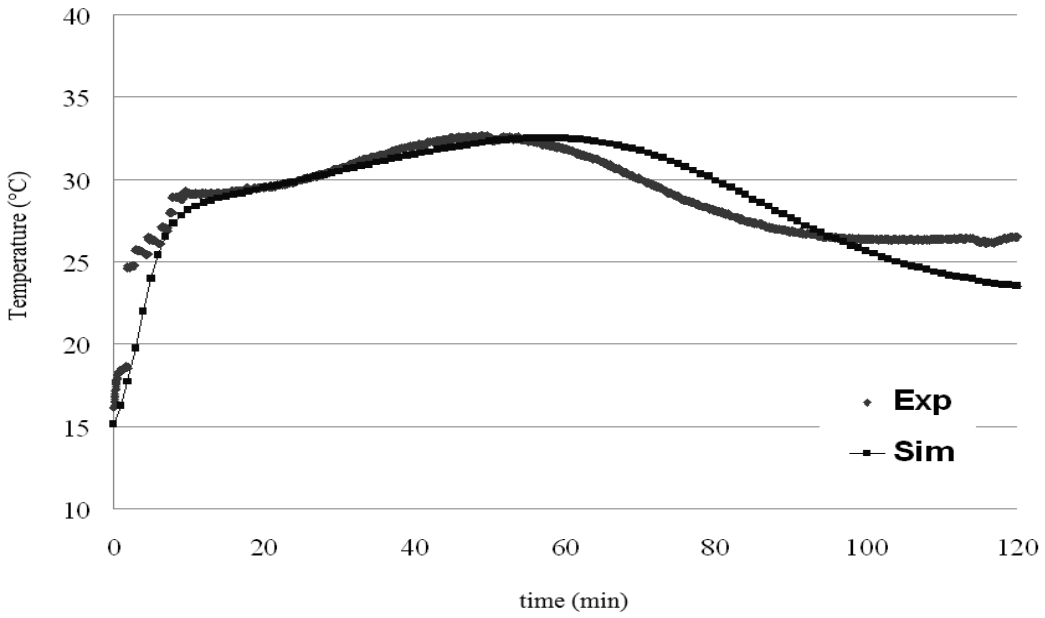

Figure 5.14 – Ethyl formate adsorption temperature profile of experiment and simulation

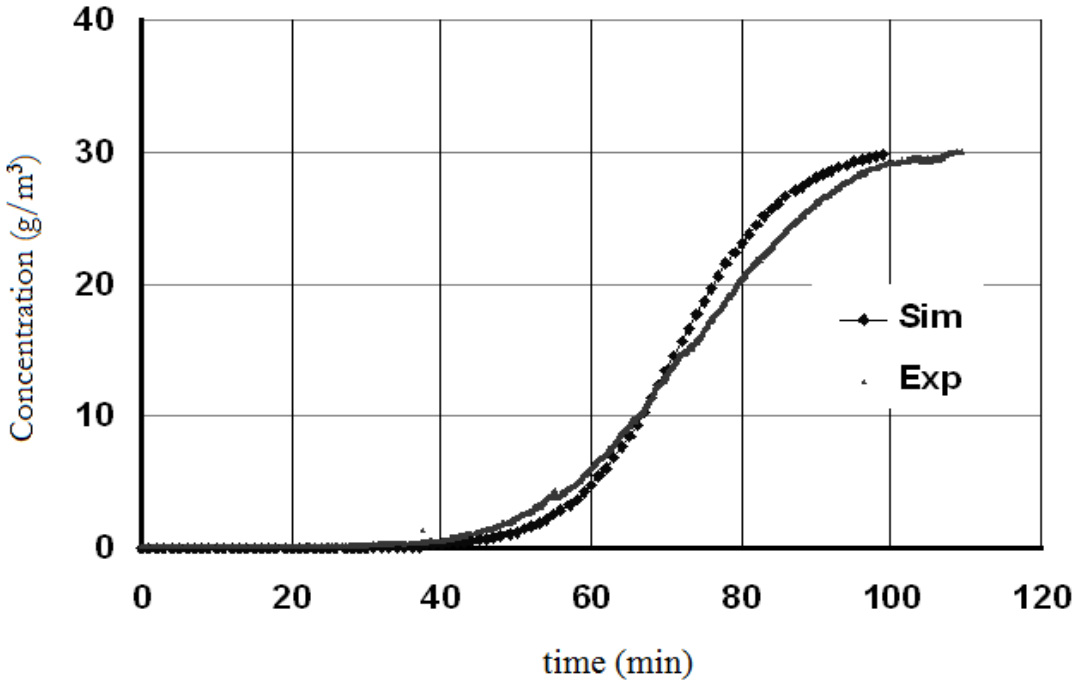

Figure 5.15 – Acetone breakthrough profile of experiment and simulation

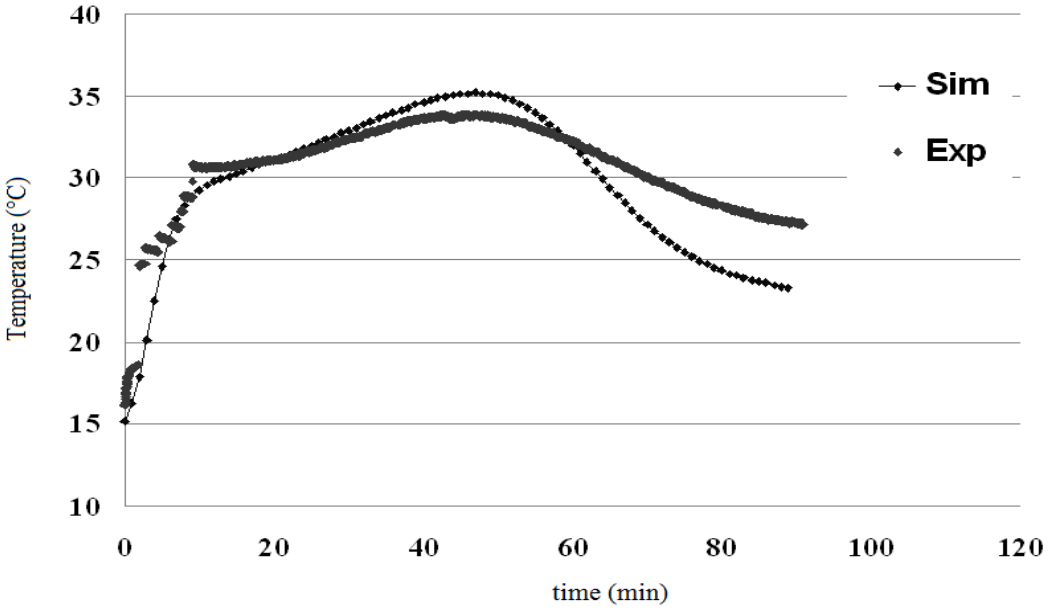

Figure 5.16 – Adsorption temperature profile of experiment and simulation

5.5.4. Comparison of hot nitrogen regeneration of acetone / dichloromethane / ethyl formate from ACV404

Table 5.4 and 5.5 summarizes the hot nitrogen regeneration operating conditions for ethyl formate, acetone and also their corresponding results such as regeneration efficiency (R_E), Operating Cost ($OP_€$). The regeneration efficiency was calculated by the ratio of mass of VOC generated to the mass of the VOC adsorbed.

Table 5.4 – Regeneration operating conditions and results for ethyl formate – ACV 404

Regeneration Experiments	Operating Conditions		Regeneration %	Operating cost
	T (°C)	v (m/s)	R_E %	$OP_€$ (€/kg)
Reg.1	170 (+)	0.17 (+)	80.0	4.47
Reg.2	170 (+)	0.10 (-)	56.6	3.83
Reg.3	130 (-)	0.17 (+)	66.0	4.91
Reg.4	130 (-)	0.10 (-)	45.9	4.73
Reg.5	150 (=)	0.14 (=)	61.1	4.42

Table 5.5 – Regeneration operating conditions and results for acetone – ACV 404

Regeneration Experiments	Operating Conditions		Regeneration %	Operating cost
	T (°C)	v (m/s)	R_E %	$OP_€$ (€/kg)
Reg.1	170 (+)	0.17 (+)	81.7	5.77
Reg.2	170 (+)	0.10 (-)	57.1	7.60
Reg.3	130 (-)	0.17 (+)	48.2	6.03
Reg.4	130 (-)	0.10 (-)	44.0	6.59
Reg.5	150 (=)	0.14 (=)	56.8	6.48

The mechanistic models for evaluating regeneration efficiency (R_E) and the operating costs ($OP_€$) obtained by doing an ANOVA with the MINITAB software. The same approach has been implemented to the other VOCs such as dichloromethane and acetone and the results of FED equation for each VOC are presented as follows:

For acetone – ACV 404 system:

$$R_{E\,\%} = 57.8 + 7.2.T + 11.65.v + 5.1.T.v \quad (5.7)$$

$$OP_{€\,(€/kg)} = 6.5 - 0.6.T + 0.2.v - 0.3.T.v \quad (5.8)$$

For ethyl formate – ACV 404 system:

$$R_{E\,\%} = 62.1 + 6.2.T + 10.9.v + 0.8.T.v \quad (5.9)$$

$$OP_{€\,(€/kg)} = 4.5 - 0.34.T + 0.21.v + 0.11.T.v \quad (5.10)$$

For dichloromethane – ACV 404 system:

$$R_{E\,\%} = 64.7 + 7.2.T + 11.2.v + 1.8.T.v \quad (5.11)$$

$$OP_{€\,(€/kg)} = 3.79 - 0.41.T + 0.11.v - 0.05.T.v \quad (5.12)$$

In Table 5.5 and 5.6, regeneration experiment Reg.5 had the operating conditions in the central point of FED (T = 150 °C, v = 0.136 $m.s^{-1}$). The experimental results were compared with the mechanistic models (equation 9) and the error percentage of the mass of regeneration of ethyl formate and acetone are under 5 %. This shows that the mechanistic model is statistically and realistically consistent within the range of operating conditions chosen. A similar central point had

been chosen for the other cases of VOCs and their respective errors on the mass regenerated were always found to be less than 7%. So the equations 5.7, 5.8, 5.9, 5.10, 5.11, and 5.12 could be used to interpolate the regeneration efficiency and the operating costs for the different families of VOCs with the activated carbon ACV 404.

Figure 5.17 and 5.18 are plotted by taking the dimensionless coefficients (from equations 5.7, 5.8, 5.9, 5.10, 5.11, and 5.12) of the corresponding operating conditions (T, v) and their interaction effect (T.v) to compare their influence on regeneration efficiency and operating costs for different VOCs with the activated carbon ACV 404.

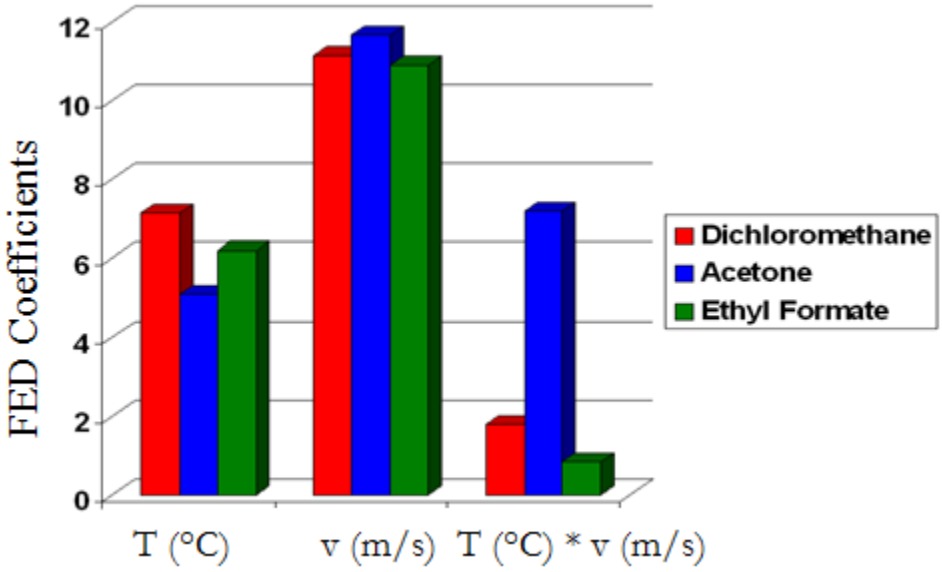

Figure 5.17 – FED measure of influence of operating conditions on regeneration efficiency

From the Figure 5.17, it could be concluded that the superficial velocity of the nitrogen (v) has influenced more on achieving higher regeneration than the nitrogen temperature (T) for all the VOCs. And also the interaction effect is significantly stronger for the case of acetone compared to dichloromethane and ethyl formate. From the Figure 5.18, it could be concluded that the increase in temperature of nitrogen has decreased the operating cost for all the cases of VOCs.

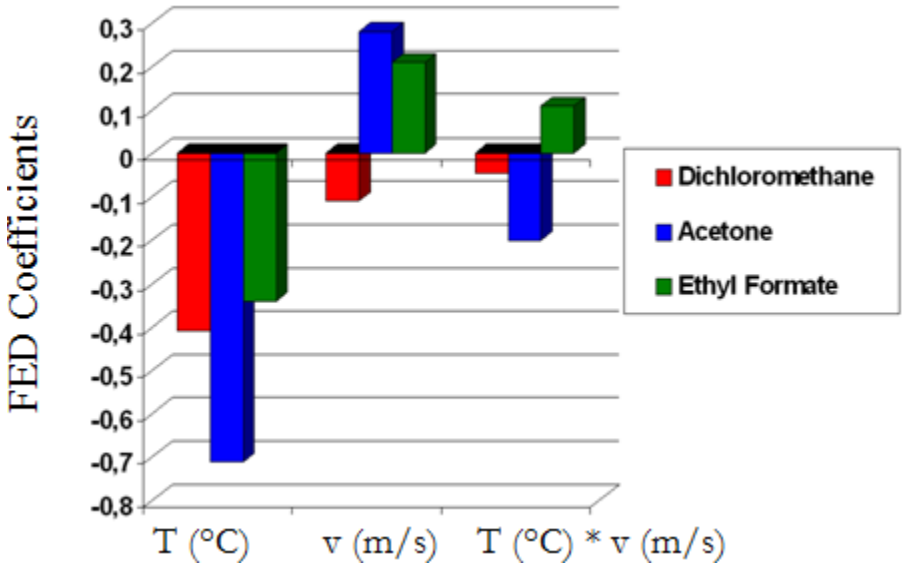

Figure 5.18 – FED measure of influence of operating conditions on operating costs

This was due to the fact of increasing the temperature had increased the regeneration of VOCs and decreased the regeneration time. The decrease in regeneration time has strictly implied less consumption of nitrogen. And the increase in superficial velocity decreased the operating cost, where as it slightly increased the cost for acetone and ethyl formate. The interaction effect in the case of acetone has decreased the operating cost significantly in case of acetone compared to the case of dichloromethane and ethyl formate.

5.5.5. Simulation results of hot nitrogen regeneration of acetone/ ethyl formate from ACV 404

Examples of simulation results of regeneration concentration and temperature profile of ethyl formate and acetone from ACV 404 have been shown in the Figures 5.19, 5.20, 5.21, and 5.22. The average error percent of the mass of acetone regenerated between the simulations and the experiments was 3.1 %. It had been noticed in Figure 5.19, there has been a delay in the regeneration concentration profile of the experimental in comparison with the simulation results. This was due to the fact of overestimation of the effective mass transfer coefficient of solid to gas (K) in the simulation model. The adjustable effective mass transfer coefficient (K) had been optimized to the best fit of the simulation curve.

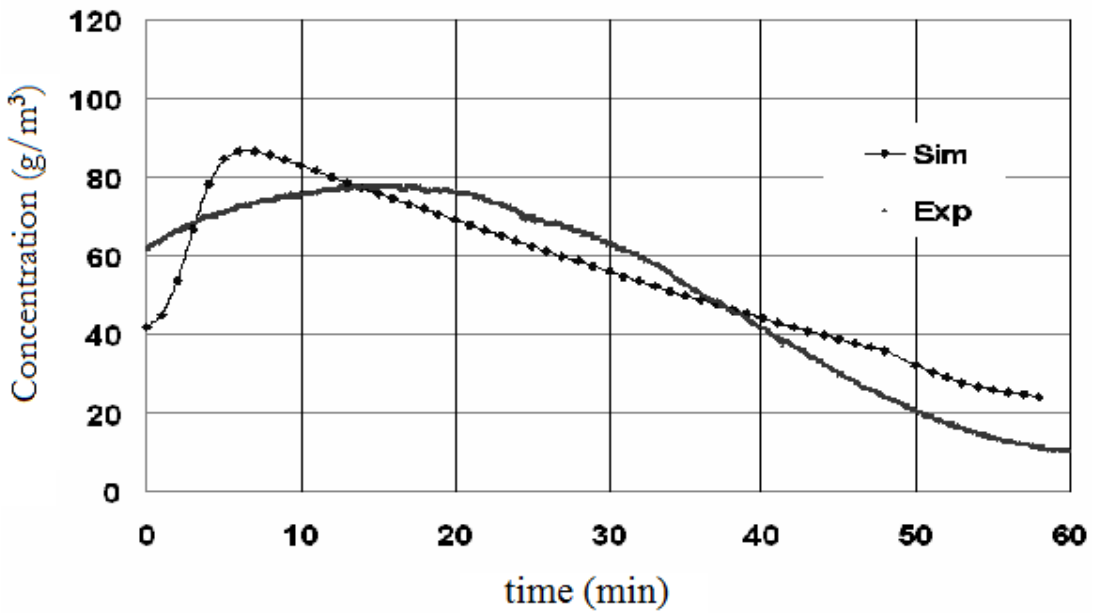

Figure 5.19 – Regeneration concentration profile of ethyl formate at 170°C and 0.17m.s^{-1}

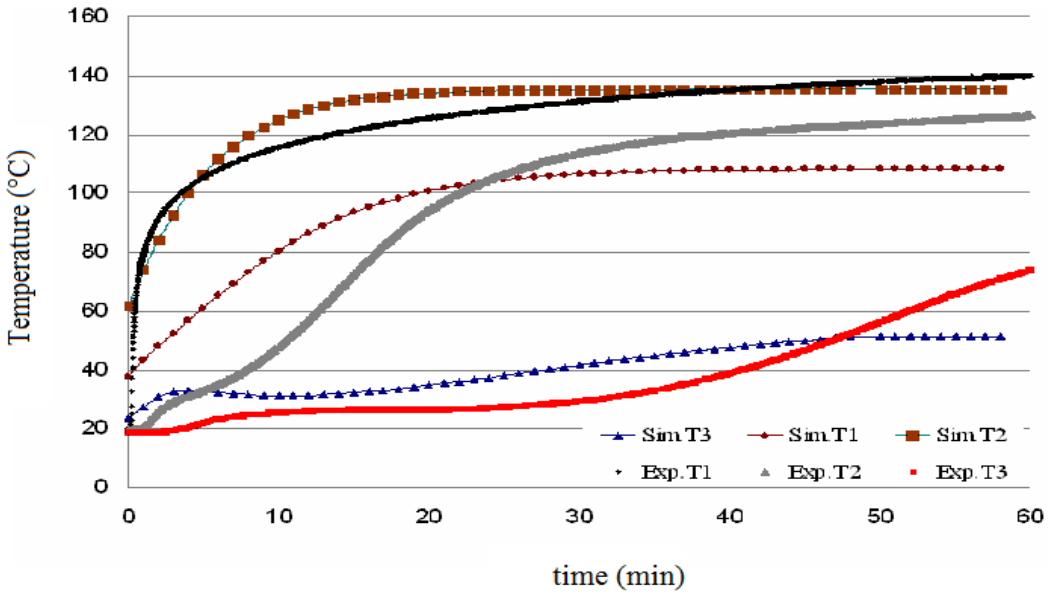

Figure 5.20 – Regeneration temperature profile of ethyl formate at 170°C and 0.17m.s^{-1}

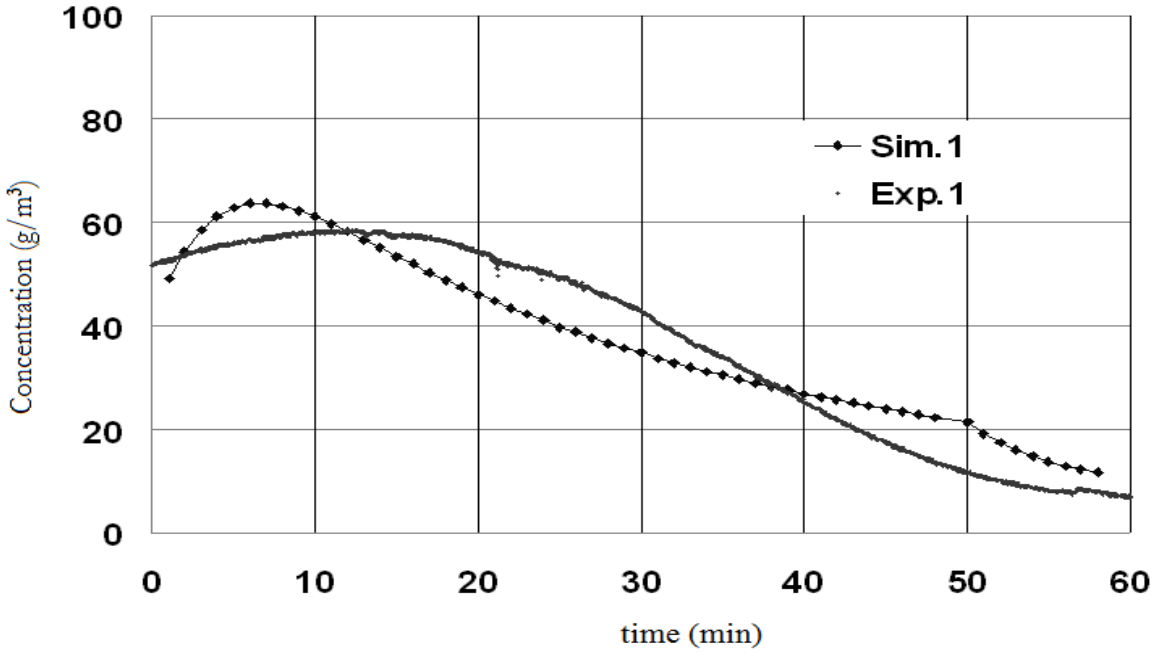

Figure 5.21 – Regeneration concentration profile of acetone at 170°C and 0.17m.s^{-1}

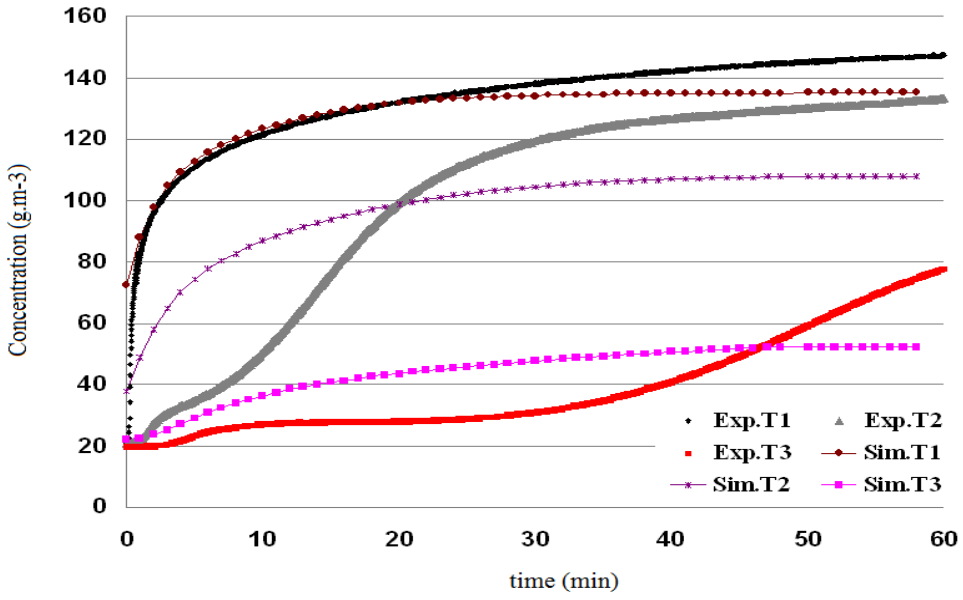

Figure 5.22 – Regeneration temperature profile of acetone at 170°C and 0.17m.s^{-1}

5.5.6. Comparison of steam regeneration results of dichloromethane / acetone from ACV 404

The selection of VOCs for steam regeneration is based on the nature of solubility. So acetone (highly soluble) and dichloromethane (almost non-soluble) are chosen for the steam regeneration experiment from ACV 404.

Steam regeneration step of dichloromethane – ACV 404 system:

For the steam regeneration, the temperatures of steam (Ts) were varied as 140 and 200°C, and the flow rate of the steam (Vs) was kept constant at 0.83 $g.s^{-1}$ by adjusting the pressure. The following Table 5.6 summarizes the operating conditions and the results obtained by the steam regeneration. The operating cost was calculated on the basis of energy required for the steam (2722 $kJ.kg^{-1}$ of steam, NIST), electricity tariff in France (60 $€.Mwh^{-1}$), cost of drying (drying time = 1 hour), and cost of water (used for the production of steam) in France (3 $€.m^{-3}$). The heating cost during drying step had been calculated based on the amount of heat energy spent to eliminate the moisture in the bed by passing hot air.

Table 5.6 – Operating conditions and results of steam regeneration of dichloromethane – ACV404

Operating Conditions			Regeneration Time (min)	Dichloromethane regenerated		$OP_€$ (€.kg^{-1})	$\sum R_R$ (g.min^{-1})
Exp	Ts (°C)	Vs (g.s^{-1})		Experiment%	Simulation%		
Reg.1	140	0.833	16	82.3	72.2	0.85	0.96
Reg.2	200	0.833	14	82.3	72.2	0.87	0.99

The Figures 5.23 and 5.24 show an example of the steam regeneration concentration and temperature profile respectively. In Figure 5.23, the regeneration profile was obtained by the simulation model. From the results in the Table 5.6, the simulation model had predicted the regenerated dichloromethane less than the experimental results and the error percentage of the mass of dichloromethane regenerated between the simulation and the experiment is 12%. This error could be due to the absence of the effect of enthalpy of latent heat of change of phase from steam to

water in the simulation model. This energy would have decreased the error difference between the simulation and experiment.

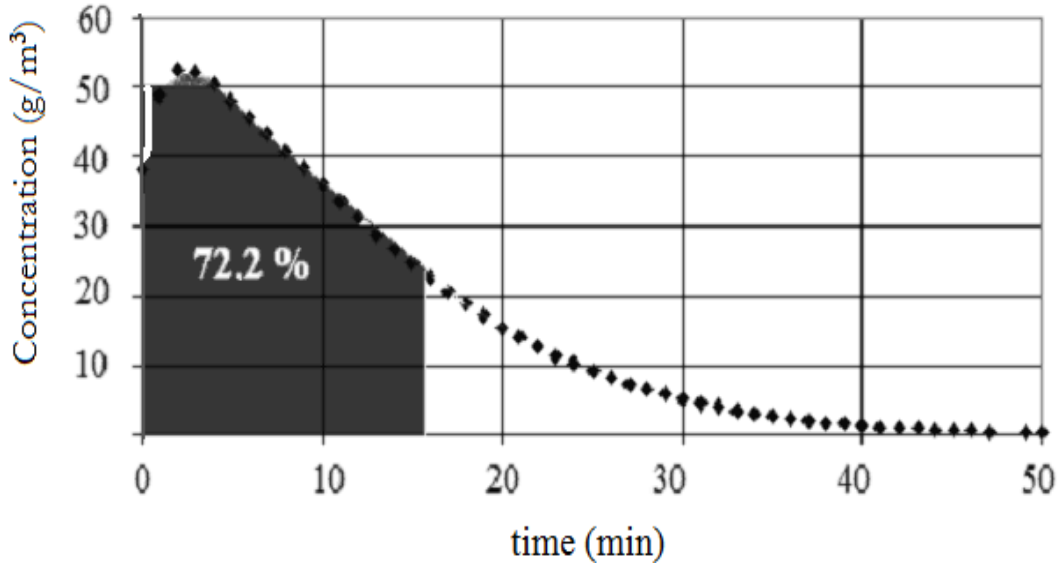

Figure 5.23 – Simulation of steam regeneration of dichloromethane - Reg.1 at 140°C and 0.83g.s^{-1}

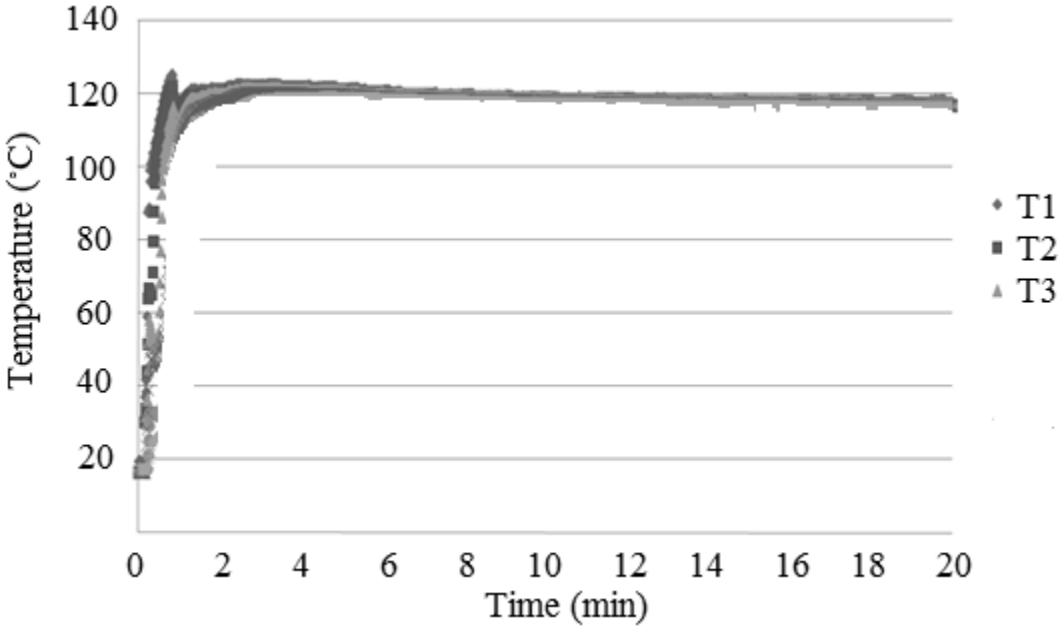

Figure 5.24 – Experimental steam regeneration temperature profile - Reg.1 at 140°C and 0.83 g.s^{-1}

From the above Figure 5.24, the temperature rise during the steam regeneration was uniform along the bed in contrary to the nitrogen regeneration in Figure 5.24.

Nitrogen regeneration had been favorable in terms of achieving slightly higher regeneration efficiency (84.8 %) and higher average regeneration rate (1.3 $g.min^{-1}$) compared to the steam regeneration. Also there was no presence of humidity after the nitrogen regeneration, which has kept the successive adsorption cycle performance consistent. Since nitrogen is inert, it would regenerate high purity of dichloromethane. Although, nitrogen regeneration was very effective in achieving slightly higher regeneration, but the operating cost was four times higher of the steam regeneration. And also, after the nitrogen regeneration, the step of separation (cryogenic condensation) of dichloromethane from nitrogen adds an additional cost. In the case of steam regeneration, it has proved that the regeneration of dichloromethane was effective (82.3 %) at a short time (16 min). But the drying step (which includes cooling time of bed) added an additional time of 1 hour to retain the bed completely dry, which has decreased the average regeneration rate (0.96 $g.min^{-1}$). But, since dichoromethane is not soluble in water, it was easy to separate by simple condensation.

Steam regeneration step of acetone – ACV 404 system:

The following table 5.7 summarizes the results of steam regeneration of acetone from ACV 404. The error between simulation and the experiment is 10% based on the regenerated acetone (g).

Table 5.7 – Operating conditions and results of steam regeneration of acetone – ACV404

Operating Conditions			Regeneration Time (min)	Acetone regenerated		$OP_{€}$ (€.kg^{-1})	$\sum R_R$ ($g.min^{-1}$)
Exp	Ts (°C)	Vs ($g.s^{-1}$)		Experiment%	Simulation%		
Reg.1	140	0.833	24	83.4	73.4	1.1	2.1

Inspite of high regeneration percent of acetone by steam regeneration (Figure 5.25 and Table 5.7), nitrogen regeneration could be preferred in the case of readily available steam in the industrial unit. It is because that acetone is highly soluble in water and so it has to be separated by multiple steps of distillation for having high purity. This additional cost has not been taken into account in the operating cost and so the nitrogen regeneration could be a better option over steam regeneration.

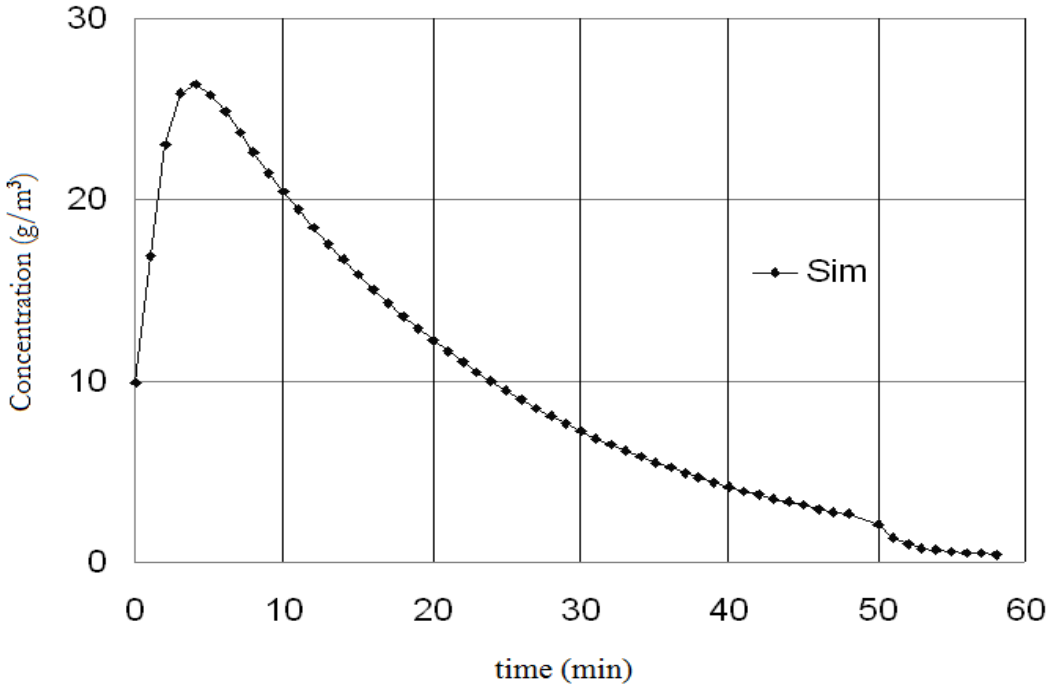

Figure 5.25 – Simulation of steam regeneration of acetone - Reg.1 at 140°C and 0.83g.s^{-1}

5.6. Conclusions

The methodologies and the explanations for choosing the activated carbon has been clearly demonstrated by comparing the adsorption and regeneration results of Dichloromethane – ACV404/ ACM 204 / BC 120 systems. ACV 404 has been the best choice because of: (1) high adsorption capacity and recovery efficiency of dichloromethane; (2) high bulk density (means more activated carbon in the same the same volume of column; (3) good simulation results of adsorption and regeneration cycles

The hot nitrogen regeneration operating condition (T = 170°C; v = 0.17 m.s^{-1}) were very effective for the VOCs involved (acetone, ethyl formate and dichloromethane) to achieve high regeneration at an optimized cost [6-7]. Thanks to the FED tool which has played a very important role in the art of designing and optimizing the hot nitrogen regeneration process. Comparison on the different families of VOC regeneration were analyzed in a detailed fashion that how each operating condition and their interaction effect contributed to the regeneration efficiency and the operating cost. The dynamic systems of adsorption and regeneration had been simulated and

validated with the experimental results. The simulation tool had been very useful in (1) choosing the right microporous activated carbon; (2) optimizing the design aspects of adsorption and regeneration process; (3) techno-economic analyses.

Steam regeneration had been a choice over nitrogen regeneration in the case of dichloromethane because of lower operating cost (0.85 €.kg-^{1}); easy choice of separation of dichloromethane of steam by simple condensation; effective regeneration efficiency (82.3%); and also readily available in the industrial units [11-12]. But in the case of acetone, it is not very clear to choose the mode regeneration because: (1) given the availability of steam in industrial unit; (2) operating cost considering the multiple distillation unit to achieve high purity; and (3) acetone purity requirements.

References

[1] P.M. Berthouex, and L.C. Brown, Statistics for Environmental Engineers, Lewis Publishers, USA, 2002

[2] S. Giraudet, Exothermicity of adsorption of volatile organic compounds in fixed activated carbon beds: modelling and simulation valdiation of experimental work, PhD dissertation, EMN, France, 2006

[3] D.M. Ruthven, Principles of adsorption and adsorption processes, John Wiley & Sons: New-York, Univ of New Brunswick: Fredericton, USA, 1984

[4] E.W. Washburn, Note on method of determining the distribution of pore sizes in a porous material. Proc.Nat. Acad. Sci 1921; 7: 115 -16

[5] Ecole des Mines de Nantes, Data sheets of tarrifs and equipment details of TSA pilot plant, France, 2010

[6] J.Ho.Yun, D. Choi, H. Moon. Benzene adsorption and hot purge regeneration in activated carbon beds, Elsevier - Chemical Eng. Sci. 2000; 55: 5857 - 72

[7] K.S. Hwang, D.K. Choi, S.Y. Gong, S.Y. Cho. Adsorption and thermal regeneration of methylene chloride vapor on activated carbon bed, Elsevier – Chemical Eng. and Pro. 1998; 46: 1111 - 23

[8] F. Delage, P. Pre, P. Le Cloirec. Mass transfert and warming during adsorption of high concentrations of VOCs on an activated carbon bed: experimental and theoretical analysis, Environ Sci Technol. 2000; 34: 4816 - 21

[9] P. Pre, F. Delage, P. Le Cloirec. Modeling the exothermal nature of V.O.C. adsorption to prevent activated carbon bed ignition, Fundamentals of Adsorption 2001; 7: 1172 – 85

[10] S. Giraudet, P. Pre, P. Le Cloirec. Modeling the Heat and Mass Transfer in Temperature Swing Adsorption of Volatile Organic compounds on to Activated Carbons, Environmental Science and Technology 2009; 43: 1173 - 79

[11] R.C. Nattkemper, Nitrogen Vs Steam Regeneration in activated carbon systems, American Carbon Society, Imation Corp., Camarillo, CA 93012, Jul 1997

[12] J. Gu, N. M. Faqir, H.J. Bart. Drying of an Activated Carbon Column after Steam Regeneration. Wiley Publications - Chemical Eng. and Tech. 1999, 22:859-64

Conclusions and Perspectives

The following section summarizes the objectives and the results obtained in the three different dimensions of the research work: (1) experimental and modeling of adsorption isotherms; (2) experimental and modeling of dynamic Vacuum Temperature Swing Adsorption (VTSA) system; (3) experimental and modeling of Temperature Swing Adsorption (TSA) system.

1. Experimental and modeling of adsorption isotherms

Equilibrium data were obtained for 5 VOCs (acetone, dichloromethane, ethyl formate, toluene, and ethyl alcohol) – 8 activated carbons systems (ACM 404, ACV 404, ACM 204, BC 120, GF 40, NC 60, NC 100, and BPL). Each system of VOC – activated carbon system has isotherm data at four different temperatures at 20, 40, 60 and 80°C, and so in total there are 120 isotherms. The range of concentration used for the isotherm experiment varies from the lowest concentration 1 $g.m^{-3}$ to the highest concentration 170 $g.m^{-3}$.

Different isotherm models (like Langmuir, Langmuir-Freundlich and Dubinin Raduskevich) had been chosen and modeled to find out the coefficients involved in each of the model. Langmuir-Freundlich isotherm model has worked better than Langmuir and DR model for all the VOCs – activated carbon systems. This is because of the greater flexibility of the model with an additional parameter (n) in the isotherm model. The coefficients of the different model have been determined by using the Gauss Newton method for non-linerar regression. These coefficients had been used in the simulation tool PROSIM for dynamic process of adsorption and regeneration.

Multiple Linear Regression (MLR) models have been established based on the properties of VOCs and the activated carbons for the characteristic adsorption energy (E) of DR model and the enthalpy of adsorption (H) of Langmuir model. Since the micropore volume is determined by the nitrogen analysis, by substituting the only unknown value of characteristic adsorption (E) in the DR model, the adsorption capacity can be determined for any concentration of VOCs (acetone, dichloromethane, ethyl formate, ethanol and toluene) to be treated. A similar approach had been tried for the other coefficients of Langmuir isotherm, but it has been unsuccessful.

So by implementing the DR-MLR model for characteristic adsorption for the 4 VOCs, it would bring down the difficulties of performing adsorption isotherm experiments. And hence, the dynamic simulation becomes simple and efficient.

2. Experimental and modeling of dynamic VTSA system

The VTSA system which has been experimented was very different from the industrial practice. Usually in industries, simple TSA systems such as hot nitrogen and steam regenerations are used for VOC recovery process. Here in this system once after the dichloromethane adsorption step, the column is completely closed and heated by hot oil bath for 40 minutes (preheating). During this time, the adsorbed dichloromethane is partially desorbed. Then the hot nitrogen was passed for a period to achieve the intermediate regeneration. Once the intermediate regeneration is achieved, the vacuum mode of regeneration was applied for further regeneration and cooling benefits at the end of regeneration. The cooling at the vacuum regeneration is an advantage over normal TSA system, because it brings the temperature down close to 40°C and so the time of cooling is saved. Vacuum regeneration had been tried to apply at an intermediate regeneration point for achieving high final regeneration at an optimized cost. Thanks to factorial experimental design which has helped to achieve this optimization.

The adsorption and regeneration experiments carried out were validated by the simulation tool PROSIM. Inspite of the fact that there was high level of regeneration and cooling benefits of VTSA systems, the additional capital cost for vacuum pump, hot oil bath, valves and other components would certainly have a drawback over normal TSA system. Also there should be an additional measurement required for determining the intermediate regeneration to apply the vacuum regeneration. Hence, the VTSA system has been very interesting from the research point of view, but because of additional capital cost and complex of operation, it leads to difficulties for an industrial practice.

3. Experimental and modeling of dynamic TSA system

The two different systems such as hot nitrogen and steam regeneration had been thoroughly investigated for different VOCs and different activated carbons. The TSA system experimented here is exactly identical to the industrial process in terms of operation, just by passing the hot nitrogen or steam for regenerating the activated carbons. The three activated carbons (ACV 404, ACM 204 and BC 120) were selected carefully to represent the diversity of their characteristics and the VOCs are

selected based on: (1) being really hazardous (dichloromethane); (2) widely used as industrial solvents (acetone and ethyl formate). From the all the hot nitrogen experiments of dichloromethane – ACV 404/ ACM 404/ BC120, the activated carbon ACV 404 has been selected as the best activated carbon because of: (1) high adsorption and regeneration performance; (2) higher bulk density.

The operating conditions for nitrogen regeneration have been optimized by changing the temperature and the superficial velocity of the nitrogen. The optimization has been done by using 2x2 FED to determine the effect of the operating conditions on the VOC regeneration efficiency and the operating costs. The ANOVA equation sets for the regeneration efficiency and the operating costs from the 2x2 FED had been established with dimensionless influence of operating conditions and their interaction effect. In all the cases of high VOCs regeneration efficiency, the superficial velocity (0.17 $m.s^{-1}$) had been the dominant factor. The influence of temperature of nitrogen, superficial velocity of nitrogen and their interaction effect on the operating cost had been different from each case of VOC – activated carbon system. Thus the understanding of these influences is very vital in designing an efficient VOC regeneration system at an optimized cost. The simulation PROSIM had been proved to be robust for having good agreements with experimental results (adsorption and regeneration) of the 3 VOCs – activated carbon systems.

The steam regeneration had been used for 2 VOCs [dichloromethane (non-soluble), acetone (soluble)] – ACV 404 systems. The temperature and the flow rate of the steam had been optimized to achieve high regeneration at a low operating cost. The major disadvantage of steam regeneration is the drying step after regeneration. If the drying is not properly done, there will be problems to have good successive VOC adsorption capacities. In the case of dichloromethane, steam regeneration is a preferred choice over hot nitrogen regeneration because of: (1) ready availability of steam in industries; (2) simple separation of dichloromethane from steam by condensation. But in case of acetone, it is unclear because it depends on the following: (1) if the steam is readily available in the industrial unit; (2) purity of acetone required; (3) cost of multiple distillation of acetone after steam regeneration to have high purity.

Perspectives

The short term perspectives from this research work could be: (1) developing more adsorption isotherm data for other VOCs on activated carbon systems; (2) implementing the DR-

MLR in the dynamic process simulation of adsorption and regeneration; (3) inspite of less error (under 7%) on mass of adsorption and regeneration for the VOCs – activated carbon systems, it could be a good improvement to develop new mass transfer and heat transfer models for their respective coefficients to overcome the lead of simulation regeneration results compared to the experimental regeneration results of TSA (4) adding the latent heat effect (phase change from steam to liquid) in the simulation model would decrease the error observed between the simulation and the experiment of steam regeneration; (5) adding a sensitivity analysis tool in the simulation tool to optimize the operating conditions both for adsorption and regeneration according to customary needs.

The long term perspectives from this research could be: (1) developing isotherm equilibrium data for multiple VOCs systems; (2) performing multiple dynamic adsorption and regeneration of VOCs on activated carbon; (3) adapting the simulation tool to the Pressure Swing Adsorption process (PSA), for example CO_2 capture to produce high purity methane in the biogas process applications.

Resume en Francais

1. Contexte et objectifs

Les procédés d'adsorption sur charbon actif (CA) sont fréquents pour remédier aux émissions atmosphériques industrielles et traiter les polluants tels que les composés organiques volatils (COV). Notre travail de recherche vise à développer des outils numériques de simulation qui puissent prédire l'efficacité du procédé dans sa phase de séparation mais aussi prédire les conditions d'échauffement ; et ainsi garantir la sécurité des installations. En outre, une partie du travail expérimental se concentre sur la phase de régénération des lits fixes de charbon actif. Des perspectives d'amélioration de la conduite des procédés sont attendues.

Les simulations numériques requièrent des données sur le procédé relatives aux :

- caractéristiques du charbon actif : propriétés texturales, densités du matériau, composition chimique, chaleur spécifique;
- propriétés physico-chimiques des COV : masse moléculaire, polarisabilité, potentiel d'ionisation, moment dipolaire, tension de surface, température d'ébullition ;
- conditions opératoires : diamètre et hauteur du lit fixe de charbon actif, conditions aérodynamiques, concentration des COV à traiter, conditions de régénération (température, gaz vecteur, etc.).

L'ensemble de ces données, fournies par l'utilisateur, sont transmises au modèle développé avec la collaboration du partenaire spécialisé, Prosim. Les principales informations fournies par la simulation sont alors les courbes de percée (efficacité du procédé), les profils de température au cœur du lit (sécurité du procédé pendant la phase d'adsorption et réduction des coûts énergétiques pendant la phase de régénération).

Dans ce contexte, nos objectifs sont de :

- mesurer les données utilisateur essentielles pour la simulation (EMN-ENSCR)
    - Sélection de COV et des CA à tester (panels représentatifs des conditions d'utilisation industrielles)
    - Caractérisation des CA

  - Equilibres d'adsorption
- générer une base de données expérimentale pour tester les capacités de prédiction de l'outil numérique (EMN)
- étudier les différents modes de régénération et définir un protocole de régénération optimal pour un coût énergétique minimal (EMN - Arkema)
- préparer le modèle global d'adsorption et de régénération qui sera ensuite valider sur la base de données expérimentales (EMN-ENSCR- Prosim).

Le présent rapport se divise suivant les objectifs précédemment cités ; en commençant par la sélection des COV et des CA, leur caractérisation puis la mesure des isothermes d'adsorption (phase 1). Les travaux de modélisation relatifs à l'amélioration de l'outil de simulation de l'étape d'adsorption sont ensuite présentés (phase 2). Enfin, dans la dernière partie du document, on décrit l'avancement des travaux concernant l'étude expérimentale des cycles TSA (phase 3).

2. Phase 1 : Etude des équilibres d'adsorption non isothermes COV-charbons actifs

2.1 Sélection des COV et charbons actifs

L'ensemble des composés organiques et des charbons actifs (Tableau 1) a été choisi avec une attention particulière. En effet, dans le but de décrire un éventail d'applications le plus large possible, les couples COV-CA doivent couvrir l'ensemble des interactions, des plus faibles aux plus fortes. D'une part, pour les COV, nous avons sélectionné, parmi les polluants industriels courants, des composés de familles chimiques différentes (cétones, composé halogéné, alcool, composés aromatiques) qui de plus possèdent des propriétés physico-chimiques variées (par exemple, par rapport au point d'ébullition entre l'acétone et le butan-2-one).

D'autre part, les charbons actifs ont été choisis parmi les produits commerciaux proposés par différents producteurs (Pica, Norit, Ceca, Chemviron). Ces CA sont fabriqués à partir de diverses matières premières (tourbe, noix de coco, bois, etc.) et suivant deux modes d'activation différents (physique ou chimique) à conditions opératoires variables. Ainsi, la composition et les textures de chacun de ces adsorbants couvrent le panel des matériaux utilisés industriellement.

Composés organiques volatils		Charbons actifs		
Nom	Famille chimique	Fabricant	Nom	Mode d'activation
Acétone	Cétone	Pica	NC60	Physique
Butan-2-one	Cétone	Pica	NC100	Physique
Dichlorométhane	Chloré	Pica	BC120	Chimique
Ethanol	Alcool	Norit	GF40	Chimique
Toluène	Aromatique	Chemviron	BPL	Physique
Xylène	Aromatique	Ceca	ACM404	Physique
Acétate d'éthyle	Ester	Ceca	ACM403	Physique
		Ceca	ACV404	Physique
		Ceca	ACV20	Physique

Tableau 1- Liste des sept composés organiques volatils et des neuf charbons actifs étudiés

2.2 Caractérisation des charbons actifs

La capacité d'adsorption et l'intensité des interactions entre molécules adsorbées et la surface des charbons actifs sont principalement liées aux propriétés de porosité et aux caracteristiques chimiques de la surface. Ainsi, les méthodes de caractérisation suivantes ont été utilisées :

- Adsorption du diazote à sa température de liquéfaction (77 K) pour déterminer la microporosité du CA (surface spécifique et volume microporeux) ;
- Porosimétrie à mercure pour évaluer la méso- et la macro-porosité ainsi que l'espace intergranulaire (degré de vide) ;
- Analyse élémentaire pour mesurer la composition du matériau (en pourcentage atomique de carbone, hydrogène, oxygène et soufre).

Chacune de ces techniques est sommairement présentée ci-dessous et les principaux résultats sont analysés.

2.2.1. Par l'isotherme de diazote à 77 K

Cette isotherme est réalisée par le système ASAP 2010 de Micromeritics pour l'analyse des surfaces spécifiques. Avant toute mesure, les échantillons de CA étaient dégazés pendant 48 heures à 250°C. Ensuite, les échantillons sont transférés sur la cellule de mesure où la courbe d'équilibre est effectuée dans un bain d'azote liquide (-196 °C) par des incréments de pression de diazote. L'isotherme en tant que telle ne donne accès qu'à une information limitée et principalement qualitative. Ainsi, des modèles théoriques sont appliqués pour déterminer les surfaces spécifiques, les volumes microporeux et la taille moyenne des micropores. L'enjeu pour l'expérimentateur est alors de vérifier l'applicabilité du modèle théorique (vérification des hypothèses) afin de disposer de mesures sûres [1-3].

Deux méthodes de calcul ont ici été retenues :

- modèle B.E.T. pour déterminer la surface d'échange totale (ou surface spécifique) ;
- modèle d'Horwart Kawazoe pour obtenir le volume microporeux.

A titre d'exemple, la Figure 1 montre une courbe d'équilibre à 77 K entre le diazote et le Pica BC120. Grâce à cette courbe, le modèle B.E.T. est appliqué (Figure 2). La relation linéaire, uniquement valable pour une plage restreinte de pressions, permet de déterminer la surface spécifique.

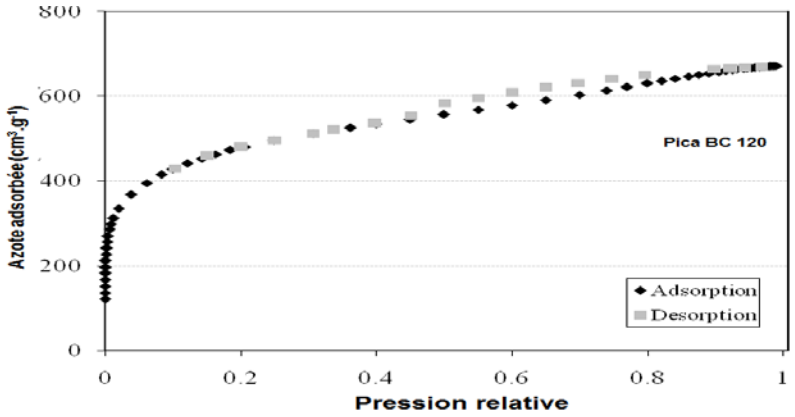

Figure 1 - Isotherme d'adsorption de l'azote à 77 K par le Pica BC120

Les résultats pour l'ensemble des charbons actifs sont rapportés dans le Tableau 2 ci-dessous.

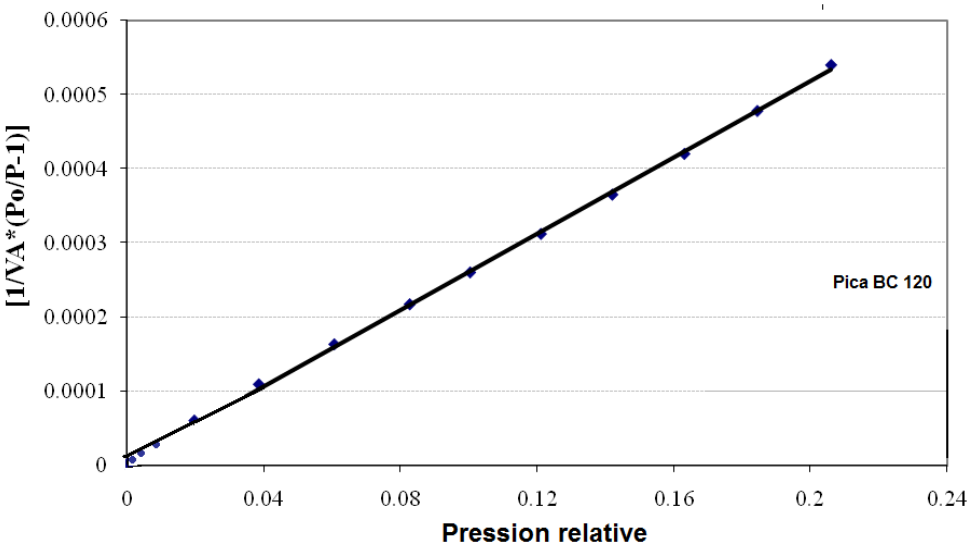

Figure 2 - Modèle B.E.T. appliqué à l'adsorption de azote à 77 K par le Pica BC120

2.2.2 Par porosimétrie à mercure

Cette technique, développée en 1921 par Washburn [4], est utilisée pour déterminer les propriétés physiques des matériaux poreux. Ces expériences ont été conduites avec le porosimètre Autopore IV 9500 de Micromeritics. La méthode consiste en une intrusion contrôlée de mercure dans la porosité du charbon actif. Le mercure n'ayant aucune affinité avec les surfaces carbonées (angle de contact supérieur à 140°), le volume de mercure introduit dans la structure de l'adsorbant est corrélé à la taille des pores par l'équation de Washburn [5-6]. A partir du volume poreux total (meso + macro), la densité du charbon actif est calculée (Tableau 2).

Figure 3 - Volume poreux total (meso + macro) et micropore en fonction du type de CA

Charbon actif	Densité ($g.m^{-3}$)	Volume microporeux ($cm^3.g^{-1}$)	Surface BET ($m^2.g^{-1}$)	Volume poreux total (meso + macro) ($cm^3.g^{-1}$)
Pica BC120	0,26	0,66	1687	1,89

Norit GF40	0,39	0,70	1881	1,01
Pica NC60	0,47	0,43	1028	1,40
Pica NC100	0,30	0,54	1430	2,36
Chemviron BPL	0,50	0,40	955	0,64
Ceca ACV404	0,42	0.54	1256	0,60
Ceca ACM404	0,46	0.44	1063	0,55
Ceca ACM403	0,53	0.47	1126	0,52
Ceca ACM204	0,59	0.30	698	0,38

Tableau 2 - Principales caractéristiques de texture des charbons actifs étudiés

Le tableau 2 montre qu'encore une fois deux classes de charbons actifs sont distinguées. En effet, contrairement aux charbons activés physiquement, les charbons activés chimiquement développent un volume mésoporeux beaucoup plus important que les CA produits par activation physique. Des données sont manquantes pour les charbons actifs produits par Ceca et restent à mesurer.

2.3. Mesures des isothermes d'adsorption

2.3.1. Méthode expérimentale

Les isothermes d'adsorption représentent les limites thermodynamiques du couple COV – CA. Ces données sont donc essentielles pour la modélisation. En outre, la relation d'équilibre entre le COV et le charbon actif sera fortement influencée par la température. Les courbes d'équilibre seront donc mesurées à quatre températures : 20, 40, 60 et 80°C. Finalement, pour sept COV et neuf CA, un total de 252 isothermes est nécessaire.

Décrivons brièvement le protocole expérimental. La mesure d'une isotherme d'adsorption est assez simple à réaliser. Dix réacteurs sont utilisés en parallèle dont chacun est empli d'air sec avec une masse constante de charbon actif (0,2 g) contenue dans une nacelle au centre du réacteur (Figure

4). Chaque réacteur est placé dans un bain thermostaté et quand la température atteinte à l'intérieur est celle désirée, un volume connu de COV liquide y est injecté. Durant ces expériences, les mesures de température réalisées au cœur des réacteurs ont montré que cette variable était précise à ±2°C autour de la valeur exigée. Après un temps d'équilibre (préalablement déterminé), la concentration en COV dans la phase gaz est mesurée par un détecteur à ionisation de flamme après une éventuelle séparation par chromatographie phase gazeuse. La quantité adsorbée est calculée par le bilan massique suivant [8-9] :

$$q_e = \frac{(C_0 - C_e)V}{m_{CA}}$$

avec

q_e : quantité adsorbée à l'équilibre ($mol.g^{-1}$)

C_0 : concentration initiale en COV ($mol.m^{-3}$)

C_e : concentration à l'équilibre ($mol.m^{-3}$)

V : volume du réacteur (m^3)

m_{CA} : masse de charbon actif (g)

Une partie des isothermes à mesurer ont déjà été obtenues au cours d'un travail de recherche précédent [9]. Afin de valider nos mesures expérimentales et avant de continuer la construction de la base de données existante, nous avons réitérer certaines de ces mesures. Ainsi, un exemple de reproductibilité des mesures est présenté sur la Figure 5 pour l'adsorption de dichlorométhane sur le charbon Pica NC60. La concordance entre les mesures réalisées et la référence montre la validité du protocole opératoire mis en place. De plus, la répétabilité des mesures est confirmé par trois essais consécutifs aboutissant à des courbes quasi-confondues.

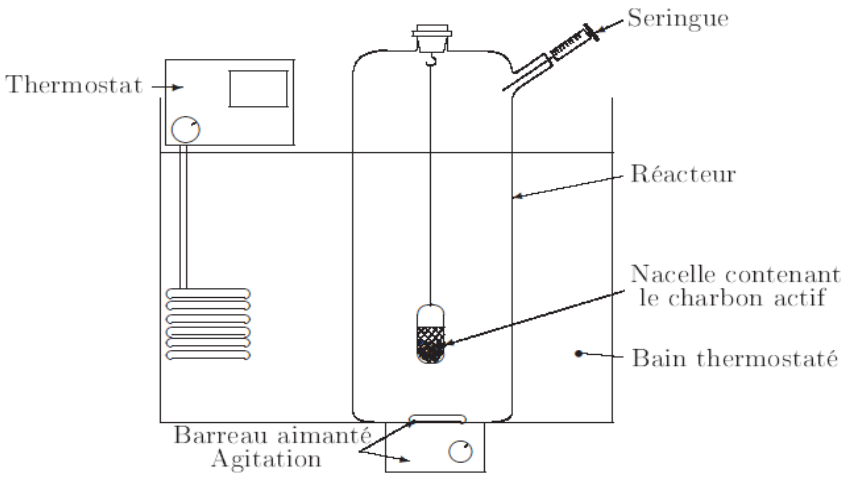

Figure 4 - Mesure des isothermes d'adsorption

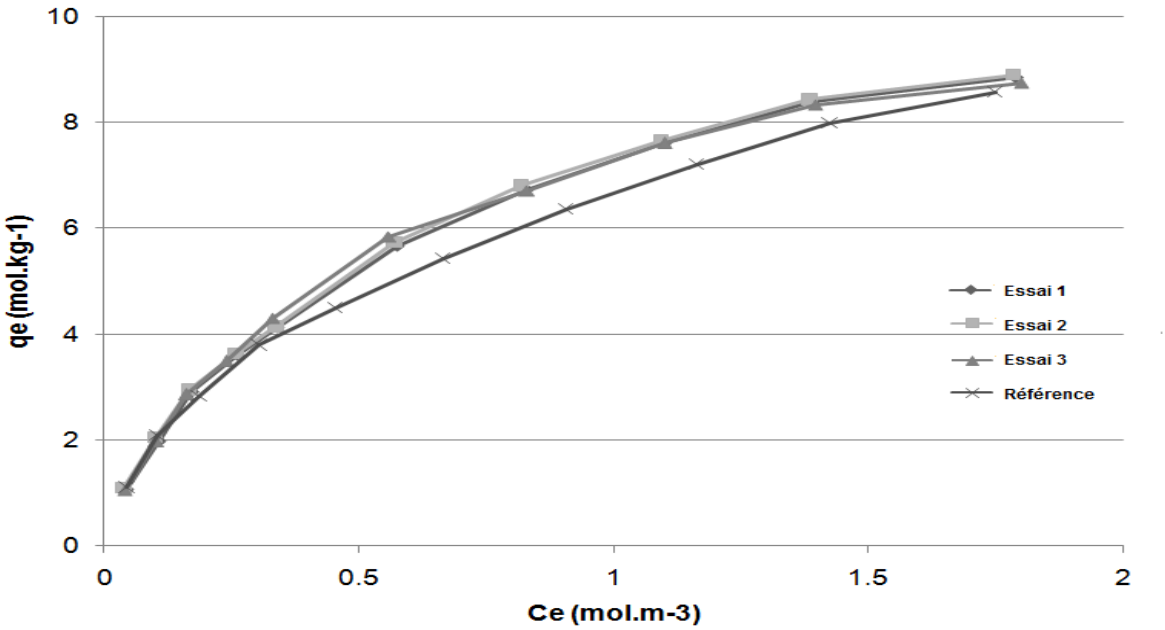

Figure 5 - Reproductibilité et répétabilité des mesures des isothermes d'adsorption du dichlorométhane sur charbon actif Pica NC60

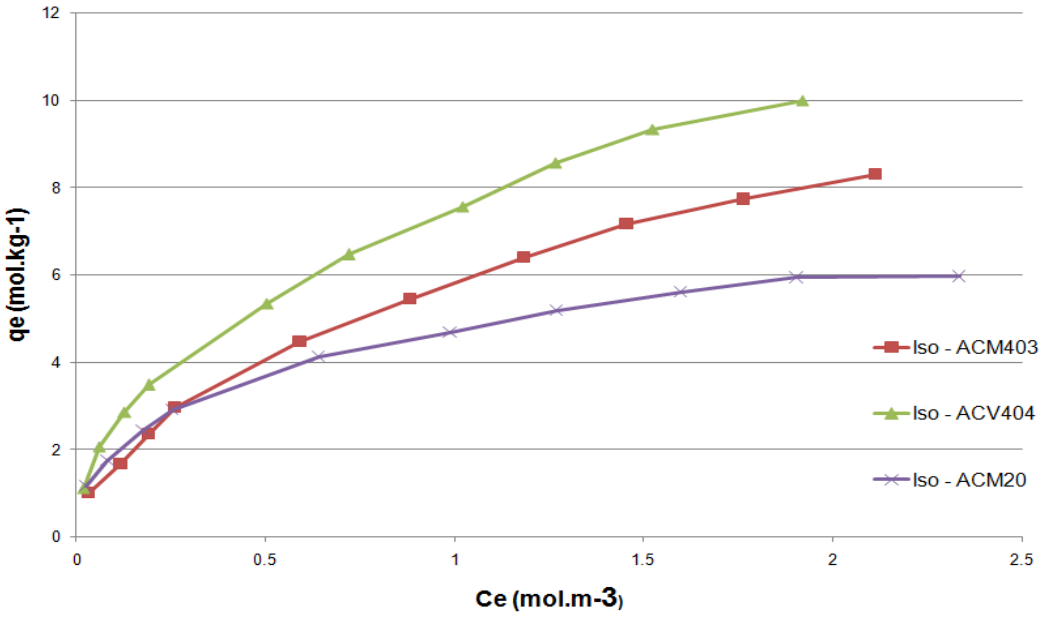

Figure 6 - Isotherme d'adsorption du dichlorométhane par trois charbons actifs produits par Ceca à 20°C

Après avoir validé le protocole expérimental, les premières courbes d'équilibre ont été tracées pour les nouveaux couples COV – CA. Ainsi, l'adsorption du dichlorométhane (CH_2Cl_2) est illustrée sur la Figure 6 pour les charbons actifs Ceca.

Un grand nombre de mesures sont encore à réaliser pour compléter la base de données (environ 180 isothermes).

2.4. Modélisation des isothermes

La modélisation des isothermes d'adsorption est un problème ancien et bon nombre de modèles ont déjà prouvé leur utilité. Chacun de ces modèles est basé sur un ensemble d'hypothèses restrictives qui s'appuient sur des mécanismes d'adsorption (site d'adsorption, potentiels d'interaction, distribution d'énergie de surface, etc.).

Néanmoins, pour notre étude, une composante principale est l'influence de la température dont le modèle doit tenir compte. Cette variable accentue considérablement les difficultés de modélisation en ajoutant des paramètres ajustables dans chaque modèle. L'objectif est alors de vérifier l'application des modèles les plus communs. Le tableau 4 montre les principaux modèles qui seront testés dans cette étude.

Nom du modèle	Equation	Paramètres ajustables
Langmuir	$q_e = \frac{q_m\, b \exp\left(\frac{H}{RT}\right) C_e}{1 + b \exp\left(\frac{H}{RT}\right) C_e}$	q_m, b, H
Dubinin – Raduskevich	$q_e = \frac{W_0}{V_m}.\exp\left(-\left(\frac{RT}{E}\ln\left(\frac{p_s}{p_e}\right)\right)^2\right)$	W_O, E
Langmuir-Freundlich	$q_e = \frac{q_m\, b \exp\left(\frac{H}{RT}\right) C_e^{1/n}}{1 + b \exp\left(\frac{H}{RT}\right) C_e^{1/n}}$	q_m, b, H, n

Tableau 4 - Principaux modèles appliqués à l'adsorption de COV

La gamme de concentration (1 à 170 gm-3) qui avait été choisi dans les expériences isothermes d'adsorption couvre un large éventail qui représente la situation typique dans les industries alimentaires, chimiques et d'hydrocarbures. Les coefficients d'adsorption isothermes pour prédire la capacité d'adsorption ont subi des tests rigoureux statistiques pour consolider la fiabilité de chaque COV - système de charbon activé. L'objectif de la création de ces vaste ensemble de données isothermes sont de les utiliser dans PROSIM simulation de processus. Même si le modèle DR-MLR pour la caractéristique de l'énergie d'adsorption (E) pour les systèmes de carbone toluène-activés n'a pas de travailler à cause des raisons invoquées dans la discussion, le modèle DR-MLR énergie caractéristique permettrait de réduire le besoin d'effectuer l'isotherme d'adsorption expériences. Les

autres valeurs telles que le volume des micropores (à partir de l'analyse d'azote), la pression de saturation et le volume molaire (à partir des propriétés de COV) sont déjà disponibles. Donc, en ayant ce modèle MLR dans l'outil de simulation, il fera la simulation efficace et simple.

3 - Phase 2 : Modélisation de l'étape d'adsorption

Cette section consiste en une étude comparative des modèles de modélisation de l'adsorption proposés par l'EMN et ProSim. Cette comparaison permet d'évaluer les spécifications en vue d'obtenir un modèle amélioré. Enfin, des résultats préliminaires sont présentés.

3-1 Analyse du modèle d'adsorption EMN et exemples de simulations

Le modèle développé à l'EMN consiste à simuler l'adsorption de COV sur un lit fixe de charbon actif industriel. L'approche globale de simulation du procédé prend en compte les transferts couplés de chaleur et de matière. Lors du transfert de matière, le mécanisme de diffusion de surface est considéré comme prédominant et le coefficient global de transfert est un paramètre ajustable. Les phénomènes de dispersion thermique et de chaleur sont également pris en compte, et les coefficients de dispersion correspondants sont aussi des paramètres ajustables.

Pour toutes les simulations, l'isotherme d'adsorption utilisée est celui de Freundlich. Le système d'équation à résoudre est limité à trois équations : le bilan massique, le bilan énergétique et le transfert de matière par adsorption (modèle de force linéaire). Enfin, la résolution du système d'équation est effectuée à l'aide de la méthode des volumes finis.

Les équations du système sont au nombre de trois:

- le bilan de matière :

$$\underbrace{-\varepsilon D_L \frac{\partial^2 C}{\partial z^2}}_{\text{dispersion}} + \underbrace{v \frac{\partial C}{\partial z}}_{\text{convection}} + \underbrace{\varepsilon \frac{\partial C}{\partial t}}_{\text{accumulation}} + \underbrace{\rho_{lit} \frac{\partial q}{\partial t}}_{\text{adsorption}} = 0$$

ε : degré de vide du lit (-)

C : concentration du COV ($mol.m^{-3}$)

v : vitesse superficielle ($m.s^{-1}$)

z : coordonnée axiale (m)

ϱlit : densité du lit ($kg.m^{-3}$)

q : quantité de COV adsorbée ($mol.kg^{-1}$)

DL : coefficient de dispersion de masse ($m2.s^{-1}$)

- le bilan énergétique :

$$\underbrace{-D_H \frac{\partial^2 T}{\partial z^2}}_{\text{dispersion}} + \underbrace{v \rho_g Cp_g \frac{\partial T}{\partial z}}_{\text{convection}} + \underbrace{\left(\varepsilon \rho_g Cp_g + \rho_{lit} Cp_s + \rho_{lit} Cp_a q\right) \frac{\partial T}{\partial t}}_{\text{accumulation}} = \underbrace{\rho_{lit}\left(-\Delta H_{ads}\right) \frac{\partial q}{\partial t}}_{\text{adsorption}} - \underbrace{4 \frac{h}{d_c}\left(T - T_0\right)}_{\text{échange}}$$

T : température (K)

ϱ_g : densité de la phase gaz ($kg.m^{-3}$)

Cpg : chaleur spécifique de la phase gaz ($J.kg^{-1}.K-^{1}$)

Cps : chaleur spécifique de la phase solide ($J.kg^{-1}.K^{-1}$)

Cpa : chaleur spécifique de la phase adsorbée ($J.kg^{-1}.K^{-1}$)

ΔHads : enthalpie d'adsorption ($J.mol^{-1}$)

h : coefficient de transfert de chaleur ($W.m^{-2}.K^{-1}$)

T0 : température ambiante (K)

DH : coefficient de dispersion de chaleur ($W.m^{-1}.K^{-1}$)

- le transfert de matière par adsorption (modèle de force linéaire):

$$\frac{\partial q}{\partial t} = k(q_e - q)$$

q : quantité adsorbée ($mol.kg^{-1}$)

k : coefficient de transfert de matière (s^{-1})

qe : quantité adsorbée à l'équilibre ($mol.kg^{-1}$)

Le coefficient de transfert s'exprime sous la forme :

$$k = \gamma \exp(\frac{0.45\Delta H_{ads}}{RT})$$

Les trois paramètres ajustables sont : γ, D_H et D_L, et les trois inconnues sont la quantité adsorbée, q, la concentration en COV, C, et la température, T.

Les hypothèses du modèle sont :

- un taux d'adsorption décrit par un modèle de force linéaire, les particules adsorbantes étant considérées comme sphériques et la diffusion homogène,

- un transfert de masse décrit par une diffusion intra-particulaire (limitée par la diffusion de surface) et extra-particulaire (D_L),

- un travail des forces de pression négligeable,

- une enthalpie d'adsorption moyenne (établie expérimentalement),

- un équilibre thermique local instantané permettant de considérer les températures du gaz et du solide égales,

- et une dispersion radiale négligée.

Les figures 7a et 7b montrent un exemple d'adsorption du formiate d'éthyle sur le charbon Pica NC60 à une concentration de 44 g.m-3 et une température de 27°C, les paramètres ajustés sont : γ = 195 s-1, D_H = 0,091 $W.m^{-1}.K^{-1}$ et D_L = 0 $m^2.s^{-2}$.

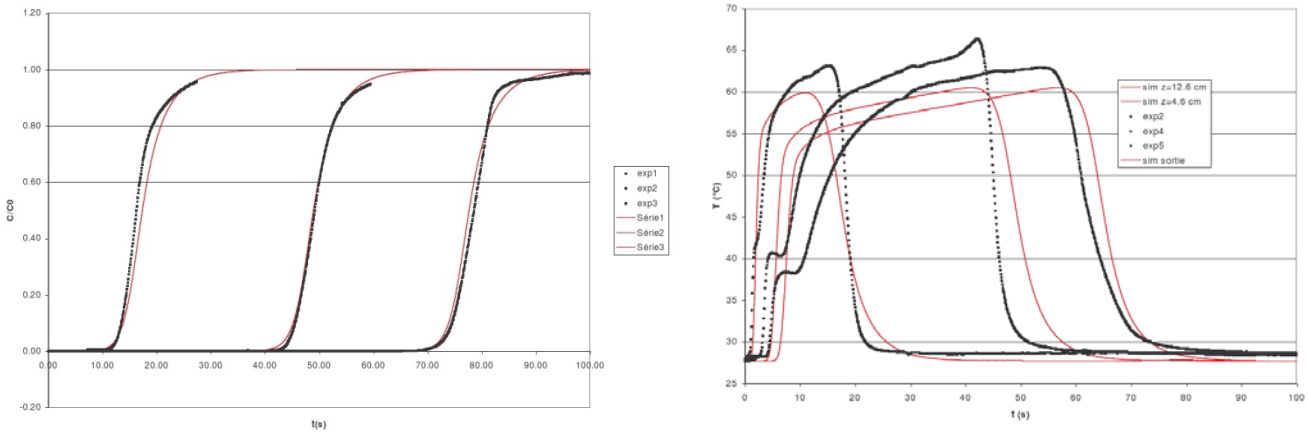

Figures 7a et 7b : Courbes de percée et profils axiaux de temperature expérimentaux et simulés dans le cas de l'adsorption de formiate d'éthyme sur PICA NC60.

Ces figures montrent un très bon accord entre les données expérimentales et la simulation. Les courbes de percées sont très bien représentées (en entrée, milieu et sortie de colonne). Les profils de températures correspondants présentent une forme globale satisfaisante, cependant la température est légèrement sous-estimée (entre 2 et 5°C environ).

On peut cependant observer les oscillations numériques pour certains profils de température et un décalage des courbes de percée en sortie de colonne, c'est le cas pour la simulation de l'adsorption du dichlorométhane sur le charbon Chemviron BPL (γ = 78,3 s-1, D_H = 0,0 $W.m^{-1}.K^{-1}$ et D_L = 0 $m^2.s^{-2}$, C0 = 47,1 $g.m^{-3}$, T0 = 23,3 °C). On remarque de plus une température sous-estimée d'environ 10°C:

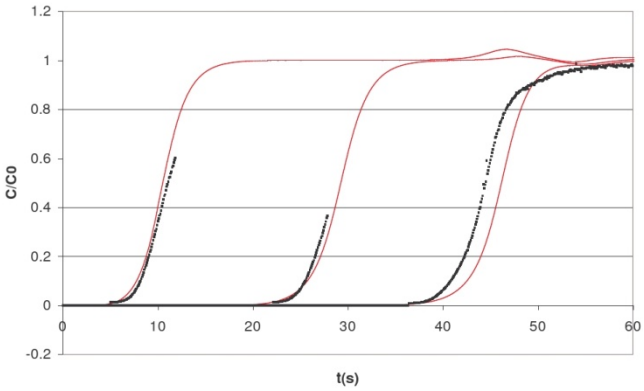

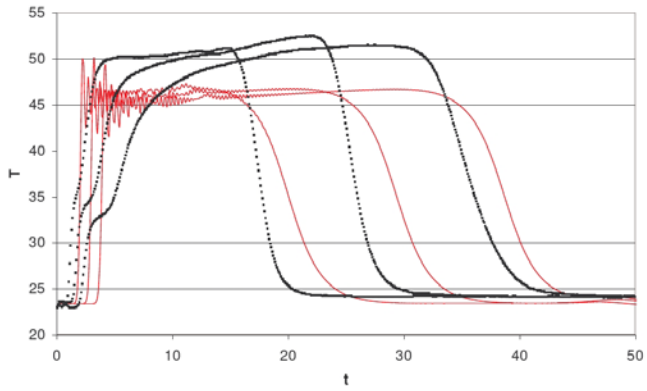

Figures 8a et 8b : Courbes de percées et profils axiaux de temperatureexpérimentaux et simùulés dans le cas de l'adsorption de dichloromethane sur charbon actif Chemviron BPL.

De façon à améliorer la forme des profils et à limiter le nombre de paramètres ajustables, nous adoptons une forme analytique pour les coefficients de dispersion D_L et D_H, ainsi seul le coefficient de transfert de masse reste ajustable. Les formes choisies pour D_L et D_H sont tirées de l'ouvrage *Perry's chemical engineers' handbook*, R.H. Perry et D.W. Green, 7th edition, 1997, 16-20 :

$$\gamma_1 = 0.45 + 0.55\varepsilon$$

$$\gamma_2 = 0.5(1 + 13\gamma_1\varepsilon/(\mathrm{Re}\,Sc))^{-1}$$

$$\mathrm{Re} = \rho_g u_0 d_p / \mu$$

$$Sc = \mu/(\rho_g D_m)$$

$$D_m = f(T, P, V_m, M)$$

$$D_H = \rho_g C p_g D_L$$

$$D_L = d_p u_0 (\gamma_1 \varepsilon / \mathrm{Re}\,Sc + \gamma_2)$$

Les figures 9a et 9b suivantes montrent les résultats de l'adsorption du dichlorométhane sur le charbon chemviron BPL vue précédemment avec ces valeurs calculé et seul γ ajusté :

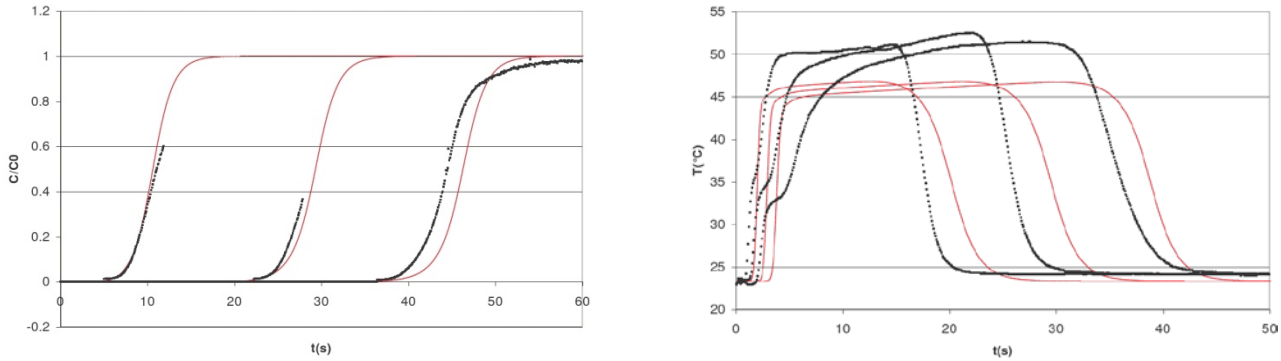

Figures 9a et 9b : courbes de percée et profils axiaux de temperature expérimentaux et simulés dans le cad de l'adsorption de dichloromethane sur charbon actif Chemviron BPL – modèle à un parameter adjustable.

Les oscillations sur le profil de température sont alors absentes. Cependant, on observe toujours un décalage sur la courbe de percée en sortie de colonne, et des températures sous-estimées.

Des simulations ont été faites avec trois COV (formiate d'éthyle, acetone et dichloromethane) sur quatre charbons actifs (Chemviron BPL, Pica NC60 et NC100, et Norit GF40). Pour tous ces couples COV/charbon, le coefficient de transfert de masse k a été ajusté de façon à le corréler à une grandeur typique du charbon actif.

Parmi les caractéristiques du charbon auxquelles nous avons accès, seule la surface spécifique semble présenter une corrélation avec le coefficient de transfert. La figure 10 présente les résultats obtenus avec les simulations les plus convaincantes.

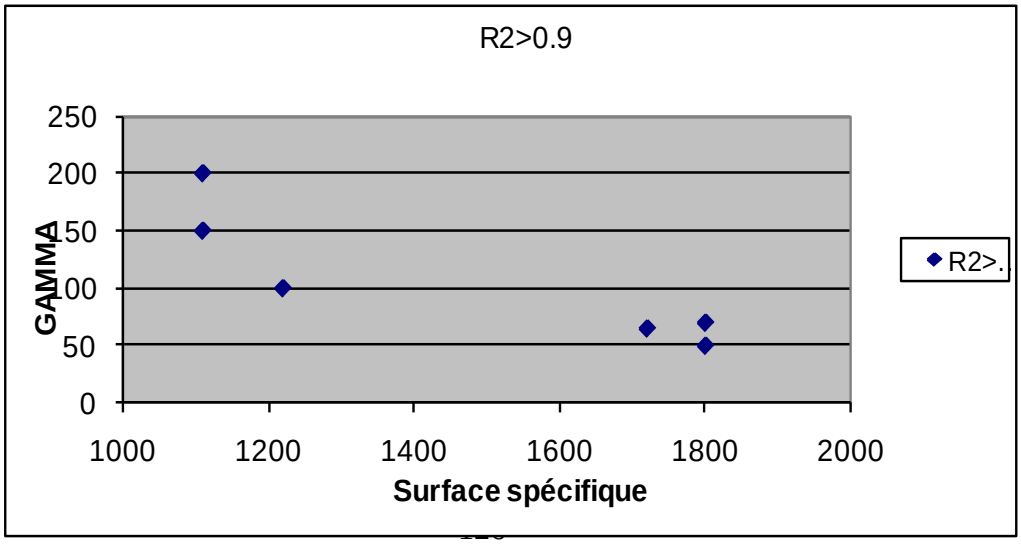

Figure 10 : Influence de la surface spécifique ($m^2.g^{-1}$) des charbons actifs sur la valeur ajustée du paramètre

Cette figure donne une tendance de la relation entre k et la surface spécifique : γ est inférieur à 100 pour des surfaces spécifiques importantes (supérieures à 1700 m^2g^{-1}) et supérieur à 100 pour des surfaces spécifiques plus faibles (inférieures à 1200 m^2g^{-1}). Cette observation suggère soit, de prendre en compte ce paramètre dans le calcul de la résistance intra- ou extra-particulaire, soit, d'introduire un aspect géométrique des particules dans le calcul de k.

En ce qui concerne le modèle développé à l'EMN, l'analyse met en évidence une bonne représentation des courbes de percée. Les profils de température simulés sont en bon accord avec l'expérience mais la valeur de la température maximale est souvent sous-estimée. Enfin, le lien apparent entre la surface spécifique et le coefficient de transfert de matière suggère de tenir compte avec précision de l'aspect géométrique des particules d'adsorbant (surface spécifique, rapport de surface sur volume de ces particules, etc.). Ce dernier point suggère de modéliser le coefficient k comme la somme de deux contributions : le transfert de matière interne, fonction du coefficient de transfert au travers de la couche limite, et externe, fonction de la diffusivité globale.

3-2 Analyse comparative du modèle d'adsorption ProSim DAC

Comme le modèle EMN, le logiciel ProSim DAC a pour but de modéliser l'adsorption de COV sur un lit de charbon actif. ProSim DAC présente une interface permettant de choisir les constituants (COV, gaz vecteur), de renseigner les caractéristiques de l'alimentation, de la colonne, du charbon et des isothermes d'adsorption. Les résultats sont directement visibles via des courbes XML, et des fichiers EXCEL sont créés pour une grande quantité de données calculées (quantité adsorbée, températures, concentrations, etc.). Il est possible d'intégrer plusieurs constituants (mélange de COV), ces derniers étant accessibles depuis une base de donnée de corps purs. Cette base de données offre également l'accès aux caractéristiques thermodynamiques de chaque constituant (masse molaire, capacité calorifique, dépendance des ces caractéristiques en fonction de la température, etc.).

La figure 11 donne un aperçu de l'interface de ProSim DAC avec la fenêtre principale, celle des caractéristiques et les courbes XML :

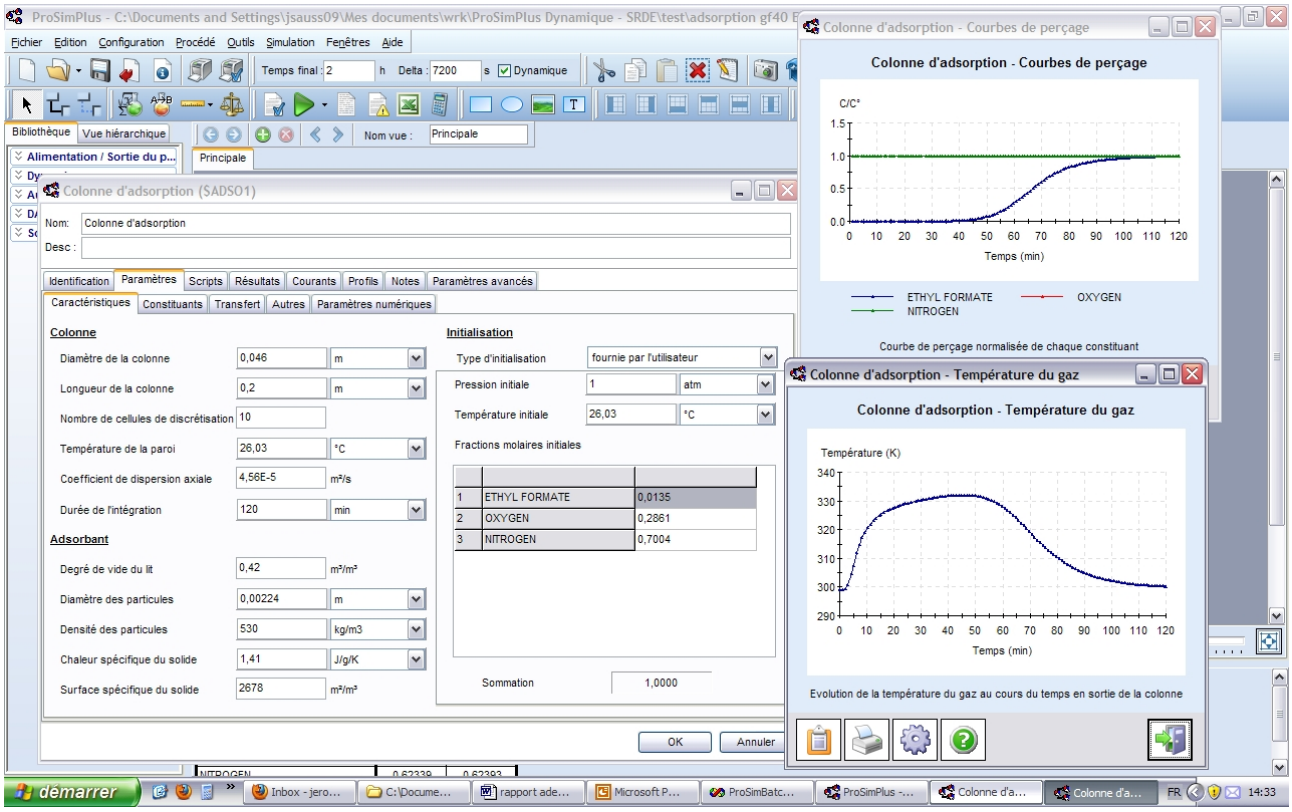

Figure 11 : Interface du logiciel Prosim DAC

Le modèle proposé dans ProSim DAC est défini par 4NC+7 équations, avec NC le nombre de constituants considérés. Le tableau 5 donne un comparatif des équations du modèle EMN et de ProSim DAC.

Le système d'équation est résolu par la méthode Gear. A ces équations s'ajoutent des coefficients de transfert de matière intra-particulaire en phase gaz et en phase solide, ainsi que des coefficients de transfert de chaleur gaz/paroi et gaz/particule. Tous ces coefficients peuvent être, soit calculés, soit entrés par l'utilisateur.

Compte tenu du nombre important d'équations dans ce modèle, le nombre d'hypothèses est limité. En effet, seuls les échanges de chaleur entre l'adsorbant et la paroi ainsi que la dispersion radiale sont négligés. Comme pour le modèle de l'EMN, le transfert de matière en phase solide est considéré comme limité par la diffusion de surface (il peut être soit calculé, soit entré par l'utilisateur).

4. Phase 3 : Etude expérimentale des cycles adsorption-régénération

Les essais d'adsorption et régénération thermique de COV sur CA seront conduits sur deux unités distinctes. L'une construite à l'EMN permettra d'étudier la régénération par injection de vapeur d'eau ou d'un gaz inerte chaud (azote). L'autre disponible à Lacq, au Centre de Recherche d'Arkema, permet d'évaluer la régénération thermique combinée à une dépressurisation sous vide de la colonne.

Nous décrivons ci-après chacune des deux unités expérimentales, ainsi que les résultats de travaux préliminaires, conduits sur le site d'Arkema, et qui ont viseé à évaluer en termes de performances et de coûts opératoires un mode de régénération thermique à l'azote chaud, combiné à une dépressurisation sous vide de la colonne (procédé VTSA « Void Thermal Swing Adsorption »).

4.1. Description de l'unité expérimentale d'adsorption modulée en température (EMN)

Une unité expérimentale permettant de réaliser des cycles d'adsorption et régénération thermique a été construite au laboratoire de l'EMN. Cette unité doit permettre de générer des données expérimentales relatives aux performances des étapes d'adsorption et désorption à la vapeur d'eau ou par un gaz inerte chaud.

4.1.1 Analyse fonctionnelle du banc d'essai

Le banc d'essai permet l'adsorption de COV sur charbon actif en grain disposé dans une colonne. La régénération de ces charbons se fait soit par circulation d'azote chauffé, ou par injection de vapeur surchauffée. L'installation permet la répétition de cycles comportant une succession d'étapes qui varient en fonction du mode de régénération appliqué.

Le Système de d'injection d'air est composé d'une entrée d'air sec, filtré et régulé (FIC11) permettant d'obtenir un débit massique maximum de 30 l/min. Une seconde entrée d'air régulée (FIC12) laissant circuler au maximum 3 l/minutes passe par le barboteur qui est placé dans un bain régulé en température (TIC17).

La prise d'échantillon FID isolée par la vanne V16 permet de vérifier la concentration en COV avant l'injection dans la colonne d'adsorption. Pendant la phase de réglage, le mélange peut être envoyé directement vers la sortie. En fonctionnement normal, il sera injecté par le bas de la colonne par la vanne V4.

La production de vapeur est assurée par un adoucisseur d'eau qui alimente un générateur électrique de vapeur de 1.6 KW. La vapeur produite traverse ensuite une surchauffeur, de 2 kW électrique, qui permet de régler la température de la vapeur jusqu'à 260°C. Le débit maximum du dispositif est de 1.14 kg/h. Il n'est pas possible de mesurer ce débit, ce dernier sera donc estimé par la pesée des condensats obtenus en sortie de la colonne.

L'azote chauffé est issue de bouteilles. Le contrôle de son débit est assuré par un régulateur de débit massique de gamme 150 l/min. La régulation de température est assurée ensuite par deux colliers (2x300 W) qui chauffent un bloc échangeur en laiton. La température de l'azote en sortie de ce réchauffeur pourra atteindre 170°C.

La colonne mesure 25 cm de hauteur et 5 cm de diamètre intérieur. Elle est isolée aux 2 extrémités pour éviter les phénomènes de condensation. Elle est entourée d'un tuyau parcouru par de l'eau du réseau qui sert à son refroidissement. Ce circuit d'eau pourra être purgé avec de l'air comprimé par la vanne V14. Un fil chauffant (500 W) est disposé en parallèle du tuyau pour chauffer la colonne avant l'injection de vapeur. Un autre sera placé sur les tuyauteries et sur les vannes d'alimentation. La colonne est équipée de 8 sondes de températures et de 3 prises d'échantillons pour la mesure de concentration en COV avec l'analyseur FID.

Le système d'acquisition permet l'affichage et l'enregistrement des débits, des températures, des concentrations ainsi que de l'humidité. Il gère aussi les différentes boucles de régulations.

4.1.2 Déroulement des cycles

Dans un premier temps, les essais seront conduits pour deux cycles successifs, incluant un mode régénération à l'azote chaud et un mode régénération à la vapeur d'eau.

Le déroulement d'un essai inclura les étapes suivantes :

1. *Adsorption*

Les vannes V1, V2, V3, V4 et V8 sont ouvertes. Le bain thermostat du barboteur a atteint sa température de consigne. Une consigne de débit est appliquée sur les deux régulateurs d'air comprimé (barbotage et dilution). Une fois les débits réglés, la concentration de COV en entrée est vérifiée à l'aide de l'analyseur à ionisation de flamme (FID). La colonne est alimentée par le mélange lorsque la vanne V16 est ouverte.

2. *Désorption à l'azote chaud*

Au cours du premier cycle, la désorption thermique sera effectuée par passage d'un courant d'azote chaud à contre-courant dans le lit. Un échangeur de chaleur permet de porter la température de l'azote à la valeur souhaitée, les vannes V7 et V4 étant ouvertes, le débit d'azote sera régulé au moyen du régulateur FIC13. Durant cette phase, la concentration en COV récupéré dans le courant gazeux en sortie de colonne est mesurée en continu.

3. *Refroidissement de la colonne*

Lorsque l'étape de désorption est terminée, le lit est refroidi à la paroi par circulation d'eau dans un serpentin. Un refroidissement convectif par circulation d'air dans le lit pourra éventuellement accélérer le refroidissement du lit.

Les étapes 1 à 4 sont répétées dans le second cycle.

4. *Désorption à la vapeur d'eau*

Une fois les consignes de température du générateur de vapeur, du surchauffeur et de la colonne atteintes, les vannes V7, V4, V15 et V17 seront ouvertes afin d'alimenter la colonne à contre-courant par la vapeur d'eau surchauffée. Les condensats seront collectés dans un réservoir amovible. Ce réservoir sera pesé en fin de désorption pour quantifier la quantité de vapeur injectée.

5. *Séchage et refroidissement du lit*

Après désorption à la vapeur d'eau, le matériau adsorbant doit être désumidifié avant d'envisager une nouvelle phase d'adsorption. Pour cela, les vannes V1, V6 et V9 sont ouvertes pour alimenter la colonne avec un débit d'air contrôlé à l'aide du régulateur FIC11. L'humidité de l'air sortant de la colonne sera mesurée par le capteur AT10.

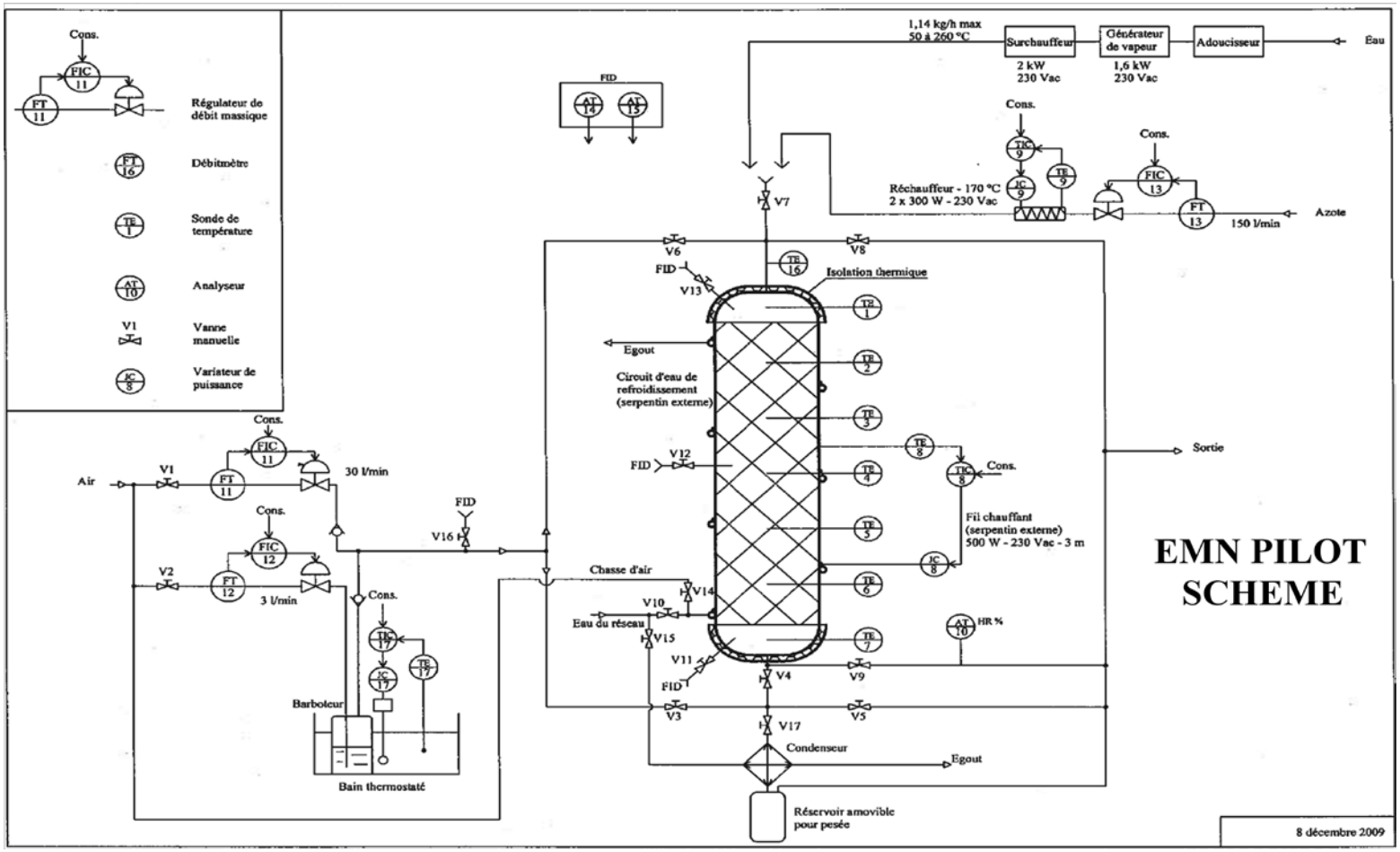

Figure 16 – Schéma de l'installation expérimentale EMN

4.2. Description de l'unité expérimentale d'adsorption modulée en température et au vide (Arkema)

L'unité expérimentale disponible sur le site de Lacq d'Arkema est montrée sur la figure 17. Elle est équipée d'une colonne mesurant 150 cm de hauteur et 5 cm de diamètre interne.
Trois thermocouples T1, T2 et T3 disposés en une hauteur de 50 cm, 25 cm et 0 cm à partir de la base du lit permettent de mesurer les profils de température au cours des cycles.

En phase d'adsorption, la colonne est alimentée par un mélange azote-COV généré au moyen d'un évaporateur, dont la température est contrôlée. Le débit d'azote en entrée est ajusté au moyen d'un débitmètre massique. Le mélange alimente la colonne du haut vers le bas. En sortie, un analyseur FID permet de mesurer la courbe de percée du filtre.

Deux modes de régénération peuvent être appliqués : sous vide ou thermique, par passage d'un gaz inerte (azote) chaud.

L'épaisseur de la paroi est élevée alors que la chaleur de l'azote lors de la régénération n'est pas suffisante. Par conséquent, il est un bain d'huile chaude (80°C) autour de la colonne.

Le bain d'huile chaude est appliquée avant la début de la régénération et d'attendre que la température pour arriver à 75°C dans le lit
Voici les conditions opératoires de la régénération

1. Température de la régénération - 85°C, 93°C et 115°C
2. Débit d'azote - 250 $L.hr^{-1}$ et 500 $L.hr^{-1}$
3. Niveau de saturation de la régénération thermique dans le lit - 55% et 75%

Ce qui suit sont les caractéristiques des importantes des équipements et le coût de l'électricité et de l'azote. Ils seront utiles dans le calcul des coûts d'exploitation et le coût de l'azote pour trouver le coût optimisé pour la régénération.

Puissance de pompe vide (KW)	0,396
Puissance de bain de l'huile chaude (KW)	2
Puissance de préchauffage (KW)	0,3
Power of cordon (KW)	0,2
Coûte de l'azote (€/m3)	0,18
Coûte de l'électricité (€/MWh)	60

4-3 Résultats d'essais préliminaires

Dans un premier temps, des essais préliminaires ont été réalisés sur l'unité expérimentale disponible à Lacq. Ces essais ont été conduits en utilisant le dichlorométhane (DCM) comme composé type, et un charbon actif sous forme d'extrudés fourni par Arkema (ACM404). Ces essais avaient pour but d'évaluer l'intérêt au plan des performances et du coût opératoire d'introduire une étape de désorption sous vide de la colonne lors de la régénération du lit.

Deux campagnes d'essais ont été réalisées. Une première a permis d'ajuster la gamme de fonctionnement opératoire de la colonne et a montré qu'une seule étape de désorption sous vide en conditions froides à l'issue de la phase d'adsorption était insuffisante pour une régénération complète du lit. A conditions initiales identiques, on montre ainsi que le taux de régénération obtenu par dépressurisation sous vide de la colonne en conditions froides n'est que de 28 %, contre 93 % par désorption thermique.

Lors de la seconde campagne, l'objectif a été d'évaluer un mode de régénération combiné thermique et sous vide, alors que le lit est encore chaud.

4-3.1 Conditions opératoires

Des cycles successifs d'adsorption-désorption ont été menés, en faisant varier les conditions de régénération. En phase d'adsorption, les conditions opératoires sont spécifiées dans le tableau 9:

COV	Dichlorométhane
Matériau	ACM404
Hauteur du lit (cm)	150
Masse du lit (kg)	1,222
Vitesse superficielle de l'azote (m/s)	0,28

Concentration COV à l'entrée (g/m^3)	50

Tableau 9 : Conditions opératoires des essais en phase d'adsorption

En phase de régénération, alors que le lit d'adsorbant est complètement saturé, la désorption est réalisée en deux étapes successives :

- Désorption thermique, par passage d'un courant d'azote chaud ;
- Dépressurisation sous vide de la colonne

Lors de la première étape, deux paramètres opératoires ont été variés : le débit et la température du courant d'azote utilisé comme agent de désorption thermique.

Lors de la seconde étape de désorption sous vide, un faible courant d'azote permettant d'évacuer le composé désorbé est maintenu en entrée de la colonne. La variable opératoire considérée a alors été le niveau de saturation du lit au moment où est démarrée la dépressurisation de la colonne.

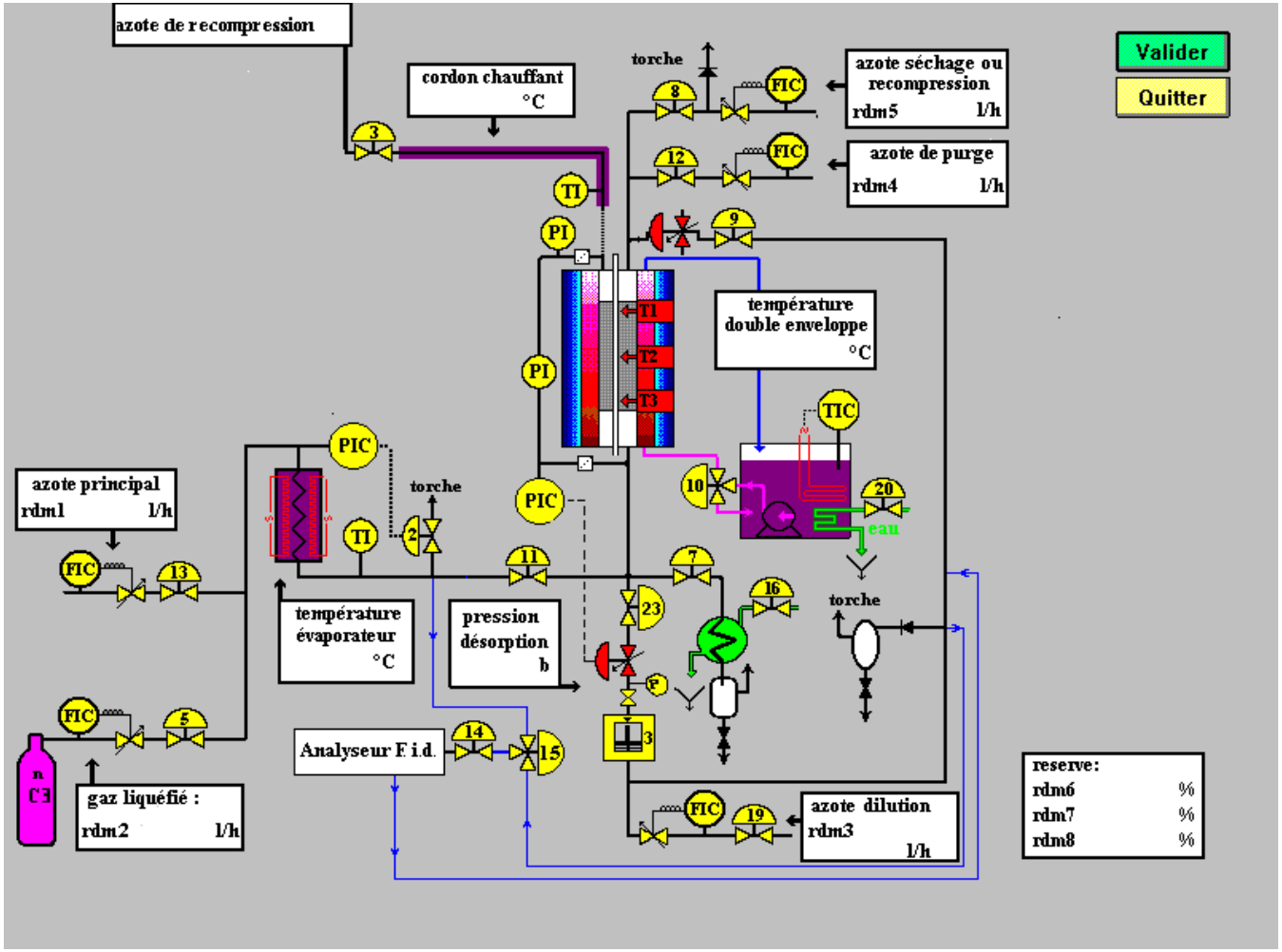

Figure 17 – Schéma de l'installation expérimentale d'Arkema, Pau

Le tableau 10 résume les conditions expérimentales testées.

Cycle	**Etape 1 : désorption thermique**				**Etape 2 : dépressurisation sous vide**		
	Tmax lit (°C)	**Débit N_2 (NL /h)**	**Durée de l'étape (min)**	**Taux de régénération du lit (%) Fin étape 1**	**Débit N_2**	**Durée de l'étape (min)**	**Taux de régénération du lit (%) Fin étape 2**
1	93	500	100	75	65	40	82
2	85	500	105	75	65	35	80
3	93	500	50	55	65	90	74
4	85	500	55	55	65	85	70
5	118	250	108	55	65	72	67
6	85	250	121	55	65	59	62
7	118	250	180	70	_	_	_
8	85	250	180	62	_	_	_

Tableau 10 : conditions opératoires appliquées lors de la phase de régénération (2nde campagne d'essais – site d'Arkema)

4-3.2 Evaluation des performances de régénération

Au cours des cycles successifs d'adsorption et de régénération, il n'a pas été observé de dégradation de la capacité d'adsorption massique du lit. La quantité de dichlorométhane adsorbé a été calculée à partir d'un bilan matière et de la mesure de la courbe de percée du filtre.
A chaque cycle, la quantité de COV adsorbée dans le lit a été évaluée à 383,33 g, soit une capacité d'adsorption massique du matériau égale à 30,34%.

Le tableau 10 reporte pour chaque cycle les taux de régénération obtenu à la fin de l'étape de désorption thermique, et après dépressurisation sous vide de la colonne. S'il est possible d'obtenir

une régénération complète du lit par désorption thermique, cela peut ne pas être le cas si la désorption thermique est partiellement compensée par une dépressurisation sous vide de la colonne. La dépressurisation sous vide est insuffisante pour régénérer complètement le lit, même après une désorption thermique partielle de 55 à 75% de la quantité de COV adsorbée à saturation. En mode combiné, le taux de régénération maximal atteint en fin de cycle est de 82%. Ce taux varie notamment en fonction du niveau de régénération partielle auquel débute la dépressurisation sous vide.

Au cours de l'étape de désorption thermique, si la température atteinte dans le lit n'influe guère sur la vitesse de régénération (cycles 5, 6, 7, 8), on constate que le débit d'azote appliqué est en revanche un paramètre opératoire déterminant. Ainsi, si l'on compare les cycles 2 et 5, un gain de 25% est obtenu sur le taux de désorption partiel à l'issue de la désorption thermique (étape 1) grâce au doublement du débit d'azote, toutes choses égales par ailleurs.

4.3.3 Analyse technico-économique

Une comparaison des coûts opératoires exprimées en termes d'énergie électrique consommée et de consommation d'azote a complété l'étude expérimentale.

Le débit d'azote chaud appliqué lors de l'étape de désorption thermique a un impact significatif non seulement sur les performances de régénération mais aussi sur les coûts opératoires. La figure 18 montre que pour réduire les coûts et accroître le taux de désorption mieux vaut appliquer un débit d'azote suffisamment élevé. Si le débit d'azote est trop faible, la vitesse de désorption est fortement ralentie. Il en résulte une baisse du taux de régénération associée à un allongement de la durée de l'étape de désorption qui accroît sensiblement la quantité globale d'azote consommée. L'augmentation du débit implique cependant une dilution plus grande des composés désorbés. Il faut ainsi considérer que le gain économique sur cette étape peut éventuellement être partiellement compensé s'il engendre un surcoût sur l'étape de séparation ultime, de condensation des COV récupérés.

En appliquant le vide dans les Reg 5 et 6 (à la fois à des débits inférieurs = 250 L. hr^{-1}), il est possible d'atteindre plus de 5 - 8% de la régénération que dans le cas de Reg 7 et 8 aux mêmes coûts (figure 19)

L'ensemble des résultats reportés sur la figure 20 indiquent que l'on peut trouver des conditions de régénération en mode combiné qui permettent d'optimiser le taux de régénération du filtre tout en minimisant les coûts opératoires.

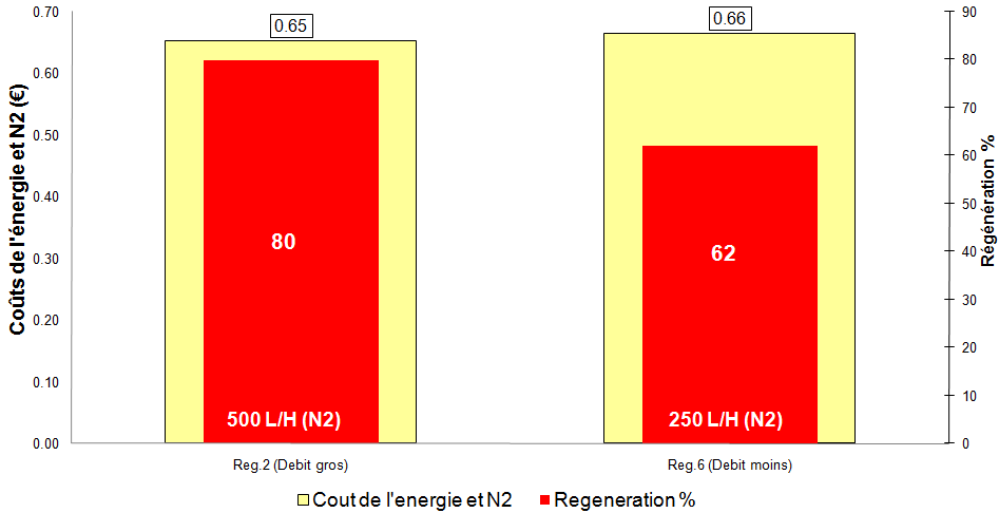

Figure 18: Influence du débit d'azote sur les performances de régénération thermique et les coûts opératoires engendrés (Cycles 2 et 6)

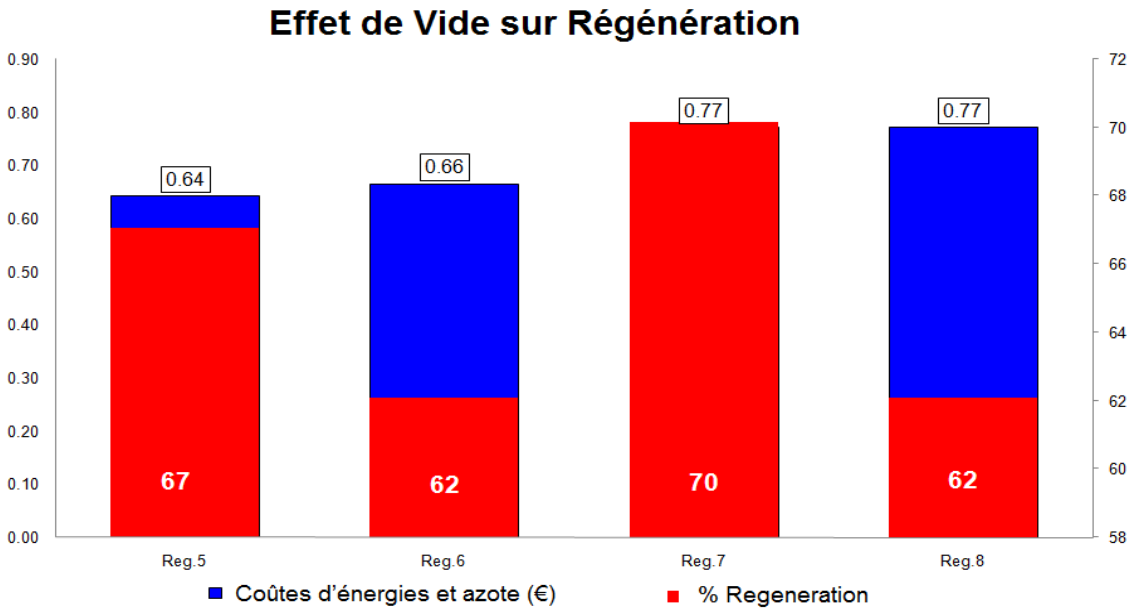

Figure 19 : Comparaison des coûts opératoires engendrés en mode de désorption thermique seul (Cycles 1 et 2) et en mode combiné à une dépressurisation sous vide (Cycles 3 et 4), pour atteindre un taux de régénération de 70%

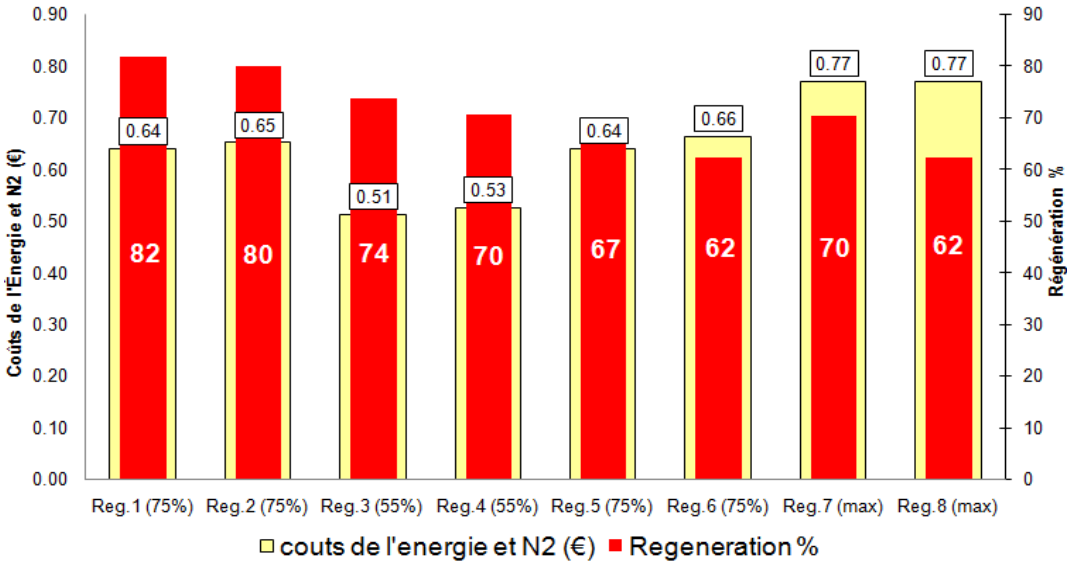

Figure 20 : Coûts opératoires et taux de régénération maximum obtenus sur les différents cycles

L'ensemble des résultats reportés sur la figure 20, l'effet de la température peut être vu en comparant les cycles successifs (comme [Reg.1 et] Reg.2, [Reg.3 et Reg.4], [Reg5 et Reg.6], [Reg.7 et Reg. 8]), il n'y a pas une grande différence dans la régénération% dans les deux cas [Reg.1 et] Reg.2, [Reg.3 et Reg.4]. C'est parce que la température du gaz a varié entre 85 et 93 C avec un débit élevé de l'azote (500 L / H). Et dans le cas de [Reg5 et] Reg.6, [Reg.7 et Reg.8], il est de 5 - 8% de différence de régénération. C'est à cause de la température a varié entre 93 à 118 C avec un faible débit d'azote (250L / H).

5. Conclusion et Perspectives

1. Certaines des caractéristiques du charbon actif sont encore à faire
2. La mesure des isothermes seront poursuivis à températures différentes avec des charbons différents et des COV différents pour construire un modèle pour l'adsorption
3. Des expériences préliminaires seront effectuées au pilote du GRL Arkema d'optimiser les conditions de opératoire pour l'adsorption
4. Des expériences préliminaires seront effectuées au pilote de l'EMN d'optimiser les conditions de opératoire pour l'adsorption
5. Les études expérimentales ont été faites pour la compréhension de l'influence de la température, du débit et du délai d'application de vide
6. Les données de la des études expérimentales seront utilisées pour la modélisation pour la simulation efficace de nouvelles études du charbon actif – COV

Références bibliographiques

[1] EUR-lex. Access to European law. Directive 2004/42/ECof the European Parliament and of the Council, Apr 2004, http://eur-lex.europa.eu/en/index.htm, accessed: 19 Jun 2011

[2] U.S. Environmental Protection Agency. Office of Pollution Prevention and Toxics (OPPT). Dichloromethane fact sheet - EPA 749-F-94-018, Aug1994, http://www.epa.gov/chemfact/f_dcm.txt, accessed: 19 Jun 2011

[3] K.S. Hwang, D.K.Choi, S.Y.Gong, S.Y.Cho, Adsorption and thermal regeneration of methylene chloride vapor on activated carbon bed, Elsevier – Chemical Eng. and Pro. 46 (1998) 1111 -1123

[4] European Parliament. Health and Environment. Dichloromethane to be banned in paint-strippers. REF: 20090113IPR46095, Jan 2009, http://www.europarl.europa.eu, accessed : 19 Jun 2011

[5] M. Worrall, AMNEC Inc., Case studies on capturing organic vapors from non-condensable gases using activated carbon technology, Jan 1998

[6] The Brownfields and Land Revitalization Technology Support Center [BTSC], U.S. EPA, Argonne National Laboratory, and the U.S. Army Corps of Engineers) – Definitions, http://www.brownfieldstsc.org

[7] C.L.Cavalacante JR et al., Industrial Adsorption Separation Processes: Fundamentals, Modeling and Applications and applications, Latin American Applied Research 2000; 30:357-64

[8] S. Giraudet, Exothermicity of adsorption of volatile organic compounds in fixed activated carbon beds: modelling and simulation valdiation of experimental work, PhD dissertation, EMN, France, 2006

[9] EPA Technical Bulletin Report, "Choosing an Adsorption system for VOC"; Clean Air Technology Centre (CATC), May 1999

[10] T. Jayabalan, Study of oxidation of carbon materials, Ph.D. Dissertation, Ecole des Mines de Nantes, France, 2008

[11] Jürgen, S.Reiner, Gas Adsorption Equilibria, Springer publications, USA, 1994

[12] D.M. Ruthven, Principles of adsorption and adsorption processes, John Wiley & Sons: New-York, Univ of New Brunswick: Fredericton, USA, 1984

[13] P. Pré, F. Delage, P. Le Cloirec. A model to predict the adsorber thermal behavior during treatment of volatile organic compounds onto wet activated carbon. Environ Sci Technol 2002; 36:4681-88

[14] F. Delage, P. Pré, P. Le Cloirec. Mass transfert and warming during adsorption of high concentrations of VOCs on an activated carbon bed: experimental and theoretical analysis. Environ Sci Technol 2000; 34:4816-21

[15] P. Pré, F. Delage, P. Le Cloirec. Modeling the exothermal nature of V.O.C. adsorption to prevent activated carbon bed ignition. In: Fundamentals of Adsorption 2001; 700-7

[16] E. Fiani, L. Perier-Cambry, G. Thomas. Non-isothermal modelling of hydrocarbon adsorption on a granulated active carbon. J Therm Anal Cal 2000; 60:557-70

[17] L. Yong, K. Sumathy. Comparison between heat transfer and heat mass transfer models for transportation process in an adsorbent bed. Int J Heat Mass Transfer 2004; 47:1587-98

[18] L. Luo, M. Bailly. Gestion de la thermique dans les procédés d'adsorption de gaz, Rev Gén Therm 1996; 35:693-7

[19] J.H. Yun, D.K. Choi, H. Moon. Benzene adsorption and hot purge regeneration in activated carbon beds. Chem Eng Sci 2000; 55:5857-72

[20]H.J. Bart, R. Germerdonk, P. Ning. Two dimensional non-isothermal model for toluene adsorption in a fixed-bed adsorber. Chem Eng Processing 1996; 35:57-64

[21]S. Giraudet, P. Pre, H. Tezel, P. Le Cloirec. Estimation of adsorption energies using physical characteristics of activated carbons and VOCs molecular properties. Carbon. 2006; 44: 1873-83

[22] D.P. Paulsen, F.S. Cannon. Polytherm model for methylisobutylketone adsorption onto coconut based granual activated carbon. Carbon. 1999; 37: 249-63

[23] G.O. Wood. Affinity coefficients of the Polanyi /Dubinin adsorption isotherm equations: a review with compilations and correlations. Carbon. 2001; 39:343–56.

[24] G.O. Wood. Review and comparisons of D/R models of equilibrium adsorption of binary mixtures of organic vapors on activate carbons. Carbon. 2000; 40:231-39

[25] C. Nguyen, DO DD. The Dubinin – Raduskevich equation and the underlying microscopic adsorption description. Carbon. 2000; 39:1327-336

[26] R.J. Dombrovski, C.M. Lastoskie, D.R. Hyduke. The Horvarth-Kawazoe method revisited. Colloids and Surfaces, A: Physicochemical and Engineering Aspects 2001;187-188:23-39.

[27] V.K. Dobruskin. Contribution of the edge effect to physical adsorption in micropores of activated carbons. Carbon 2002; 40:659-66.

[28] V.K. Dobruskin. Micropore structure of activated carbons and predictions of adsorption equilibrium. Carbon 2002; 40:1003-10.

[29] J. Wu, L.G. Hammarstrom, O. Claesson, I. Fangmark. Modeling the influence of physico-chemical properties of volatile organic compounds on activated carbon adsorption capacity. Carbon 2003;41:1322-5.

[30] A.M. Tolmachev, O.I. Trubnikov. Molecular models for vapor adsorption on microporous adsorbents. Carbon 2002; 40:1401-7.

[31] J.A. Schwarz, C.I. Contescu. Surfaces of nanoparticles and porous materials. Surfactant Sci Series, Marcel Dekker: New-York, USA, 1999

[32] Y. He, J.H. Yun, N.A. Seaton. Adsorption equilibrium of binary methane/ethane mixtures in BPL activated carbon: isotherms and calorimetric heats of adsorption. Langmuir 2004; 20:6668-78

[33] S. Giraudet, P. Pre, P. Le Cloirec. Modeling the Heat and Mass Transfer in Temperature Swing Adsorption of Volatile Organic compounds on to Activated Carbons. Env. Sci. and Tech 2009; 43:1173 – 179

[34] L.K. Wang, N.C. Pereira, Y.T. Hung. Air pollution control engineering. Humana press, Totowa, New Jersey. Volume 1, 2004

[35] R.C.Nattkemper, Nitrogen Vs Steam Regeneration in activated carbon systems, American Carbon Society, Imation Corp., Camarillo, CA 93012, Jul 1997

[36] J. Gu, N. M. Faqir, H.J. Bart, Drying of an Activated Carbon Column after Steam Regeneration. Wiley Publications - Chemical Eng. and Tech. 1999, 22:859-64

[37] J.F. Nastaj, B. Ambrożek, J. Rudnicka, Simulation studies of a vacuum and temperature swing adsorption process for the removal of VOC from waste air streams, Elsevier – Interna. Comm. of heat and mass transfer. 2006; 33: 80 - 6

[38] R.H. Zanitsch, R.T. Lynch, Carbon Adsorption Handbook, Selecting a Thermal Regeneration System for Activated Carbon, Calgon Carbon Corporation, 1997

[39] R.T. Yang, Adsorbents: fundamentals and applications, John Wiley & Sons pub., New Jersey, 2003

[40] J. Kuntzel, R.Ham, T.Melin. Steam regeneration of hydrophobic zeolites, Chemie Ingenieur Technik, 1999; 7:71 - 76

[41] J.S.J. Van Deventer, B.S. Camby, The influence of Regeneration conditions on the adsorptive behavior of activated carbon, Mineral Engg., 2003

[42] J. Bonjour, J.B. Chaflen, F. Meunier, TSA process with indirect cooling and heating, I& EC research, 2002, 41:5802-811

[43] T.C. Drage, A. Arenillas, K.M. Smith, C.E. Snape, Thermal stability of polyethylenimine based carbon dioxide adsorbents and its influence on selection of regeneration strategies, Microporous and Mesoporous Materials, 2008, 116:504-12

[44] J. Kim, S. Lee, M. Kim, J. Lee, C. Lee, Sorption equilibrium and thermal regeneration of acetone and toluene vapours on an activated carbon, I&EC Research, 2007, 46:4584-594

[45] S.G.Ramalingam, P.Pré, S.Giraudet, L.Le Coq, P.Cloirec, O.Baudouin, S.Déchelotte, Recovery comparisons - Hot Nitrogen Vs Steam regeneration of toxic dichloromethane from activated carbon beds in oil sands process 2012; 205-206:222-28

[46] T. Boger, A. Salden, G. Eigenberger, A combined vacuum and temperature swing adsorption process for the recovery of amine from foundry air, Elsevier - Chemical Eng. and Pro.,1997, 36:231-42

[47] S.G.Ramalingam, J.Saussac, P.Pré, S.Giraudet, L.Le Coq, P.Cloirec, S.Nicolas, O.Baudouin, S.Déchelotte, A.Medevielle, Hazardous Dichloromethane recovery in combined temperature and vacuum pressure swing adsorption process, Elsevier – Journal of Haz. Materials 2011; 198:95-102

[48] R.H. Perry *et al.*, Perry's Chemical Engineers Handbook, McGraw-Hill, New York, 2007

[49] P.M.Berthouex., L.C.Brown, Statistics for Environmental Engineers, Second ed., Lewis Publishers, USA, 2002

Annexes

T1, T2, T3 sont les températures en haut, milieu et bas de la colonne. P1, P2 (P-R), P3 sont les pressions en haut, entre de la pompe vide et le régulateur, et bas de la colonne.

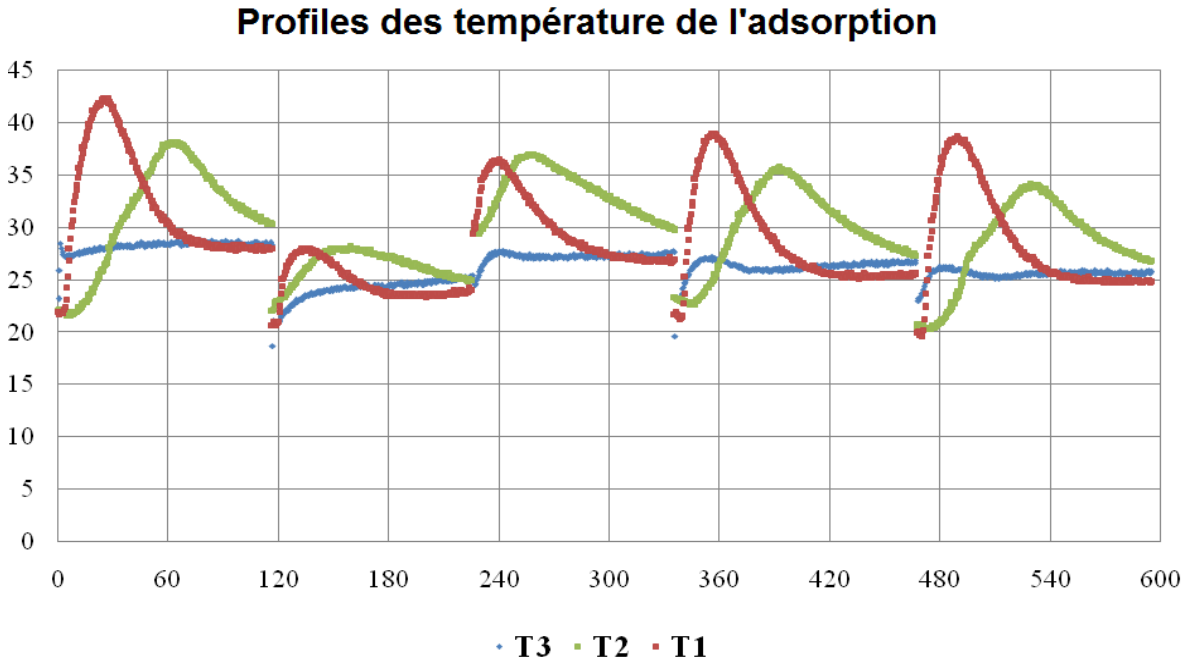

Profile des températures de l'adsorption

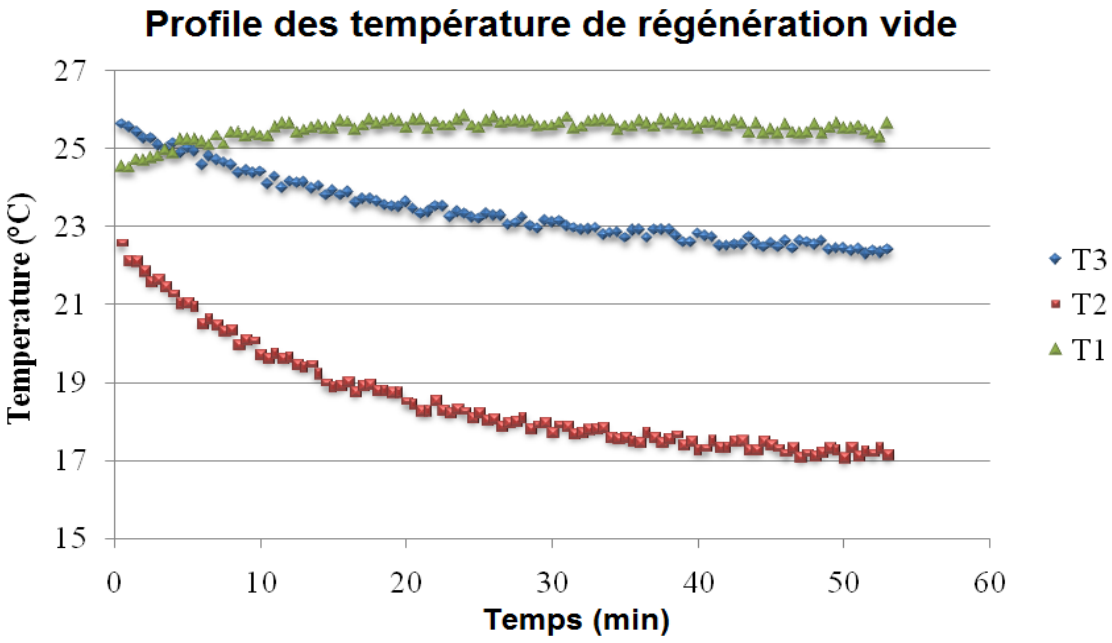

Figure 4-8 Profile des temperature de la Régénération sous Vide

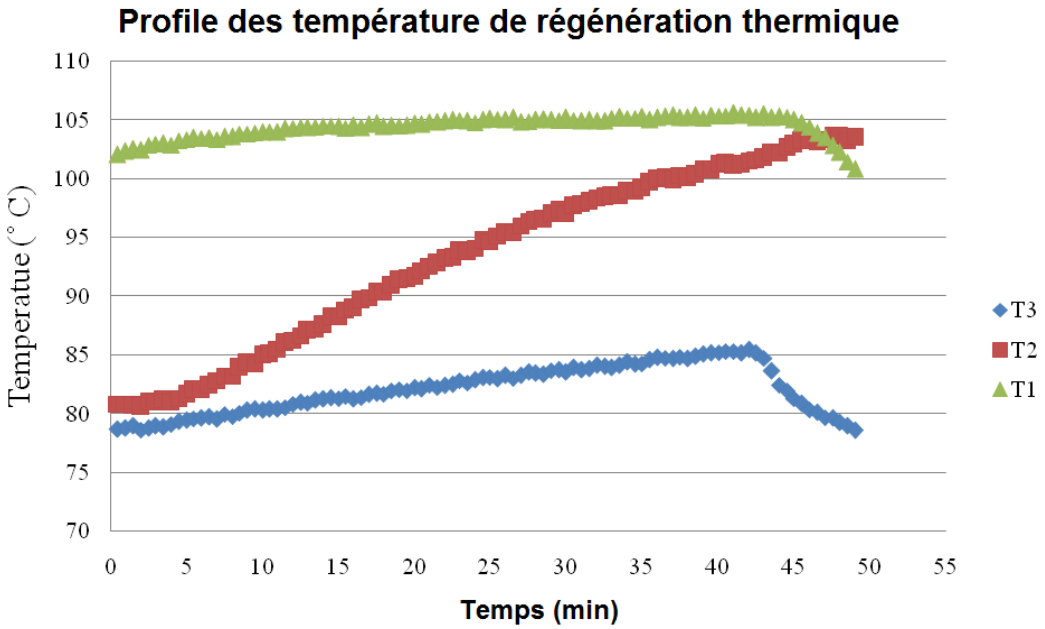

Figure 4-9 Profile des temperature de la Régénération thermique

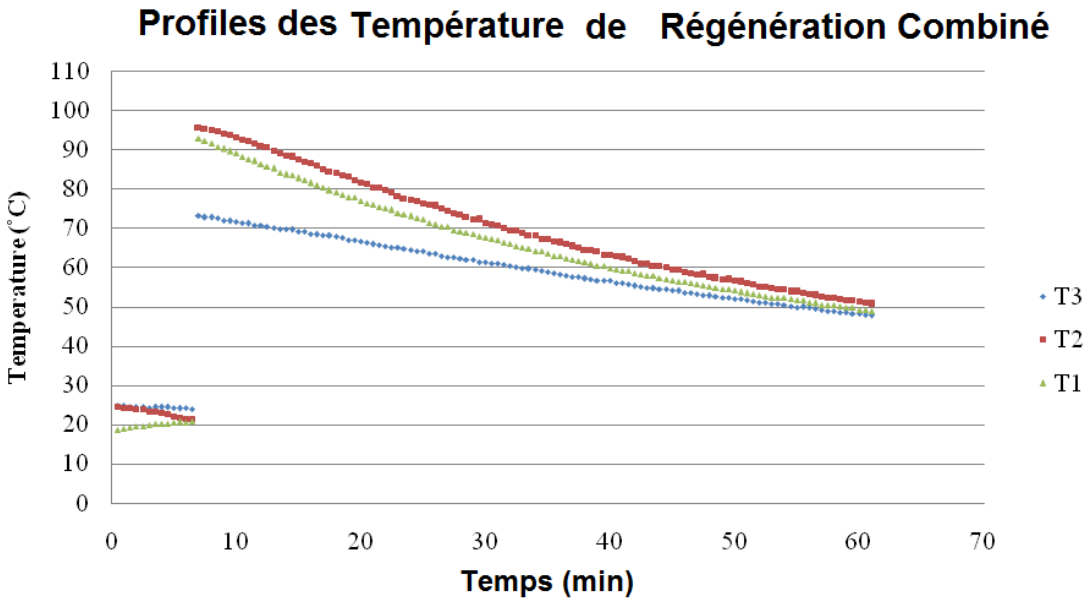

Profile des temperatures de la Régénération combinée

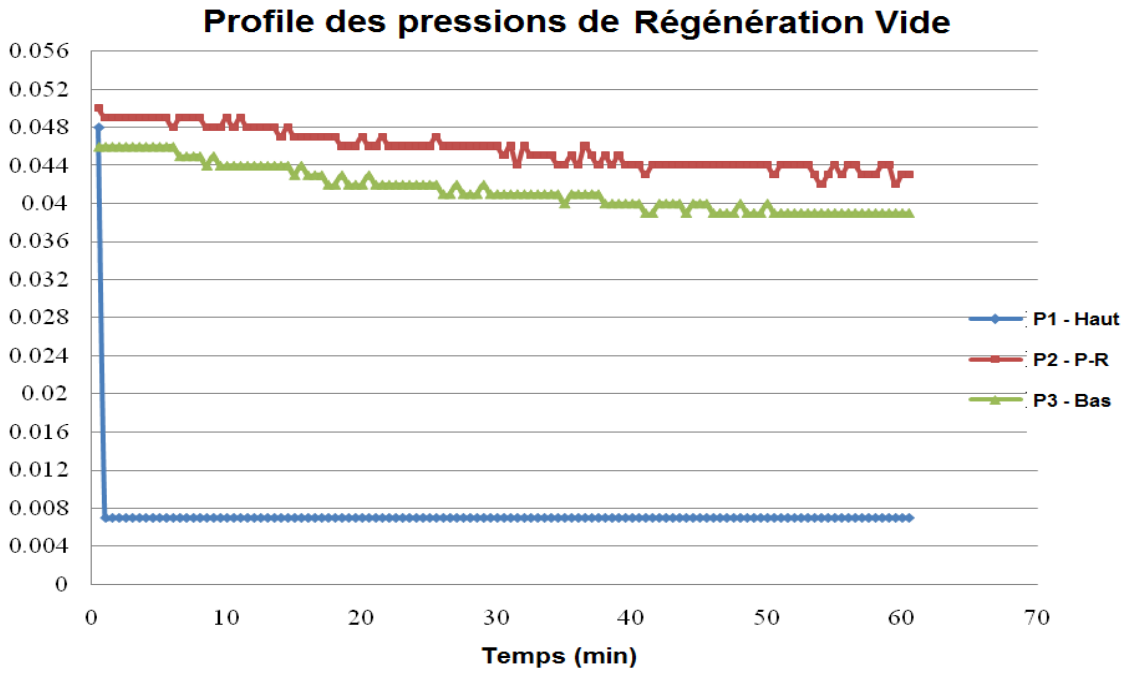

Profile des Pressions de la Régénération sous vide

1. Les pressions sont mesurées à 3 points P1 la pression au sommet de la colonne, P2 la pression entre le fond (bas) de régulateur de Pression et passent l'aspirateur la pompe et P4 la pression au fond de la colonne

2. La pression aux diminutions dans le P2 et P4, comme les revenus de régénération et c'est constant après la saturation de régénération

3. Il y a un grand saut (de 0.048 barres(bars) à 0.007 barres(bars)) dans la pression P1 dans 50 secondes et il pourrait être du à la partie supérieure de la colonne qui est vide

Summary of experimental results of coefficients of Lagmuir isotherm model

COV	CA	qm (mol.kg^{-1})	b (m^3.mol^1)	H(J.mol^1)	R^2
Ethyl Alcohol	ACM 204	4.1	1.52E-06	39060	0.93
Ethyl Alcohol	ACM 404	7.4	2.03E-04	24650	0.99
Ethyl Alcohol	ACV 404	7.6	5.87E-04	22460	0.97
Dichloromethane	ACM 204	6.8	1.57E-02	12810	0.98
Dichloromethane	ACM 404	14.5	1.90E-03	14630	0.98

Dichloromethane	ACV 404	10.8	5.73E-05	26240	0.98
Ethyl Formate	ACM 204	3.9	5.37E-03	19190	0.92
Ethyl Formate	ACM 404	5.5	5.08E-05	28370	0.95
Ethyl Formate	ACV 404	6.6	1.12E-04	26820	0.95
Acetone	ACM 204	3.3	9.05E-06	35830	0.92
Acetone	ACM 404	4.8	3.91E-04	23368	0.98
Acetone	ACV 404	4.9	9.60E-07	41840	0.95
Toluene	ACM204	5.2	5.87E-04	19630	0.94
Toluene	ACM404	8.8	2.04E-03	16740	0.95
Toluene	ACV404	10.2	4.52E-03	14370	0.98

Summary of experimental results of coefficients of Langmuir-Freundlich model

COV	CA	qm (mol.kg^{-1})	b (m^3.mol^1)	n	H (J.mol^1)	R^2
Ethyl Alcohol	ACM 204	6.3	6.33E-04	2.1	19300	0.99
Ethyl Alcohol	ACM 404	7.8	4.10E-04	1.1	22300	0.99
Ethyl Alcohol	ACV 404	9.7	3.88E-03	1.4	15320	0.99
Dichloromethane	ACM 204	12.3	4.67E-02	1.6	14170	0.99
Dichloromethane	ACM 404	24.3	3.19E-03	1.3	11380	0.99
Dichloromethane	ACV 404	25.5	9.96E-04	1.7	14830	0.99
Ethyl Formate	ACM 204	8.7	3.91E-02	2.5	17341	0.99
Ethyl Formate	ACM 404	18.3	2,16E-03	2.1	12480	0.99
Ethyl Formate	ACV 404	32.4	3.23E-03	2.4	10370	0.99
Acetone	ACM 204	5.3	3.32E-03	2.2	15354	0.97
Acetone	ACM 404	6.1	3.36E-03	1.4	15693	0.98
Acetone	ACV 404	5.9	1.83E-04	1.6	25030	0.97
Toluene	ACM204	7.9	2.48E-03	1.4	13790	0.95
Toluene	ACM404	7.8	9.23E-04	0.9	19660	0.96
Toluene	ACV404	8.9	2.21E-03	0.8	17170	0.98

Summary of experimental results of coefficients of DR isotherm model

COV	ACs	W_0 (cm^3g^{-1})	E (kJ mol^{-1})	R^2
Acetone	ACM 204	0.34	15.5	0.96
Acetone	ACM 404	0.47	13.2	0.92
Acetone	ACV 404	0.54	15.1	0.97
Dichloromethane	ACM 204	0.32	13.7	0.96
Dichloromethane	ACM 404	0.51	12.7	0.92
Dichloromethane	ACV 404	0.55	14.7	0.95
Ethyl Formate	ACM 204	0.34	13.9	0.95
Ethyl Formate	ACM 404	0.44	12.8	0.93
Ethyl Formate	ACV 404	0.53	13.7	0.92
Ethyl Alcohol	ACM 204	0.34	12.5	0.96
Ethyl Alcohol	ACM 404	0.49	10.8	0.91
Ethyl Alcohol	ACV 404	0.55	11.3	0.90

Summary of experimental results of coefficients of modified Langmuir model

Modified Langmuir model coefficients – VOC /ACV404 system				
VOCs	qm_0 ($mol.kg^{-1}$)	qm_1 (T^{-1})	k_1 (T^{-1})	k_0 (atm^{-1})
Acetone	2.79	173	4810	7.8 E-05
Ethyl Formate	3.02	243	3893	1.6 E-04
Dichloromethane	3.52	279	3087	4.0 E-03

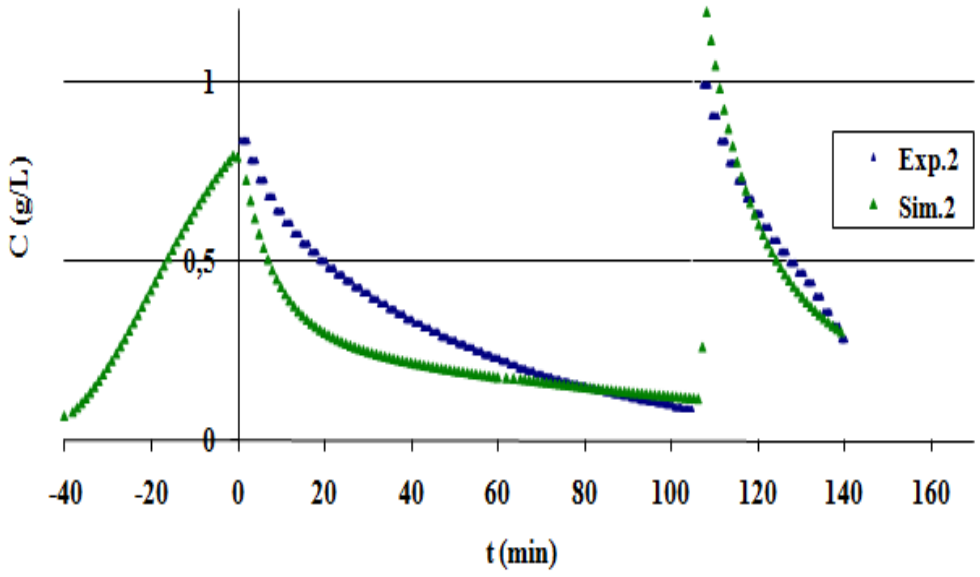

VTSA process – Regeneration 2 at 85 °C and 75% Intermediate regeneration

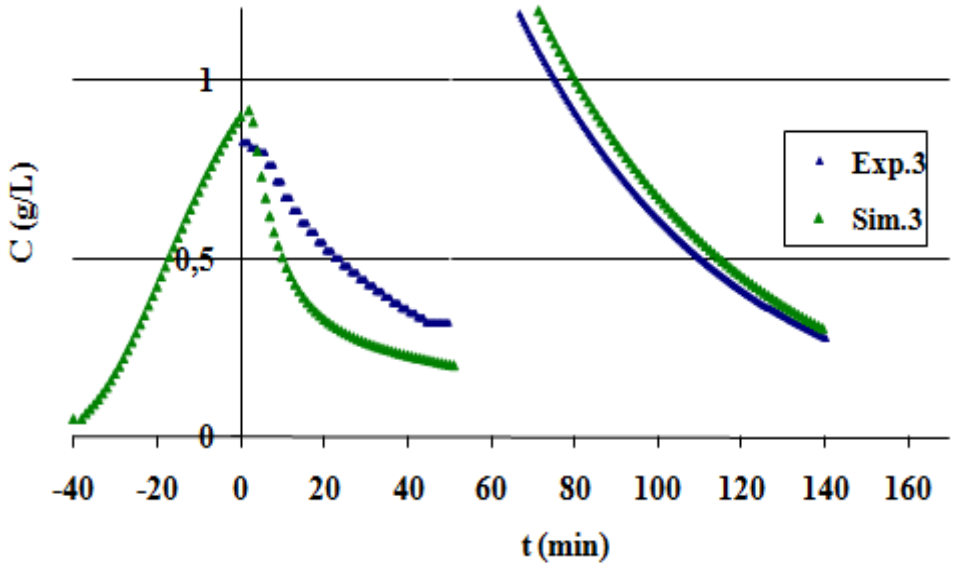

VTSA process – Regeneration 3 at 93 °C and 55% Intermediate regeneration

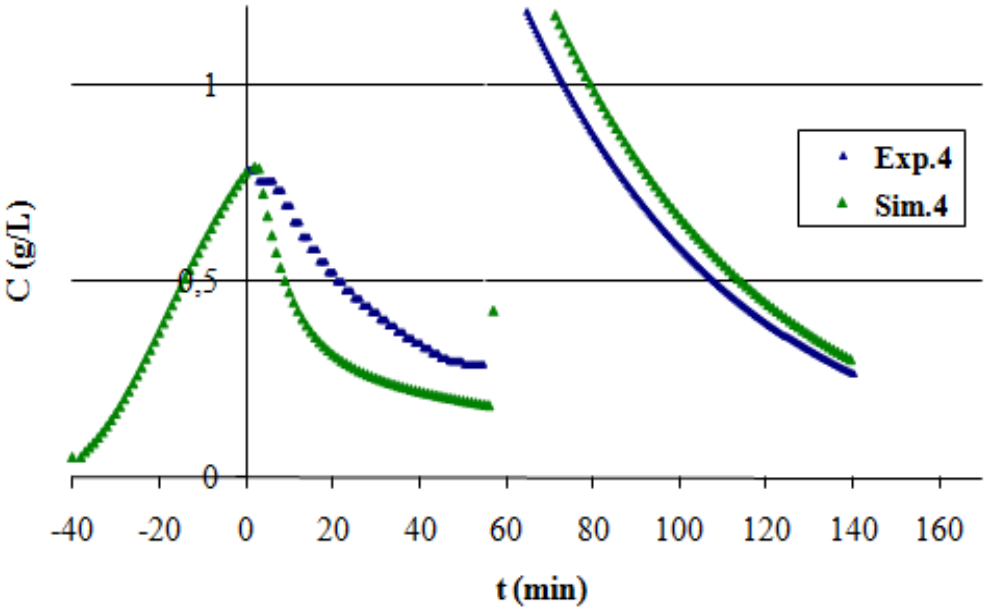

VTSA process – Regeneration 4 at 85 °C and 55% Intermediate regeneration

Summary of internal mass transfer coefficients in the simulation model

VOC - AC system	D_{gl} ($m^2.s^{-1}$)
Dichloromethane – ACM 404	0.008
Dichloromethane – ACV 404	0.009
Dichloromethane – BC 120	0.01
Acetone – ACV 404	0.003
Ethyl Formate – ACV 404	0.001

RESUME et MOTS CLES

Shivaji Ganesan Ramalingam

Adsorption de Composes Organiques Volatils et Régénération de charbon actifs – Développement d'outils de simulation

Adsorption of Volatile Organic Compounds and Regeneration of activated carbons – Development of a simulation tool

Résumé

Les vapeurs organiques émises des solvants utilisés dans le produit chimique / la nourriture / les processus pharmaceutiques, ou des stations d'entreposage de combustible d'hydrocarbure aux terminus de pétrole, peuvent être efficacement capturées par l'adsorption sur les lits de charbon actif. L'objectif général du programme de recherche est les études expérimentales et les études de simulation de l'adsorption et des pas de régénération en cas de l'enlèvement COV qui estime dans les émissions industrielles par l'Adsorption (TSA – Température Swing Adsorption et VTSA -Vacuum Température Swing Adsorption). C'est accompli par les points suivants : établir les données d'équilibre d'isotherme pour 5 COV et 8 carbones activés à 293, 313, 333 et 353 K (complètement 120 expériences d'isotherme) et les utiliser ensuite dans le modèle de simulation; développer une simulation pose pour le processus de régénération et l'adsorption; concevoir et optimiser l' expérimentale de TSA qui a été établi dans Ecole des les Mines de Nantes; concevoir et optimiser l'expérimentale de VTSA qui a été établi dans GRL ARKEMA; la validation de simulation de résultats expérimentaux de le processus TSA et VTSA. Une fois après l'achèvement de tous les objectifs, le but est de se développer et le lancement un utile de simulation complet pour l'adsorption et les pas de régénération de COV avec la coopération de la Société PROSIM

Mots clés

Adsorption, régénération, COV, charbon actif, simulation, isotherme d'adsorption

Abstract

Organic vapors emitted from solvents used in chemical / food / pharmaceutical processes, or from hydrocarbon fuel storage stations at oil terminals, can be efficiently captured by adsorption onto activated carbon beds. The overall objective of the research program is the experimental and simulation studies of the adsorption and regeneration steps in the case of VOC removal which accounts into industrial emissions by Temperature Swing Adsorption (TSA) and Vacuum Temperature Swing Adsorption (VTSA) processes. This is achieved by the following steps: to establish the isotherm equilibrium data for 5 VOCs and 8 activated carbons at 293, 313, 333, and 353 K (totally 120 isotherm experiments) and then use them in the simulation model; to develop a simulation model for adsorption and regeneration process; to design and optimize the experimental setup of Thermal Swing Adsorption (TSA) which has been established in Ecole des Mines de Nantes; to design and optimize the experimental setup of Vacuum Temperature Swing Adsorption processes (VTSA) which has been established in GRL ARKEMA unit ; simulation validation of experimental results of TSA and VTSA process. Once after the completion of all the objectives, the goal is to develop and launch a complete simulation package for adsorption and regeneration steps of VOCs with the co-operation from PROSIM Corporation

Key Words

Adsorption, Regeneration, VOC, activated carbon, simulation, adsorption isotherm